Università degli Studi di Pisa
Facoltà di Scienze Matematiche Fisiche e Naturali

Ph.D Thesis

Finite-Size Scaling in Non-Equilibrium Critical Phenomena

Massimiliano Gubinelli

Supervisor
Prof. S. Caracciolo

Pisa, Ottobre 2002

Contents

Introduction

At present, the statistical mechanics of systems in thermal equilibrium is quite well established. On the other hand, little is known in general for nonequilibrium systems. It seems therefore worthwhile to study simple models which are out of thermal equilibrium. One of such systems is the model introduced at the beginning of the eighties by Katz, Lebowitz, and Spohn [21] (described in Chapter 1), who studied the stationary state of a lattice gas under the action of an external drive. The model, hereafter called *driven lattice gas* (DLG), is a kinetic Ising model on a periodic domain with Kawasaki dynamics and biased jump rates. In a sense the DLG may be considered as the "Ising model" for nonequilibrium critical phenomena, given its simplicity and richness. Indeed although not in thermal equilibrium, the DLG has a time-independent stationary state and shows a finite-temperature transition (Section 1.2 and 1.4), which is however different in nature from its equilibrium counterpart [1].

Despite its simplicity, the DLG has not been solved exactly [2]. Nonetheless, many results have been obtained by means of Monte Carlo (MC) simulations and by using field-theoretical methods. In particular, Refs. [26, 27] developed a continuum model which is believed to capture the basic features of the transition and which provides exact predictions for the critical exponents. The analysis of Refs. [26, 27] has been recently criticized in Refs. [49, 50, 53], opening an ongoing debate we sum up in Section 1.5. Several computer simulations studied the critical behaviour of these systems in two and three dimensions [38, 40, 41, 45]. These simulations provided good support to the field-theoretical predictions, once it was understood that the highly anisotropic character of the transition required some kind of anisotropic finite-size scaling (FSS, discussed in Chapter 2).

In spite of the extensive numerical work, there are no direct studies of the correlation length so far, essentially because it is not easy to define it. Our first concern will be to define a finite-volume transverse correlation length (see Section 1.3) generalizing the definition of the second-moment correla-

[1] For an extensive presentation of the DLG and of many generalizations, see Refs. [20, 18].

[2] The DLG is soluble for infinite drive in the limit in which the ratio of jump rates parallel and perpendicular to the field direction becomes infinite [22].

tion length that is used in equilibrium systems. Because of the conserved dynamics, such a generalization requires some care. To this end, we will extend euristically our results of ref. [95] on the proper definition of correlation lenght in finite systems at fixed magnetization (or density).

Since anisotropic FSS scaling requires the preliminary knowledge of the anisotropy exponent Δ we try to understand in sec. 2.4 what can be expected, on general grounds, when the wrong value of Δ is used in simulations. This led us to the study of an exaclty soluble model to confirm our conjectures, the analisys is described in chap. 3. In general *shape mismatch* in FSS is poorly understood and more thorough investigations would be needed to assess a firm theoretical framework for anisotropic FSS. This has a huge relevance in the understanding of critical phenomena outside thermal equilibrium where strong anisotropy (correlation lengths diverging with different exponents in different directions) is a rule.

In sec. 2.5 we analyze the behaviour in a finite box of the field-theory believed to describe the critical phenomena in the DLG and compute FSS functions for several observables.

Then in sec. 4 we report the results of extensive numerical simulations of the DLG in two dimensions and compare the results with the theoretical prediction of the standard field-theory, finding a good agreement. Exploiting the correlation lenght and FSS arguments, our analysis essentially confirms the gaussian nature of transverse fluctuations in DLG as expected by field theory. A preliminary investigation of shape mismatch effects in the DLG is attempted, however the situation is still far from being clear and more insights (mainly from the theoretical side) are needed.

Finally, I would like to acknowledge the very interesting collaboration with S. Caracciolo and A. Gambassi which led to many of the results I present here.

Chapter 1

The Driven Lattice Gas

1.1 The lattice gas

A *lattice gas*[1] is a model of indistinguishable classical particles moving on a d-dimensional hypercubic lattice $\Lambda \subset \mathbb{Z}^d$ constrained by an hard-core repulsive interaction. A configuration η of the system is completely described by the occupation numbers $\eta_{\boldsymbol{i}}$ of each site $\boldsymbol{i} \in \Lambda$. We will consider only models in which at most one particle may occupy a given site, then $\eta_i \in \{0,1\}$ and the state space is given by $\mathcal{C}(\Lambda) := \{0,1\}^{\Lambda}$([2]), $\eta \in \mathcal{C}(\Lambda)$ is a particular configuration of the gas. Unit vectors in the principal directions of the lattice Λ will be denoted $\hat{\boldsymbol{e}}_\mu$, $\mu = 1, \ldots, d$, $|\boldsymbol{i} - \boldsymbol{j}|$ is the distance between $\boldsymbol{i}, \boldsymbol{j} \in \Lambda$, $|\boldsymbol{i} - \boldsymbol{j}| = 1$ when $\boldsymbol{i}$ and $\boldsymbol{j}$ are nearest-neighbours (NN). Given a configuration $\eta \in \mathcal{C}$ we will denote with $\eta^{\boldsymbol{ij}}$ the configuration

$$\eta^{\boldsymbol{ij}}(\boldsymbol{k}) := \begin{cases} \eta(\boldsymbol{j}), & \text{if } \boldsymbol{k} = \boldsymbol{i}, \\ \eta(\boldsymbol{i}), & \text{if } \boldsymbol{k} = \boldsymbol{j}, \\ \eta(\boldsymbol{k}), & \text{otherwise.} \end{cases}$$

i.e. $\eta^{\boldsymbol{ij}}$ is obtained from η by exchanging site $\boldsymbol{i}$ with site $\boldsymbol{j}$.

The gas evolves through random jumps of particles to neighboring sites. This can be conveniently described prescribing the rates $c(\boldsymbol{i}, \boldsymbol{j}, \eta)$ of transition form the configuration η to the configuration $\eta^{\boldsymbol{ij}}$.

Consider a finite volume Λ and let $P_0(\eta)$ be the an initial probability distribution over $\mathcal{C}(\Lambda)$, let $P_t(\eta)$ be the probability of finding the gas in configuration η at time t. It obeys the *Fokker-Planck equation*

$$\frac{d}{dt} P_t(\eta) = L^* P_t(\eta) = \frac{1}{2} \sum_{i,j \in \Lambda} \{c(\boldsymbol{i}, \boldsymbol{j}, \eta^{\boldsymbol{ij}}) P_t(\eta^{\boldsymbol{ij}}) - c(\boldsymbol{i}, \boldsymbol{j}, \eta) P_t(\eta)\}. \quad (1.1)$$

[1] Its simplest form was used as a model in seminal works on phase transitions [2, 4].

[2] Dynamics may restricts configuration to a subset of $\{0,1\}^{\Lambda}$.

A Markov process over the state space $\mathcal{C}(\Lambda)$ is canonically associated with this evolution equation for P_t (for details see e.g. [3]).

The dynamics is *conservative* and the density

$$\rho_\Lambda(C) := \frac{1}{|\Lambda|}\sum_{\boldsymbol{i}\in\Lambda}\eta_{\boldsymbol{i}}, \tag{1.2}$$

does not change in time: the configuration space is decomposed into invariant subspaces with different densities, i.e. $\mathcal{C} = \cup_\rho \mathcal{C}_\rho$, where $\mathcal{C}_\rho = \{C \in \mathcal{C} \,|\, \rho_\Lambda(C) = \rho\}$. With some conditions on the rates (satisfied in the models we will consider) the dynamics is irreducible [62] in every $\mathcal{C}_\rho$, i.e. from each state it is possible to get to each other state by a finite number of allowed transitions. This is sufficient to ensure that there exists a unique invariant probability (i.e. a stationary solution of (1.1)) $P^s_\rho(C)$ in each $\mathcal{C}_\rho$ and that it is independent of the initial configuration chosen. Consider the lattice gas as a thermodynamical system allowed to exchange energy with a thermal bath, then we are led to formulate two main constraints on the allowed dynamics: first, the stationary measure P^s should be a Gibbs measure for a suitable energy function $H : \mathcal{C}(\Lambda) \to \mathbb{R}$ and parametrized by the temperature of the thermal bath. Second, the stochastic process associated to Fokker-Planck eqn. (1.1) should be *stochastically reversible* [3], that is in the stationary state the law of the associated Markov process must be invariant by time-reversal. By well known arguments, this implies that the rates $c(\boldsymbol{i}, \boldsymbol{j}, \eta)$ must satisfy the *detailed balance* condition

$$P^s(\eta)c(\boldsymbol{i}, \boldsymbol{j}, \eta) = P^s(\eta^{\boldsymbol{ij}})c(\boldsymbol{j}, \boldsymbol{i}, \eta^{\boldsymbol{ij}}), \qquad \forall \boldsymbol{i}, \boldsymbol{j} \in \Lambda. \tag{1.3}$$

If $P_s(\eta) = Z^{-1}\exp\left(-H(\eta)\right)$ then

$$\frac{c(\boldsymbol{i}, \boldsymbol{j}, \eta)}{c(\boldsymbol{j}, \boldsymbol{i}, \eta^{\boldsymbol{ij}})} = \exp\Big(H(\eta) - H(\eta^{\boldsymbol{ij}})\Big), \qquad \forall \boldsymbol{i}, \boldsymbol{j} \in \Lambda \tag{1.4}$$

which can be satisfied by choosing rates c satisfying

$$c(\boldsymbol{i}, \boldsymbol{j}, \eta) = w(H(\eta) - H(\eta^{\boldsymbol{ij}}))$$

where w is an aribitary function such that $w(-x) = \exp(x)w(x)$. Different dynamics correspond to different choices for w. The stationary distribution on $\mathcal{C}(\Lambda)$ of the resulting Markov process is, nevertheless, the same, irrespective of the specific dynamics chosen [3].

A non-equilibrium steady state can be produced by perturbing an equilibrium dynamics satisfying (1.3) by coupling the lattice gas with external

[3] One popular choice for w is the Metropolis rate

$$w(x) = \min\{1; e^{-x}\} \quad .$$

force fields acting on the bulk. The essential features of the class of models called *driven lattice gases* (DLG) is the presence of an external field $\boldsymbol{E}$ acting on every bond of the lattice in such a way that the detailed balance in the local form (1.4) is modified in

$$\frac{c_E(\boldsymbol{i},\boldsymbol{j},\eta)}{c_E(\boldsymbol{j},\boldsymbol{i},\eta^{\boldsymbol{ij}})} = \exp\Big(H(\eta) - H(\eta^{\boldsymbol{ij}}) + \beta|\boldsymbol{E}(\boldsymbol{i},\boldsymbol{j})|\ell\Big) \tag{1.5}$$

for $\boldsymbol{i},\boldsymbol{j}$ nearest neighbours in Λ and where $\ell = -1, 0, +1$ for jumps of particles in the direction of $\boldsymbol{E}$, in trasverse directions and in the opposite direction, respectively. This modification takes into account the work done by the external field. If $\boldsymbol{E}$ is integrable, i.e. there exists a function $-V$ on Λ whose discrete gradient is $\boldsymbol{E}$ then the stationary measure for the rates c_E is just the Gibbs measure associated to the energy function $H_E = H + V$. The driven lattice gases are obtained taking $\boldsymbol{E}$ constant and imposing periodic boundary conditions (allowing particles to jump across the boundaries of Λ for landing at the opposite boundary). In this situation there not exists a global potential function V and the stationary state carries a non-zero flux of particles along $\boldsymbol{E}$ explicitly violating time-reversal symmetry. The stationary measure is not known *a-priori*.

1.2 The KLS model

A simple example of DLG was introduced by Katz, Lebowitz and Spohn in 1984 [21]. This model, which we will call the KLS model (and will be our standard model of DLG), is specified by requiring that the particle interacts with NN attractive couplings: the energy function is then

$$H_\Lambda = 2\beta J \sum_{\langle \boldsymbol{i},\boldsymbol{j}\rangle} \eta(\boldsymbol{i})\eta(\boldsymbol{j}) := \beta\mathcal{H}_I, \tag{1.6}$$

where angular brackets means summation over NN pair of sites $\boldsymbol{i},\boldsymbol{j} \in \Lambda$.

With vanishing external field ($\boldsymbol{E} = 0$) the stationary state is the Gibbs measure associated to H_Λ in $C_N(\Lambda)$. Introducing Ising spins $\sigma(\boldsymbol{i}) = (2\eta(\boldsymbol{i}) - 1)$ the Hamiltonian $\mathcal{H}_I$ is exaclty that of an Ising model and β is proportional to the inverse of the temperature of the thermal bath $k_B T = \beta^{-1}$. Gas particles and holes corresponds respectively to positive and negative spins, density $\rho = N/|\Lambda|$ becomes magnetization $m = 2\rho - 1$ which thus is conserved. The Gibbs measure is then

$$Z^{-1}\exp(-\beta\mathcal{H}_I)\delta\left(\sum_{i\in\Lambda}\sigma_i - m|\Lambda|\right) \tag{1.7}$$

In the thermodynamic limit this ensemble is equivalent to the standard Ising model where the magnetic field is such that the mean magnetization is m.

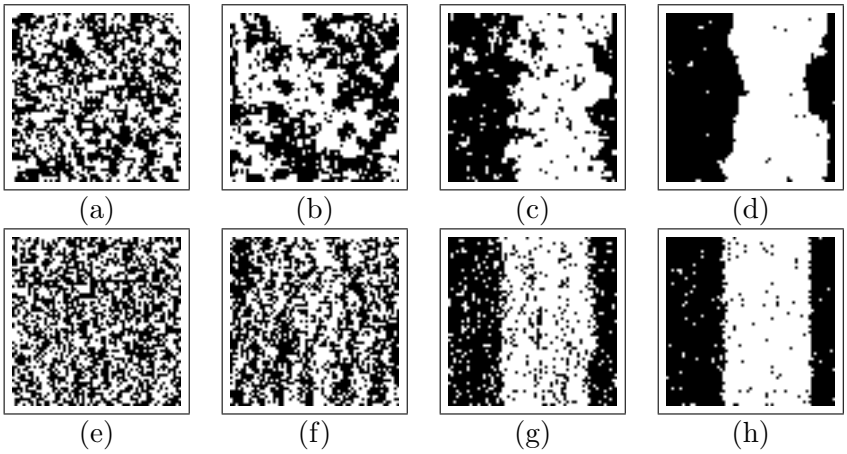

Figure 1.1: Typical configurations of the 2d KLS model on a 64×64 lattice. Temperature is decreasing from the left to the right: (a,b,e,f) $T > T_c(E)$; (c,d,g,h) $T < T_c(E)$. (a,b,c,d) refer to ordinary lattice gas $E = 0$. (e,f,g,h) refer to DLG with a saturating electric field $E = \infty$, along the vertical direction

At half density ($\rho = 1/2$) the corresponding magnetization is zero and the second-order phase transition point of the Ising model is accessible by tuning T to the critical temperature T_c (in two dimensions Onsager's result gives $\beta_c = 1/(k_B T_c) = \log(1+\sqrt{2})/2 \approx 0.44$). From the point of view of the lattice gas this is a "gas-liquid" transition: the gaseous phase with $T > T_c$ (cfr. Fig. 1.1 (a,b)) has homogeneous density and $\langle \sigma_{\boldsymbol{i}} \rangle = 0$ for every $\boldsymbol{i} \in \Lambda$. In liquid phase (cfr. Fig. 1.1 (c,d)) there is segregation of a particle-rich phase $\langle \sigma_{\boldsymbol{i}} \rangle = +m(T)$ and an hole-rich phase $\langle \sigma_{\boldsymbol{i}} \rangle = -m(T)$. The presence of the interface is due to the global conservation law. This transition is of course well understood both from the thermodynamical point of view [5], and for what concerns dynamical effects [1].

The key feature of the KLS model is that there are strong numerical evidences that the phase transition is present also in the case $E := |\boldsymbol{E}| > 0$ (Fig. 1.1 (e,f,g,h)) and that for $\rho = 1/2$ it is a continous phase transition (we will see below which is the meaning of this statement). (numerical evidences in $d = 2$ and $d = 3$, can be found in a lot of papers, see [20, 18] for comprehensive reviews) This transition occours at an inverse temperature $\beta_c(E)$ which, in two dimensions, saturates at $\beta_c(\infty) \approx 0.709(5)\beta_c(0)$ [39, 40, 41]. For $\beta < \beta_c(E)$ particles are homogeneously distributed in space, while for $\beta > \beta_c(E)$ the gas segregates in two regions, one almost full and the other almost empty, with interfaces parallel to $\boldsymbol{E}$, as shown in Figure 1.1.

Symmetries

Let us define the following transformations for the DLG model:

$$\begin{cases} C : \eta_{\boldsymbol{i}} \overset{C}{\mapsto} 1 - \eta_{\boldsymbol{i}} & \forall \boldsymbol{i} \in \Lambda \\ R : \boldsymbol{E} \overset{R}{\mapsto} -\boldsymbol{E} \\ P : \widehat{\boldsymbol{x}} \overset{P}{\mapsto} -\widehat{\boldsymbol{x}} \end{cases} \tag{1.8}$$

It's easy to realize that transition rates (and so the model) are invariant for lattice translations of both initial and final configurations and for all possible pairings of the transformations (1.8), i.e. CR, CP and PR. Moreover any ortogonal transformation in the transverse space is a symmetry. These symmetries play special rôle to set up a mesoscopic description of the observed phase transition, see Section 1.4 and 1.5.

1.3 Observables

In this section we define observables which will allow us to characterize quantitatively the phase transition of the DLG and which can be measured in numerical simulations [56]. Our principal concern is with the $2d$ DLG so we will refer to this case even though the given definitions can readily be generalized to generic d.

We consider a finite square lattice of size $L_{\parallel} \times L_{\perp}$ with periodic boundary conditions.

A very important feature of the model is the fact that total magnetization is constant (and set to zero to be able to reach the critical regime) and thus does not allow to distinguish between the two phases. The signal of the transition is encoded into long-wave disomogeneities of local magnetization. A natural object of interest is then the Fourier transform of the magnetization field $\sigma_{\boldsymbol{i}}$ which we will denote $\phi(\boldsymbol{k})$:

$$\phi(\boldsymbol{k}) := \sum_{\boldsymbol{j} \in \Lambda} e^{i \boldsymbol{k} \cdot \boldsymbol{j}} \sigma_{\boldsymbol{j}}, \tag{1.9}$$

where the allowed momenta are

$$\boldsymbol{k}_{n,m} := \left(\frac{2\pi n}{L_{\parallel}}, \frac{2\pi m}{L_{\perp}} \right), \tag{1.10}$$

with $(n, m) \in \mathbb{Z}_{L_{\parallel}} \times \mathbb{Z}_{L_{\perp}}$. At half filling, i.e. for $\rho = 1/2$ we have

$$\sum_{\boldsymbol{j} \in \Lambda} \sigma_{\boldsymbol{j}} = 0, \qquad \text{i.e.} \qquad \phi(\boldsymbol{k}_{0,0}) = 0. \tag{1.11}$$

In the ordered phase $|\phi(\boldsymbol{k})|$ takes its maximum for $\boldsymbol{k} = \boldsymbol{k}_{0,1}$, and the expectation value on the steady state of its module

$$m(L_\parallel, L_\perp) := \frac{1}{|\Lambda|}\langle|\phi(\boldsymbol{k}_{0,1})|\rangle \tag{1.12}$$

is a good order parameter.

In momentum space the static structure factor

$$\tilde{G}(\boldsymbol{k}; L_\parallel, L_\perp) := \frac{1}{|\Lambda|}\langle|\phi(\boldsymbol{k})|^2\rangle \tag{1.13}$$

vanishes at $\boldsymbol{k}_{0,0}$ because of Eq. (1.11) and is maximal at $\boldsymbol{k}_{0,1}$, so that it is natural to define the susceptibility as[4]

$$\chi(L_\parallel, L_\perp) := \tilde{G}(\boldsymbol{k}_{0,1}; L_\parallel, L_\perp). \tag{1.14}$$

In Fig.1.2 we reported results from Monte Carlo simulations showing χ as a function of E and β on a finite lattice. It is evident the onset of long-range order when β increases. Note how the effect of the external fields saturates rapidly. Figure 1.3 shows a characteristic feature of the transition: we compared χ with its longitudinal counterpart $\chi_\parallel = \langle|\phi(\boldsymbol{k}_{1,0})|^2\rangle$ to illustrate the fact that ordering is expected only in the transverse direction.

Another interesting observable is a generalization of Binder's cumulant [70] adapted to our transverse order parameter:

$$g(L_\parallel, L_\perp) := 2 - \frac{\langle|\phi(\boldsymbol{k}_{0,1})|^4\rangle}{\langle|\phi(\boldsymbol{k}_{0,1})|^2\rangle^2}. \tag{1.15}$$

If $\phi(\boldsymbol{k}_{0,1})$ has a Gaussian law in the stationary state, then $\langle|\phi(\boldsymbol{k}_{0,1})|^4\rangle = 2\langle|\phi(\boldsymbol{k}_{0,1})|^2\rangle^2$ and $g = 0$. This is expected in the high-temperature phase of the model. At low temperature, where long-range order sets it we expect on the other hand that $\langle|\phi(\boldsymbol{k}_{0,1})|^n\rangle \approx \langle|\phi(\boldsymbol{k}_{0,1})|\rangle^n$ giving $g = 1$.

1.3.1 The correlation length

Next, we would like to define a correlation length. In infinite-volume equilibrium systems there are essentially two different ways of proceeding. One can define the correlation length in terms of the large-distance behavior of the two-point function or by using the small-momenta behavior of the two-point function (e.g. second-moment correlation length). In the DLG both methods require careful considerations. Indeed a well estabilished feature of non-equilibrium steady states of conservative dynamics is that they develop generic long-range correlations in the disordered phase [20, 18, 19].

[4] We must note that the susceptibility defined by using the linear response theory does not coincide in general non-equilibrium system with that defined in terms of the Fourier transform of the two-point correlation function.

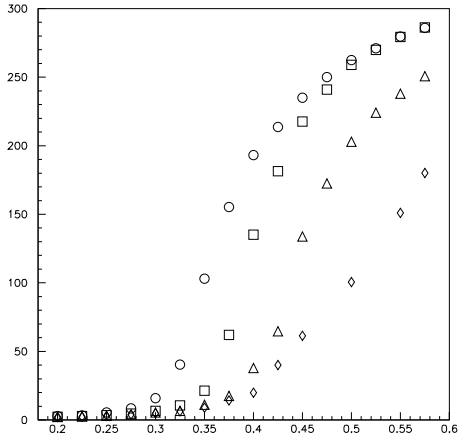

Figure 1.2: Plot of χ on a 30×30 lattice for various values of β and different values of the external field $E = 5(\circ)$, $0.75(\square)$, $0.3(\triangle)$, $0(\Diamond)$.

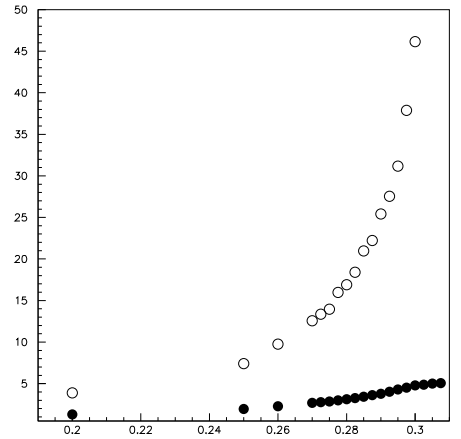

Figure 1.3: Comparison between χ ($\circ$) e $\chi_{\|}$ ($\bullet$) ($\chi_{\|} = \langle|\phi(\boldsymbol{k}_{1,0})|^2\rangle$) for various β on a 32×128 lattice.

In our case, the two-point function

$$G(\boldsymbol{x}-\boldsymbol{y}) = \langle \eta_{\boldsymbol{x}} \eta_{\boldsymbol{y}} \rangle = \frac{1}{L_\perp L_\parallel} \sum_{\boldsymbol{k}} \widetilde{G}(\boldsymbol{k}) e^{-i\boldsymbol{k}\cdot(\boldsymbol{x}-\boldsymbol{y})}$$

has already been studied by MC simulations and approximate analytic methods [20, 18]: it shows a generic power-law behaviour

$$G(\boldsymbol{x}) \propto |\boldsymbol{x}|^{-d} \tag{1.16}$$

and is not positive-definite (as a consequence of (1.16) and of the conservation law), see Fig. 1.3.1.

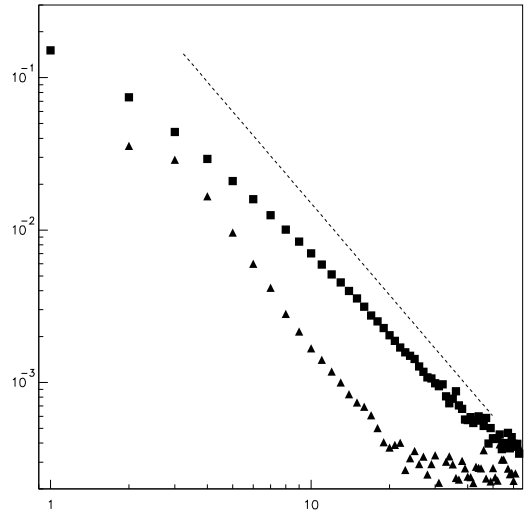

Figure 1.4: $G(\boldsymbol{x})$ for the DLG on a 2d 128×128 lattice in the high-temperature region ($\beta \ll 1$) and for $E = \infty$. (■) is $G(\boldsymbol{x})$ for $\boldsymbol{x} \| \boldsymbol{E}$; (▲) $-G(\boldsymbol{x})$ for $\boldsymbol{x} \perp \boldsymbol{E}$. Note that transverse correlations are negative. The dotted line has a slope of -2.

The algebraic power–law decay of correlations, as expressed by Eq. (1.16), gives rise to a discontinuity of the static structure factor $\tilde{G}(\boldsymbol{k})$ for $\boldsymbol{k} = \boldsymbol{0}$. Figure 1.5 shows the function $\tilde{G}(\boldsymbol{k})$ for the DLG on a 2d 128×128 lattice obtained by a MC simulation. The discontinuity is quite evident.

From this peculiar behaviour one problem arise: how can we define a correlation length for this system? At equilibrium correlations decay exponentially with distance, at least in the high–temperature phase, so that a natural length scale emerges in that context. But here correlations decay *generically* following a power–law and there is no evident emerging length

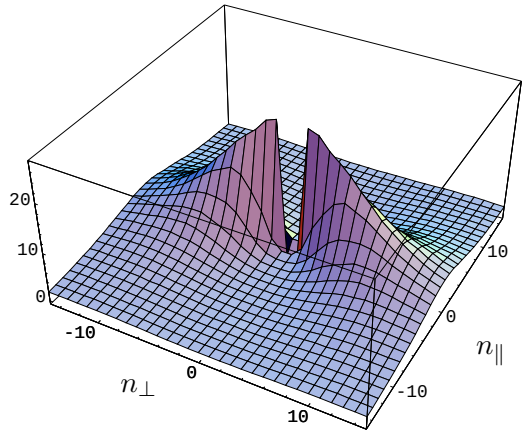

Figure 1.5: $\tilde{G}(\boldsymbol{k})$ for the DLG in $d = 2$, $L_\parallel \times L_\perp = 128 \times 128$ lattice. $n_\parallel, n_\perp$ are wave-numbers: $k_{\parallel,\perp} = 2\pi n_{\parallel,\perp}/L_{\parallel,\perp}$ where $\parallel, \perp$ denote directions parallel and transverse to $\boldsymbol{E}$.

scale. Nevertheless it is possible to show that if one considers the mean correlation of two points on the solid angle, an exponential decay is recovered (see, for details, [20]).

Fig. 1.6 shows the crossover in the two-point function $G(\boldsymbol{x})$ of the 2d-DLG as the temperature approach the phase transition point. Clearly the power-law behaviour associated with the critical state sets in first at small distances, while the long-range behaviour is still described by Eq. (1.16). Then we would like to identify the characteristic length scale at which the crossover takes place.

In Refs. [47] a parallel correlation length is defined. However, this definition suffers from many ambiguities (see the discussion in Ref. [20]) and gives results for the exponent $\nu_\parallel$ which are not in agreement with the theory [38]. Even more difficult appears the definition of a transverse correlation length because of the presence of negative correlations at large distances [38, 20].

To overcome the difficulties of the real-space strategy we will define the correlation length by using the two-point function for small momenta. We follow Ref. [95], where we discussed the possible definitions of correlation length in the absence of the zero mode, as it is the case here.

We consider the structure factor in finite volume at zero longitudinal momenta

$$\tilde{G}_\perp(q; L_\parallel, L_\perp) := \tilde{G}((0, q); L_\parallel, L_\perp), \tag{1.17}$$

(note that the conservation law implies $\tilde{G}_\perp(0; L_\parallel, L_\perp) = 0$) and introduce a

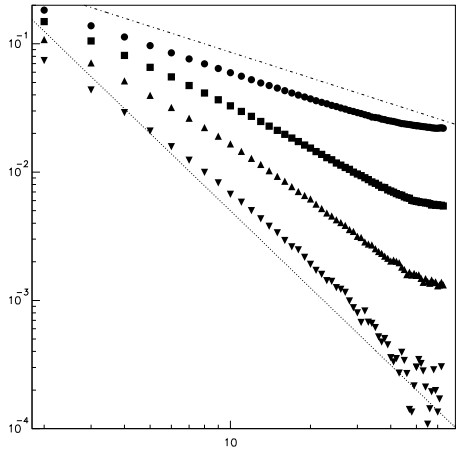

Figure 1.6: 2d-DLG : The function $G(\boldsymbol{x})$ for $\boldsymbol{x} \| \boldsymbol{E}$ for different $\beta = 0.2$ (▼),0.25 (▲), 0.28 (■), 0.3025 (•). Lattice size is 128×64, $E = \infty$ and $\beta_c \approx 0.313$. Straight lines have slope -2 and $-2/3$.

finite-volume (transverse) correlation length

$$\xi_{ij}(L_\parallel, L_\perp) := \sqrt{\frac{1}{\hat{q}_j^2 - \hat{q}_i^2}\left(\frac{\tilde{G}_\perp(q_i; L_\parallel, L_\perp)}{\tilde{G}_\perp(q_j; L_\parallel, L_\perp)} - 1\right)}, \tag{1.18}$$

where $\hat{q}_n = 2\sin(\pi n / L_\perp)$ is the lattice momentum.

Some comments are in order:

(i) If we consider an equilibrium system or a steady state in which correlations decay exponentially, then we have for $q \to 0$ that

$$\tilde{G}_\perp^{-1}(q; L_\parallel, L_\perp) = \chi(L_\parallel, L_\perp)^{-1}(1 + \xi_{ij}^2(L_\parallel, L_\perp)\, q^2 + O(q^4, L^{-2})). \tag{1.19}$$

where $\chi(L_\parallel, L_\perp)$ is the susceptibility. Thus, $\xi_{ij}^2(\infty, \infty)$ is a good definition of correlation length which has an infinite-volume limit independent of i and j.

(ii) Since $\tilde{G}_\perp(0; L_\parallel, L_\perp) = 0$, q_i and q_j must not vanish. Moreover, as discussed in Ref. [95], the definition should be valid for all T in finite volume. Since the system orders in an even number of stripes, $\tilde{G}_\perp(q_i; L_\parallel, L_\perp) = 0$ is zero for i even as $T \to 0$. Therefore, if our definition should capture the nature of the phase transition, we must require i and j to be odd. Although any choice of i, j is conceptually good, finite-size corrections increase with i, j, a phenomenon which

should be expected since the critical modes correspond to $q \to 0$. Thus, we will choose $(i, j) = (1, 3)$.

Another quantity which is considered in the analysis is the amplitude A_{13} defined by

$$A_{13}(L_{\parallel}, L_{\perp}) := \frac{\xi_{13}^2}{\chi}. \tag{1.20}$$

1.4 Field-theory of the DLG

There are many examples of non–equilibrium systems in which, by adjusting the value of some parameter, a phase transition can occur. See, for some examples, [20, 18] and references therein. Among lattice models we want to recall percolation, low dimensional models as one dimensional non–equilibrium systems (for recent reviews see [16, 17]), and many generalizations of standard DLG as *randomly driven* lattice gas [31, 32, 20], *two–temperatures* lattice gas [28, 29, 30, 20], DLG with *tilted or open* boundary conditions [33, 34] and DLG *with quenched disorder* [35] to cite only some of them.

All of them are lattice models. However, in a neighborhood of the critical point (critical region) we can limit ourselves to consider slowly-varying (in space and time) observables. At criticality (corresponding to the onset of long-range order) the lattice spacing a is negligible compared to the length and time scales at which long-range order is established so that it can be removed by taking the formal limit $a \to 0$. In this way, it is possible to formulate a description of the system in terms of *mesoscopic* variables defined on a continuum. In principle, the dynamics of such variables can be obtained by coarse graining the microscopic system. However, given the difficulty of performing a rigorous coarse-graining procedure, one postulates[5] a continuum field theory, in the form of a stochastic Langevin equation for the order parameter, that has all the symmetries of the microscopic lattice model. We will discuss this point again in Section 1.5, giving an overview of a recent still ongoing debate.

By universality [6] the continuum model should have the same critical behaviour of the microscopic one. This statement has quite rigorous foundations in the theory of equilibrium critical phenomena, from both static and dynamical point of view, and may be explained by means of the *Renormalization Group* (RG) approach to the problem. As far as dynamical aspects of the problem are concerned, we want to point out that we expect that the microscopic dynamics play a rôle in the problem only in determining conservation laws to which the system is subjected during time evolution.

[5] In some simple cases it is possible to derive, at least heuristically and in a mean-field approximation (factorization of joint probabilities in the Master equation), the mesoscopic equation from the microscopic model [55].

Accordingly, we expect no dependence of the critical behaviour of the system from the exact realization of the lattice dynamics employed to generate the equilibrium state.

On the other hand this fact is not evident at all in the case of non–equilibrium critical phenomena which depend strongly on dynamical realization of the system. To what extent universality applies to this case is not clear. We discuss this issue in Section 1.5.

Assuming universality, a field theory for the DLG (see discussion in Sec. 1.5) has been proposed [26, 27] (see also Ref. [20]) and analyzed, giving rise to exact predictions for critical exponents in space dimension d with $2 < d < 5$([6]).

Using standard methods it is possible to analyze the continuum theory in terms of a dynamical functional [11, 12, 13, 14] which reads (neglecting terms which are irrelevant by power-counting) [26]

$$J[\varphi,\tilde{\varphi}] = \int \left\{ \tilde{\varphi}[\lambda^{-1}\partial_t + \Delta_\perp(\Delta_\perp - \tau) - \rho\Delta_\parallel]\varphi + \frac{1}{2}u_0\nabla_\parallel\tilde{\varphi}\,\varphi^2 + \tilde{\varphi}\Delta_\perp\tilde{\varphi} \right\} \tag{1.21}$$

where $\varphi(\boldsymbol{x},t)$ is the local "density" field (actually, the coarse-grained version of $\sigma_{\boldsymbol{i}}$), $\tilde{\varphi}$ is the Martin-Siggia-Rose response field[11], $\parallel$ and $\perp$ subscript means spatial direction parallel and perpendicular to the external field, τ is the effective distance from the critical point, ρ is a parameter and u_0 the coupling-constant of the theory, proportional to the coarse-grained microscopic force field, and takes into account its leading effects. The upper critical dimension for this theory turns out to be $d_c = 5$. Power counting allows the conclusion that only the parameter ρ is renormalized by interactions. A dangerous irrelevant operator is also present. Renormalization group analysis leads to the following scaling form for $\Gamma_{\tilde{n}\,n}$ (1PI vertex functions with $\tilde{n}$ fields $\tilde{s}$ and n fields s)

$$\begin{aligned} &\Gamma_{\tilde{n}\,n}(\{p_\parallel,\boldsymbol{p}_\perp,\omega\};\tau,u,v) = \\ &\quad l^{Q_{\tilde{n},n}}\Gamma_{\tilde{n}\,n}\left(\left\{\frac{p_\parallel}{l^{2+\eta}},\frac{\boldsymbol{p}_\perp}{l},\frac{\omega}{l^4}\right\};\frac{\tau}{l^2},u^*,l^{\kappa^*}v\right) \end{aligned} \tag{1.22}$$

where $u \propto \mu^{-\epsilon}\rho^{-\frac{3}{2}}u_0^2$, $\epsilon = 5-d$, μ is a momentum scale, $l \ll 1$ in the scaling limit, $u^* = O(\epsilon)$ is the non trivial IR fixed-point value of the coupling u, v is the coupling of the dangerous irrelevant operator. $\eta = (5-d)/3$ exactly and $\kappa^* = \frac{2}{3}(d-2)$;

$$Q_{\tilde{n},n} = -2\,\eta\left(\frac{n+\tilde{n}}{4} - \frac{1}{2}\right) + d + 5 - \tilde{n}\frac{d+3}{2} - n\frac{d-1}{2}$$

[6] A field theory for the DLG was also derived in Ref. [25], starting from the standard Model B dynamics. The external drive partially breaks the supersymmetry (SUSY) of Model B, giving rise to a crossover towards a new fixed point in $d = 5$, with a residual symmetry ($\frac{1}{2}$SUSY of Ref. [25]).

From (1.22) we see that when considering time-independent observables at vanishing $p_{\|}$ the scaling form obtained is that of a *mean-field* theory for $2 < d < 5$ (with a dangerous irrelevant operator).

1.5 On the universality class of the DLG

We said that the rigorous mapping between lattice models and corresponding continuum field theories is rather difficult and seldom rigorously obtained. Then, in principle, every postulated field theory may be questioned. In recent years the field theory (1.21) proposed to describe the physics of DLG has been criticized by some authors. We want here to take a quick survey of this open debate (to which we wish to contribute with our findings [56]).

Episode I: 1986

The theory proposed, from various perspectives, in [27, 26, 25] is based on a Langevin equation for the order parameter, derived from the heuristic arguments we want to describe briefly.

We expect that the description of DLG from a mesoscopic point of view may be formulated in terms of the order parameter which is readily identified in numerical simulation with the scalar field of particle density. Our interest will be in its fluctuations around the mean spatial value (fixed by some initial condition), i.e. in the fluctuating field $\varphi(\boldsymbol{x}, t)$. DLG dynamics is a conservative one: this means that this field satisfies continuity equation

$$\partial_t \varphi + \nabla \cdot \boldsymbol{J} = 0 \quad . \tag{1.23}$$

In the theory of dynamical critical phenomena [5, 6] we assume that $\boldsymbol{J}$, the particel current, is given by Model B [1]:

$$\boldsymbol{J} = -\lambda \nabla \frac{\delta \mathcal{H}}{\delta \varphi} + \boldsymbol{J}_L \quad , \tag{1.24}$$

where λ plays the rôle of a diffusion constant and $\mathcal{H}$ is assumed to be a Ginzburg–Landau–Wilson Hamiltonian (GLW):

$$\mathcal{H} = \int d^d \boldsymbol{x} \left\{ \frac{1}{2} (\nabla \varphi)^2 + \frac{\tau}{2} \varphi^2 + \frac{f}{4!} \varphi^4 \right\} \quad ,$$

where τ is the deviation from a reference temperature T_0, i.e. $\tau \propto T - T_0$. The choice of GLW is due to the fact that it includes all those operators (according to RG classification) that are relevant at the Gaussian fixed point. $\boldsymbol{J}_L$ is a stochastic current that takes into account microscopic fluctuations around the deterministic part of the evolution equation for φ (with $\langle \cdots \rangle$ we mean an average over possible noise realizations),

$$\begin{gathered} \langle J_{L,i}(\boldsymbol{x}, t) \rangle = 0 \quad , \\ \langle J_{L,i}(\boldsymbol{x}, t) J_{L,j}(\boldsymbol{x}', t') \rangle = 2\lambda \delta_{ij} \delta^d(\boldsymbol{x} - \boldsymbol{x}') \delta(t - t') \quad , \end{gathered} \tag{1.25}$$

we assume $\boldsymbol{J}$ to have a Gaussian distribution.

These are standard definitions in the context of weak perturbation around a thermodynamical equilibrium state. For example (1.24) has its meaning in the context of linear response theory [9].

By means of standard manipulations one gets

$$\begin{gathered}\partial_t\varphi = \lambda\Delta\frac{\delta\mathcal{H}}{\delta\varphi} + \nu_L \quad \text{where} \quad \nu_L = -\nabla\cdot\boldsymbol{J}_L \quad \text{and} \\ \langle\nu_L(\boldsymbol{x},t)\rangle = 0 \quad , \\ \langle\nu_L(\boldsymbol{x},t)\nu_L(\boldsymbol{x}',t')\rangle = -2\,\lambda\,\Delta_{\boldsymbol{x}}\delta^d(\boldsymbol{x}-\boldsymbol{x}')\delta(t-t') \quad ,\end{gathered} \tag{1.26}$$

which is exactly Model B. If one now introduces the external field $\boldsymbol{E}$ we expect (a) an additional contribution to $\boldsymbol{J}$ in (1.23), due to the mesoscopic version of enhanced transition in the direction of the field (a sort of "conduction"), of the form $\boldsymbol{J}_E = \sigma(\varphi)\boldsymbol{E}$ (linear approximation is assumed) and (b) anisotropy of diffusion coefficients. The latter means that the breaking of isotropy in the system may give rise to mesoscopic anisotropic coefficients, as it has been showed in [25]. We expect anisotropic expression for GLW as well. In RG language we can say that the anisotropy introduced by the field may drive the RG isotropic fixed point towards an anisotropic one (this means that even the field propagator shows anisotropic scaling).

Taking into account all this factors one ends up with [20]

$$\begin{gathered}\partial_t\varphi = \lambda[\Delta_\perp(\tau_\perp - \kappa_\perp\Delta_\perp) + \rho\Delta_\parallel(\tau_\parallel - \kappa_\parallel\Delta_\parallel) - \kappa\Delta_\parallel\Delta_\perp]\varphi - \boldsymbol{E}\cdot\nabla\sigma(\varphi) + \nu_L \\ \langle\nu_L(\boldsymbol{x},t)\nu_L(\boldsymbol{x}',t')\rangle = -2\lambda(\gamma\Delta_\perp + \varsigma\Delta_\parallel)\delta^d(\boldsymbol{x}-\boldsymbol{x}')\delta(t-t') \quad ,\end{gathered} \tag{1.27}$$

where we assumed a constant $\boldsymbol{E}$. $\parallel$ and $\perp$ subscript means spatial direction parallel and perpendicular to $\boldsymbol{E}$, respectively. All the parameters in this equation are introduced to take into account anisotropy. Let us note that we now have two temperature parameters, namely $\tau_\perp$ and $\tau_\parallel$, which the onset of transverse or longitudinal order depends on. We have, in general

$$\sigma(\varphi) = \sigma_0 + \sigma_1\varphi + \sigma_2\varphi^2 + \cdots \quad , \tag{1.28}$$

by means of symmetry arguments it is easily shown that only σ_2 matters [26]. Now we can discuss the dynamical functional associated with the Langevin equation (1.27) and determine the critical dimensions of its possible fixed points. To this end we take advantage of the classification of operators according their scaling dimensions and behaviour under RG flow into relevant, irrelevant and marginal ones [6]. It is not difficult to realize that the case corresponding to numerically observed ordered state (see Fig. 1.1) is the one giving rise to the dynamic functional (1.21).

Now the question is whether the field-theoretical results obtained from the standard RG analysis of (1.21) agree with numerical data or not.

As we can see from Tab. 1.2, early numerical simulations [47] seemed in agreement with theoretical predictions apart from a quite different value of the critical exponent β (we want to remark that the theoretical result $\beta = 1/2$ may be affected by logarithmic corrections in $d = 2$, given the presence of a marginal field). A better understanding of FSS in anisotropic systems (we discuss this issue in section 2.3), led to a reconciliation between numerics and theory ([39, 40]). Indeed in [39] (whose expanded version is in [40]) it was shown (in a quite clear way) that an effective exponents $\beta_{\text{eff}} \approx 1/3$ may be a consequence of an incorrect FSS, in which one tries to collect on a single scaling plot, data coming from systems with different small shape factor S (see sec. 2.4). In a sense, β_{eff} describes the cross-over to the case $S = 0$. Nevertheless, some doubts remained, and numerical analysis was debated [44, 49].

To have a flavour of such a debate let us have a look at literature. In [42] the main concern is the two–layers DLG[7] but, as a byproduct of their numerical analysis, it is claimed that Leung's results [39, 40] are incorrect, and that correct scaling plots ruled out the value $\beta = 1/2$. A reply to these criticism appear in [43]: There it is shown (using as an example the well–known 2D Ising model) that results in [42] are due to the inclusion in scaling plots of data well outside what we expect to be a reasonable critical region. Subsequent papers bear evidence supporting the standard picture [41] even if discrepancies are still numerically observed [44] (also this last papers deals with two-layer DLG).

Episode II: May 1997

Following a proposed criticism [48] (also supported by some numerical observation [44]) to the widely accepted naïvely determined mesoscopic equation, Garrido, los Santos and Muñoz [49] introduced a new Langevin equation for driven diffusive systems in which the effects of the microscopic dynamics were carefully taken into account. They claimed that the aboved-mentioned discrepancy between field–theoretical results and MC simulations was due to the fact that microscopic DLG master equation and the mesoscopic equation used to analyze critical behaviour in driven diffusive systems were not describing the same physics. In particular the mesoscopic equation derived in [49], has coefficients depending in a quite precise way on microscopic parameters which the dynamics of the underlying lattice model depends on (especially the microscopic driving field $\boldsymbol{E}$), while in the standard case [26, 27] it is not possible to determine this dependence. For finite value of $\boldsymbol{E}$ the

[7] It is defined as the union of a pair of parallel copies of DLG, so that each site in one of them has the corresponding one into the other. Inter–copy jumps are allowed only between corresponding sites, according to Metropolis rate, without any interaction Hamiltonian between copies.

equation of [49] is the same as that of [26, 27][8], they write in the form

$$\partial_t\varphi = \frac{e(0)}{2}\left[-\Delta_\perp(\Delta_\perp - \tau)\varphi + \frac{g}{3!}\Delta_\perp\varphi^3\right] + \\ -\tau h'(E)\Delta_\parallel\varphi - E\,h'(E)\nabla_\parallel\varphi^2 + \sqrt{e(0)}\nabla_\perp\cdot\zeta_\perp \quad , \tag{1.29}$$

where ζ is a δ-correlated gaussian noise, $h'(E)$ is a function of the microscopic field strenght E, and all others are given parameters. The current term is $-E\,h'(E)\nabla_\parallel\varphi^2$.

But for $|\boldsymbol{E}| = \infty$ [9](this case is sometimes called infinitely fast driven lattice gas – IDLG), i.e. when jumps against field are not allowed in the lattice model, a non trivial result is obtained only in the isotropic case (the same scaling for all directions at least naïvely, i.e. $\Delta = 0$ at tree level, see Tab. 1.1), with an upper critical dimension $d_c = 4$ instead of 5, and the equation turns out to be quite different from the previous one:

$$\partial_t\varphi = \frac{e(0)}{2}\left[-\Delta_\perp(\Delta_\perp - \tau)\varphi + \frac{g}{3!}\Delta_\perp\varphi^3\right] + \\ -\tfrac{e(0)}{2}\Delta_\perp\Delta_\parallel\varphi + \sqrt{e(0)}\nabla_\perp\cdot\zeta_\perp + \sqrt{\tfrac{e(0)}{2}}\nabla_\parallel\cdot\zeta_\parallel \quad . \tag{1.30}$$

Indeed the term proportional to the current disappears in the critical theory, showing that *particle current is not a relevant feature of the dynamics*. As a consequence of Eq. (1.30) we expect a different set of critical exponents (although, at variance with the standard case, not exactly computable), resulting also in a *different universality class*.

The observed discrepancy between simulations and theory is then traced back to the fact that the former may be affected by strong cross–over effects between the two possible theories, depending on the value of E used in simulations.

Even though the statements made by authors of [49] are all resonable we have to notice that arguments leading to their conclusions are quite questionable. Their "derivation" of the newly proposed Langevin equation has, to our concern, less rigour than claimed and, moreover, it fails to reproduce some well–established properties of the microscopic model (see [54]).

In a subsequent paper by the same authors [50] details of the new derivation were given in a more extensive way, but again with some quite heuristic assumption.

Then a paper devoted to the RG analysis at one loop of the new model [49] for the IDLG appeared [51]. We checked the calculation reported there and

[8] In some papers, including [49], mesoscopic equations describing a diffusion mechanism coupled to an external drive, as it is the case of DLG equation of [26, 27], are termed driven diffusive systems – DDS.

[9] We want to point out that even if microsopic driving field is infinite, the coarse–grained one may be finite.

found a combinatorics error [52]. Even more severe were the generic IR problems of this theory [52]. Meanwhile a paper appears by other authors bearing evidences against the theory and pointed also out those mistakes [54]. In particular it is easy to realize that equation (1.30) obeys a spurious conservation law [52, 54, 53], given that if one defines a "row density", i.e.

$$\rho_r(x_\parallel, t) := \int d^{d-1}\boldsymbol{x}_\perp \, \varphi(\boldsymbol{x}, t) \quad ,$$

then, after averaging on the noise, it is a conserved quantity $\forall x_\parallel$. This is an additional conservation law which is not present in the original model and it causes the IR problems of the theory (as one easily realize putting the theory on finite volume), and an ill–defined static structure factor (with a line of singularities in momentum space instead of only one point of discontinuity).

Moreover in [54] it was pointed out that Langevin equation in [49] has a symmetry not observed in MC simulations. Indeed the absence of a coupling with external field results in a theory with Ising up–down symmetry (particle–hole symmetry $\varphi \mapsto -\varphi$, i.e. the C-symmetry of Eq. (1.8) for density fields), leading to a vanishing three–point correlation function for all $T \geq T_c$ in disagreement with existing numerical data. Thus, in a sense, mesoscopic theory has an higher degree of symmetry than the microscopic one. This may be justified only showing explicitly that the corresponding fixed point is stable against perturbations by symmetry-breaking operators [54].

Episode III: January 2000

A new paper by Garrido, Muñoz and de los Santos [53], appear to correct the previously proposed Langevin equation, following suggestions and observations of Refs. [52, 54]. By means of heuristic arguments they introduce a new term $\rho\nabla_\parallel\varphi(\boldsymbol{x}, t)$ in the Langevin equation, suitable for healing IR divergencies, and due, in their opinion, to a correct evaluation of the "entropic term" was overlooked in the previous derivation (we are still waiting for an analytic proof of the new term, see Ref. [18] in [53]). This term changes a lot of features of the theory previously proposed in [49]: The naïve (tree level) anisotropic scaling is recovered and, by power–counting analysis, the critical theory (there called *anisotropic diffusive system* – ADS) turns out to be a well–known Langevin equation, i.e. that of the *randomly driven lattice gas* (RDLG). This model was introduced in [31] (and discussed in a detailed way in [32]), to describe, from a mesoscopic point of view, a lattice gas with annealed randomness given by a fluctuating gaussian random driving field (insted of a fixed one, as in the case of standard DLG). The naïve Langevin equation associated with this model has no current term, for obvious symmetry reason: The random field causes anisotropy but not an overall current. The relevant non–linearity is due to a cubic term in s, instead of the usual quadratic one given by the non linear dependence of "conductivity"

$\sigma(\varphi)$ from the density (see Eq. (1.28)), coupled to mesoscopic external field. Then the conclusion of [53] was, again, that at least for the infinite driving field case, the *particle current is not the relevant features of the* DLG. This is due, in their opinion, to a saturation of microscopic transition rates in the Master–Equation, that, in a sense, wipes out any dependence from the precise value of the field and so from the current coupled to it [53]. For the ADS upper critical dimension is $d_c = 3$ (compare to 5 of the standard case, see Tab. 1.1). At variance with microscopic DLG model, the ADS (i.e. RDLG) shows again an up–down symmetry ($\varphi \mapsto -\varphi$) resulting in a vanishing three point correlation function [53, 54], which may be irrelevant at the critical point. Indeed the closely related triangular anisotropies seems to disappear in the limit of large (compared to typical energy scale) external driving field [58, 59].

A brief summary of theoretical predictions of these models is reported in Tab. 1.1.

A contribution to this debate appeared in [55], where an heuristic and approximate scheme is presented to derive the mesoscopic kinetic equations from the microscopic dynamics of the system. The method consists of two steps:

- a mean-field type factorization of joint probabilities, appearing into the Master equation, into single variable ones (i.e. correlations are neglected),
- a naïve continuum expansion, in which probabilities are replaced by the corresponding mesoscopic density fields. In this way a *deterministic* (there is no noise term) kinetic equation for these field is obtained.

By applying this method, it is possible to determine the dependence of mesoscopic parameter from microscopic ones. In [55] 1D, 2D and 3D Ising model with Glauber (i.e. spin flip) dynamics are considered, and quite good estimates for critical temperatures are obtained in the last two cases. The kinetic equation derived is, of course, a time dependent Ginzburg–Landau equation. The case of 1D (with only hard–core interaction) and 2D (with heat–bath rates) DLG is also considered, the latter leading to a deterministic kinetic equation in agreement with standard theory [26, 27, 25]. Even the explicit temperature dependence of the mesoscopic transverse and parallel mass parameters ($\tau_\perp$, $\tau_\parallel$), is in qualitative agreement with what was stated heuristically in [27, 26]. Moreover for $|\boldsymbol{E}| = \infty$ (being $\boldsymbol{E}$ the microscopic field), the relevant non-linearity still come from the coupling of the current with external field, at variance with [53].

Episode IV: June 2001

Recently we concluded our FSS analysis of DLG [56], finding good agreement between numerical results and theoretical predictions of [26, 27]. We

	DLG [26, 27]†	IDLG [51]‡	RDLG [53, 31, 32]
Current	Yes	No	No
Symmetries*	CP, CR, PR	C, P	C, P
d_c	5	4	3
$\eta_\perp^{**}$	0	$O(\epsilon^2)$	$\frac{4}{243}\epsilon^3 + O(\epsilon^4)$
$\nu_\perp^{**}$	$\frac{1}{2}$	$\frac{1}{2} + \frac{\epsilon}{12} + O(\epsilon^2)$	$\frac{1}{2} + \frac{\epsilon}{12} + \frac{\epsilon^2}{18}\left[\frac{67}{108} + \ln\frac{2}{\sqrt{3}}\right] + O(\epsilon^3)$
$z = z_\perp$	4	$4 + O(\epsilon^2)$	$4 - \frac{4}{243}\epsilon^3 + O(\epsilon^4) := 4 - \eta$
β	$\frac{1}{2}$	$\frac{1}{2} - \frac{\epsilon}{6} + O(\epsilon^2)$	$\frac{1}{2} - \frac{\epsilon}{6} + \frac{\epsilon^2}{18}\left[-\frac{7}{54} + \ln\frac{2}{\sqrt{3}}\right] + O(\epsilon^3)$
Δ	$1 + \frac{\epsilon}{3}$	$O(\epsilon^2)$	$1 - \frac{2}{243}\epsilon^3 + O(\epsilon^4) := 1 - \frac{\eta}{2}$

Table 1.1: Theoretical predictions for (transverse) critical exponents for Langevin equations recently proposed to describe DLG. $\epsilon := d_c - d$ where d_c is showed in the table. We define these transformations [58]: $s \overset{C}{\mapsto} -s$, $\boldsymbol{E} \overset{R}{\mapsto} -\boldsymbol{E}$, $\hat{\boldsymbol{x}} \overset{P}{\mapsto} -\hat{\boldsymbol{x}}$. We recall that $\nu_\parallel = (1+\Delta)\nu_\perp$, $z_\parallel = z_\perp/(1+\Delta)$. * We do not indicate the obvious $O(d-1)$ symmetry in transverse space, common to all these models. † Exponents *exactly* known for $2 < d < 5$. ‡ This theory has severe IR problems [52, 54]. ** Exponent inferred from the scaling form in momentum space (for strongly anisotropic systems it differs from that emerging from real space scaling forms, see Ref. [20]).

performed various cross-checks, as discussed in chapter 4, studing a suitably defined correlation length and several observables, defined in section 1.3.

Before entering into details of our work, we have to say that shortly after our paper, a new one by Achahbar, Garrido, Marro and Muñoz [57] appeared supporting their previous conclusions in a surprising way. By means of MC simulation and a suitable anisotropic FSS, they conclude that:"*..., MC results support strongly that both the IDLG and the RDLG belong in the same universality class, and share not only critical exponents and scaling functions, but also the scaling amplitudes*" (quotation from [57]). Summing up, they carried out MC simulations of both RDLG and IDLG, on lattices 20×20, up to 125×50. By using Binder's cumulant crossing method (see section 2.2.1) they determined critical temperatures for both models and then perform an anisotropic FSS analysis (see sections 2.3) for the finite volume magnetization, susceptivity and Binder's cumulant. In order to have a good data collapse (where the goodness is judged by eye inspection) one has to adjust some parameters, whose values are related to critical exponents, as explained in section 2.2.1. Estimated values (though authors do not perform any error analysis, judged to be "*... inessential in this context.*"–quotation from [57]) of critical exponents are in agreement with theoretical ones (even though computed within ϵ–expansion) for RDLG see Tab. 1.1. Moreover,

$d=2$								
	DLG	IDLG	RDLG	MC				
	[26, 27]	[51]	[53]*	[47]	[39]	[44]	[41]	[57]
Δ (†)	2	0	1	0	2	0	$1.98(4)^\ddagger$	~ 1
$\eta_\perp$	0	0	0					
$\nu_\perp$	1/2	2/3	0.626	$0.62(12)^a$	0.5	0.7		0.625
z	4	4	4					
β	1/2	1/6	0.334	0.23(2)	0.5	0.3	$1.00(2)\nu_\perp$	0.33
γ	1	4/3	1.25				$2.03(3)\nu_\perp$	1.22

Table 1.2: Theoretical predictions for (transverse) critical exponents for a two–dimensional DLG (these results come from ϵ–expansion results listed in Tab. 1.1, up to $O(\epsilon^2)$, and naïvely extended to the proper value of ϵ, without any resummation attempts and neglecting possible logarithmic corrections due to marginal operators in $d = 2$), compared to MC results. Remember that $\gamma = \nu_\perp(2 - \eta_\perp)$. * See also [31, 32]. † To perform an anisotropic FSS of MC data, the value of Δ has to be assumed. ‡ Assuming results from [46] it is possible to determine Δ (by using FSS cross-over). Indeed it was found $\nu_\perp/\nu_\parallel = 2.98(4) := 1 + \Delta$. (^{a}) This result is reported in [47] as $0.55^{+0.20}_{-0.05}$.

unexpectedly, FSS functions turns out to be exactly the same for the two models, without having to adjust any amplitude [57].

Episode V: April 2002

Very recently Ref. [61] appeared in the literature, announcing unexpected numerical results and making the statement of Ref. [57], about universality classes, even stronger. At variance with previous studies, the numerical investigation of the DLG and some related models, is there carried out by means of short-time dynamic MC method. This numerical technique has been extensively used to investigate dynamical and static properties of several well-known equilibrium models (see Ref.s [97] for early works and review), giving exponents in good agreement with those obtained by standard MC simulations. The general underlying ideas are related to the short-time universal scaling behaviour observed in relaxation processes starting from a prepared initial condition (fully ordered and completely disordered ones are considered in Ref. [61]). Remarkably enough, short-time MC simulations do not suffer the problem of critical slowing down [97] and even finite-size effects do not play the same rôle as they do in standard MC simulations (at least in the very early stages of relaxation). In Ref. [61] the DLG with finite and infinite driving field (there called FKLS and IKLS, respectively), the RDLG with infinite random field (called IRDLG) and the driven lattice gas

with an oscillatory field [10] (introduced in Ref. [36]) in the limit of infinite field (IOKLS) are studied to clarify the long-standing controversy about the universality class of the DLG. At variance with previous works, the analysis of the numerical results should not be influenced by the problem of the strongly anisotropic FSS, and this should make the results more reliable and not biased by theoretical expectations (no value of the anisotropy exponent Δ is required and, indeed, it is possible to measure it). The main results of this work are

- As a consequence of the short-time scaling forms assumed in the paper, the critical exponents of all the models studied are the same as those predicted by the field-theory of the RDLG [31, 32], while there is a quantitative disagreement with the prediction of Ref.s [27, 26]. Short-time scaling forms differ only for nonuniversal amplitudes.

- The models IKLS, FKLS, with a macroscopic current and IRKLS and IOKLS, without any current, have the same critical exponents, and thus belong to the universality class. This observation support the conclusion of Ref. [57], that the relevant feature of DLG is the anisotropy and not the current (which does not paly any role neither to determine the universality class nor to give rise to strong anisotropy).

First of all we note that these results go well beyond the statements done in Ref. [51, 57]. There it was argued that the IKLS, i.e. the DLG driven with an infinite field, should be in the same universality class as the RDLG, while for finite driving (FKLS) the field-theory of Ref.s [27, 26] should be the correct one to describe critical properties. In a sense the limit of infinite driving was regarded as a singular one. Here the stronger statement is made that in *all the cases* the critical behavior is that of the RDLG.

We remark that the conclusion of this work depend crucially on some assumptions on the short-time scaling forms made in the paper. These generalize in a nontrivial way standard scaling arguments usually done when dealing with short-time scaling forms in finite systems. For example the authors implicitly assume that there is only one exponent $z = z_{\parallel}$, instead of the two standards $z_{\perp}$, $z_{\parallel}$ and thus, depending on the chosen initial condition, $t \sim \tau^{-\nu_{\parallel} z}$, or $t \sim \tau^{-\nu_{\perp} z}$ (t is the typical time scale of the dynamics and τ measures the distance from the critical point). This is not usually the case. In Ref. [61] there is no attempt to justify these unnatural assumptions. Moreover, if one tries to analize the results of this paper following a more reasonable extension of short-time scaling forms [11], one finds these results in disagreement with both proposed field-theoretical descriptions of critical

[10] The field acts along a given lattice axis exactly as in the standard definition of the DLG but its sign is reversed once every 10 MC sweeps [36].

[11] For example keeping in mind that at least in principle $z_{\perp} \neq z_{\parallel}$, as also predicted by field-theoretical approach of both Ref.s [27, 26] and Ref. [57]

properties. We refer to Ref. [61] for the numerical results of that paper, not reported in Table 1.2.

We believe that these unclear aspects of the work reported in Ref. [61] should be clarified before making any statement based on it.

Chapter 2

Finite-size scaling

Phase transitions are characterized by a non-analytic behaviour at the critical point [2, 4, 6]. These non-analyticities are however observed only in the infinite-volume limit. If the system is finite, all thermodynamic functions are analytic in the thermodynamic parameters, temperature, applied magnetic field, and so on. However, even from a finite sample, it is possible to obtain many informations on the critical behaviour. Indeed, large but finite systems show a universal behaviour called finite-size scaling (FSS). The FSS hypothesis, formulated for the first time by Fisher [7, 67, 68] and justified theoretically by using renormalized continuum field theory [66, 71] and conformal field theory (a collection of relevant articles on the subject appears in [73]), is a very powerful method to extrapolate to the thermodynamic limit the results obtained from a finite sample, both in experiments and in numerical simulations. In particular, the most recent Monte Carlo studies rely heavily on FSS for the determination of critical properties (see, e.g., [76, 85, 86, 87, 75, 78, 88, 89, 90] for recent applications in two and three dimensions; the list is of course far from being exhaustive).

2.1 Thermodynamic limit

We will describe FSS in the context of continuous (second-order) phase transitions in systems controlled by a single scalar parameter T which we assimilate to a temperature. We assume the existence of a thermodynamic description of the system in a finite box Λ (e.g. a bounded subset of a discrete lattice where spin-like variables live): given any observable $\mathcal{O}$ we can compute its value on the thermodynamic state determined by T and Λ as

$$\mathcal{O}_\Lambda(T) := \langle \mathcal{O} \rangle_\Lambda(T)$$

where $\langle \cdot \rangle_\Lambda(T)$ is the appropriate averaging. The infinite system is then understood in terms of the *thermodynamic limit*. Given an increasing sequence $\{\Lambda_n\}_n$ of boxes, the value $\mathcal{O}_\infty(T)$ of the observable in the infinite-volume

system is given by

$$\mathcal{O}_\infty(T) := \langle \mathcal{O} \rangle_\infty := \lim_{n\to\infty} \mathcal{O}_{\Lambda_n}(T).$$

Usually this limit exists for a wide class of $\mathcal{O}$ and taking arbitrary shapes for Λ_n. Boundary conditions can influence the limiting procedure in the cases where there are more than one thermodynamical phases coexisting at the same value of T. Moreover in non-equilibrium steady states the thermodynamic limit of certain observables may depend on the shape of the box even in the disordered phase [23, 24].

The correlation length. The existence of the thermodynamic limit is tightly linked to the decay of correlation functions for local observables. In particular, in systems with short-range interactions, the (connected) correlation function

$$G_{\phi,\infty}(x) := \langle \phi(x); \phi(0) \rangle_\infty$$

of a general local observable ϕ has an exponential decay. Equivalently the corresponding Fourier trasform $\widehat{G}_{\phi,\infty}(k)$ (the *structure factor*) is an analytic function of k in a neighborhood of the origin.

It is then possible to define a *exponential* correlation length $\xi^{(\exp)}_{\phi,\infty}$ for ϕ as

$$\xi^{(\exp)}_\infty := -\lim_{|x|\to\infty} \frac{|x|}{\log |G_\infty(x)|},$$

note that a-priori this correlation length will depend also on the direction along which we take the limit $|x| \to \infty$. We will elaborate on this point below.

Another possible definition of infinite-volume correlation length is give by *second moment* correlation length $\xi^{(2)}_{\phi,\infty}$

$$\xi^{(2)}_{\phi,\infty} := \left(\frac{1}{2d} \frac{\sum_x G_\infty(x)|x|^2}{\sum_x G_\infty(x)} \right)^{1/2} = \left[\frac{1}{2d\widehat{G}_\infty(0)} \left. \frac{d^2 \widehat{G}_\infty(q)}{dq_i dq^i} \right|_{q=0} \right]^{1/2}. \quad (2.1)$$

which captures the quadratic behaviour of the inverse structure factor $\widehat{G}_\infty(k)^{-1}$ in the neighborhood of $k = 0$. Of course if $\hat{G}(k)$ happens to be dominated by a single pole the two definitions of correlation length will be stricly related. The simplest example of $\hat{G}_\infty(k)$ is given by the structure factor of the order parameter in isotropic mean-field models where fluctuactions are gaussian and

$$\hat{G}_\infty(k) = \frac{Z}{|k|^2 + \lambda}.$$

In this case $\xi^{(\exp)}_\infty = \xi^{(2)}_\infty = \lambda^{-1/2}$.

In finite volume does not exists a natural definition of correlation length and the exponential correlation length cannot be generalized to finite volume. However, if we consider a finite d-dimensional box Λ of linear sizes $(L_1, \dots, L_d)$ with periodic boundary conditions, the two-point function $G_{\phi,\Lambda}(\boldsymbol{x})$ will be periodic and its Fourier transform $\widehat{G}_{\phi,\Lambda}(\boldsymbol{q})$ will be defined for discrete values of $\boldsymbol{q} = \boldsymbol{q_n} = (2\pi n_1/L_1, \dots, 2\pi n_d/L_d)$. So we can devise definitions that converge to $\xi_\infty^{(2)}$ as $\Lambda \to \infty$: for instance

$$\xi_L^{(2a)} := \left[\frac{\widehat{G}_{\phi,\Lambda}(0) - \widehat{G}_{\phi,\Lambda}(\boldsymbol{q}_{\min})}{\hat{\boldsymbol{q}}^2_{\min} \widehat{G}_{\phi,\Lambda}(\boldsymbol{q}_{\min})} \right]^{1/2},$$

where $\boldsymbol{q}_{\min} = (2\pi/L_1, 0, \dots, 0)$ and

$$\hat{\boldsymbol{q}}^2 = \sum_{i=1}^{d} 4 \sin^2(q_i/2).$$

In general there are $2d$ inequivalent definitions of $q_{\min}$ which give rise to different correlation lengths. When the finite-sistem enjoys cubic symmetry it is possible to show that this definition converges to $\xi_\infty^{(2)}$ (which is intrinsically isotropic).

The definition is motivated by the desire to have, also for finite L, the same relation between ξ and λ in the case of mean-field models (or, more concretely, in mean-field approximations to interacting theories). Indeed, in this case, we would have

$$\widehat{G}_L(\boldsymbol{q}) = \frac{Z_L}{\hat{\boldsymbol{q}}^2 + \lambda_L}$$

so that

$$\xi_L^{(2a)} = \lambda_L^{-1/2},$$

exactly. However, equally valid definitions would be

$$\xi_L^{(2b)} := \left[\frac{\widehat{G}_{\phi,\Lambda}(\boldsymbol{0}) - \widehat{G}_{\phi,\Lambda}(\boldsymbol{q}_{\min})}{\hat{\boldsymbol{q}}^2_{\min} \widehat{G}_{\phi,\Lambda}(\boldsymbol{0})} \right]^{1/2},$$

which gives

$$\xi_L^{(2b)} = \left(\lambda_L + \hat{\boldsymbol{q}}^2_{\min}\right)^{-1/2},$$

or

$$\xi_L^{(2c)} := \left[\frac{\widehat{G}_{\phi,\Lambda}(\boldsymbol{0}) - \widehat{G}_{\phi,\Lambda}(\boldsymbol{q}_{\min})}{\hat{\boldsymbol{q}}^2_{\min} (2\widehat{G}_{\phi,\Lambda}(\boldsymbol{q}_{\min}) - \widehat{G}_{\phi,\Lambda}(\boldsymbol{0}))} \right]^{1/2},$$

which gives

$$\xi_L^{(2c)} = \left(\lambda_L - \hat{\boldsymbol{q}}^2_{\min}\right)^{-1/2}.$$

For $L \to \infty$ at T fixed (i.e. $\lambda_L \to \lambda_\infty$ asymptotically constant)

$$\xi_L^{(2a)} \approx \xi_L^{(2b)} \approx \xi_L^{(2c)} \to \xi_\infty^{(2)},$$

so that all of them recover the correct thermodynamic limit, but a relevant issue is whether all of them have the correct FSS properties. In Ref. [95] we study the large-N limit of the N-vector model, and we show the existence of several constraints on the definition of the finite volume correlation length if regularity of the finite-size scaling functions and correct anomalous behaviour above the upper critical dimension are required. Moreover these constraints also ensure the correct behaviour taking into account logarithmic corrections at the upper critical dimension [96]. Then, we study in detail the N-vector model ($N \mapsto \infty$) in which the zero mode is dynamically constrained, as it is the case of the lattice gas. Also in this case, we find that the finite-volume correlation length must meet some requirements in order to obtain regular finite-size scaling functions, and, above the upper critical dimension, an anomalous scaling behaviour.

Critical singularities. When $T \to T_c$ there are quantities $\mathcal{O}_\infty$ which behave as

$$\mathcal{O}_\infty(t) \sim |t|^{-x_\mathcal{O}} \qquad \text{for } t \to 0 \tag{2.2}$$

where $t{:=}(T - T_c)/T_c$ is the reduced temperature and where $\sim$ means that $|t|^{x_\mathcal{O}}\mathcal{O}_\infty(t)$ has a finite limit as $t \to 0$. Along with these diverging quantities it is possible to identify a distinguished local operator ϕ (the order parameter) for which the associated exponential correlation length $\xi_\infty{:=}\xi_{\phi,\infty}^{(\exp)}$ diverges as

$$\xi_\infty \sim |t|^{-\nu}. \tag{2.3}$$

If the exponent ν characterizing the diverging correlation length does not depend on the direction along which ξ is measured we will say that the system undergoes an *isotropic* phase transition (note that this does not means that the system itself is isotropic); otherwise the phase transition will be *anisotropic*.

Usually in the isotropic case $\xi_{\phi,\infty}^{(2)}$ has a singular behaviour described by the same exponent ν. This can be easily understood on a dimensional ground assuming that ξ_∞ is the only relevant scale of length in the neighborhood of the phase transition point.

As we already remarked, in the finite systems all thermodynamic functions have an analytic dependence on control parameters which means that the interchange of the infinite-volume limit with the limit $t \to 0$ is in general not permitted:

$$\lim_{t\to 0}\lim_{\Lambda\uparrow\infty} |t|^{x_\mathcal{O}}\mathcal{O}_\Lambda(t) \neq \lim_{\Lambda\uparrow\infty}\lim_{t\to 0} |t|^{x_\mathcal{O}}\mathcal{O}_\Lambda(t) = 0$$

if, for example, $x_{\mathcal{O}} > 0$.

FSS theory predicts the asymptotic shape of the function $\mathcal{O}_\Lambda(t)$ when $\Lambda \to \infty$ and $t \to 0$ in a well-determined fashion. We will review the phenomenological approach to FSS theory [67, 69] for isotropic (or weakly anisotropic) phase transitions with the aim of extending the results to the anisotropic case, relevant to our analysis of the critical behaviour of the DLG. Note that, in the context of DLG, a phenomenological approach to FSS has been discussed in [47], keeping into account the strong anisotropy observed in the transition (for $d = 2$ see Refs. [41, 40, 46], for $d = 3$ see Refs. [45]).

2.2 Isotropic FSS

In the case of isotropic phase transitions a natural way of taking the infinite-volume limit is to consider boxes of size L in all directions. Denote the corresponding averages with $\langle\cdot\rangle_L$. When $t \to 0$ there is a (essentially unique) correlation length ξ which diverges. If L is large and if there are not other characteristic lengths of magnitude comparable to that of ξ or L [1] we can write $\mathcal{O}_L(t)$ as a function of $\xi_\infty(t)$ and L:

$$\begin{aligned} \mathcal{O}_L(t) &\approx F_{\mathcal{O},0}(\xi_\infty(t), L) = \xi_\infty(t)^{y_{\mathcal{O}}} F_{\mathcal{O},0}(1, L/\xi_\infty(t)) \\ &= \xi_\infty(t)^{y_{\mathcal{O}}} F_{\mathcal{O},1}(\xi_\infty(t)/L) \end{aligned} \tag{2.4}$$

where $\approx$ means equality modulo terms which are asymptotically negligible as $L, \xi_\infty \to \infty$. Indeed it is clear that, being ξ_∞ and L the only dimensionful quantities present, the function $F_{\mathcal{O},0}(x, y)$ must be an homogeneous function whose degree $y_{\mathcal{O}}$ can be determined by letting $L \to \infty$ with ξ_∞ fixed:

$$\mathcal{O}_\infty(t) = \lim_{L\to\infty} \mathcal{O}_L(t) = \xi_\infty(t)^{y_{\mathcal{O}}} F_{\mathcal{O},1}(0) \sim |t|^{-y_{\mathcal{O}}\nu}$$

giving $y_{\mathcal{O}} = x_{\mathcal{O}}/\nu$. Note that the existence of a finite limit for $F_{\mathcal{O},1}(z)$ when $z \to 0$ depends on two main assumptions:

i) the existence of a well defined thermodynamic limit for the quantity $\mathcal{O}_L$;

ii) the possibility to interchange the FSS limit with the thermodynamic limit.

While the first of these assumptions depends only on the observable, the validity of the second assumption depends also on the specific way the FSS limit is attained as we will explore below (chap. 3). For the time being we

[1] If it is not the case we have *violations* of FSS and hyperscaling relations fail, generally because of dangerously irrelevant operators [8]

will assume both of them and the reader must realize that many results of FSS rely crucially on their validity.

Another way of rephrasing eq. (2.4) is

$$\mathcal{O}_L(t) \approx L^{x_\mathcal{O}/\nu} F_{\mathcal{O},2}\left(\frac{\xi_\infty(t)}{L}\right), \tag{2.5}$$

for $L \to \infty$ with $z{:=}\xi_\infty/L$ constant, where $F_{\mathcal{O},2}(z)$ has a finite limit for $z \to \infty$ and

$$F_{\mathcal{O},2}(z) \sim |z|^{x_\mathcal{O}/\nu} \qquad \text{for } z \to 0.$$

For a good finite-volume definition of correlation length ξ_L we obtain similarly

$$\xi_L(t) \approx L F_{\xi,2}\left(\frac{\xi_\infty(t)}{L}\right) \tag{2.6}$$

since in this case $x_\xi = \nu$. Moreover

$$\lim_{z\to 0+} \frac{F_{\xi,2}(z)}{z} = 1.$$

2.2.1 Asymptotic FSS

The functional relation expressed by eq. (2.5) cannot be direclty used to analyze simulation (or experimental) data since usually the infinite-volume correlation length is an unknown quantity – inaccessible, if we are not able (or do not want) to perform the infinite volume limit. A very common approach to overcome this problem is that of substituting the asymptotic expression of ξ_∞ as a function of t in (2.5) resulting in:

$$\mathcal{O}_L(t) \approx L^{x_\mathcal{O}/\nu} G_\mathcal{O}\left(tL^{1/\nu}\right). \tag{2.7}$$

The function $g_\mathcal{O}(z)$ is finite and non-vanishing in zero, and should satisfy[2]

$$g_\mathcal{O}(z) \sim |z|^{-x_\mathcal{O}} \qquad \text{for} \quad z \to \infty. \tag{2.8}$$

In eq. (2.7) only accessible quantities appear: t can be tuned by the experimentalist while $\mathcal{O}_L(t)$ is directly measurable. Even if the (infinite-volume) correlation length does not shows up explicitly it is always lurking in the background as witnessed by the presence of the related critical exponent ν. This form of FSS relies heavily on the knowledge of the critical temperature T_c (present in the definition of t). In this approach there are two widely used tecniques to locate T_c from finite-sample data: the first is to study the shape of some quantity like the finite-volume susceptibility χ which in

[2]Note that the behaviour of $|z|^{x_\mathcal{O}} g_\mathcal{O}(z)$ for $z \to \infty$ is not directly related to the finite-size corrections to $\mathcal{O}_L(t)$ for $L \to \infty$ at t fixed in the limit of small t. See the detailed discussion in Refs. [91].

infinite volume diverges at T_c while in finite-volume has a peak whose size grows with L, by eq. (2.7) we have

$$\chi_L(T) \approx L^{\gamma/\nu} G_\chi(tL^{1/\nu})$$

where $\gamma = x_\chi$ as usual. Then if we call $T_c(L)$ the value of T for which $\xi_L(T)$ attains its maximum we have

$$T_c(L) \approx T_c + T_c u^* L^{-\omega}$$

where $u^* = \text{argmax}_u G(u)$ and $\omega = \min(1/\nu, 1)$. Then using an extrapolation it is possible to locate T_c. The second widely used method is more closely related to FSS and is based on the observation that in many systems it is possible to find an observable $\mathcal{O}$ such that $x_\mathcal{O} = 0$, that is without scaling dimension. For example, for systems in the universality class of the φ^4 field theory, we can define an adimensional ratio of moments of the order parameter Φ like the *Binder's cumulant* [70] g defined, for instance, as

$$g := \frac{\langle \Phi^4 \rangle}{\langle \Phi^2 \rangle^2}. \tag{2.9}$$

FSS predicts for g the following behaviour ($x_g = 0$)

$$g_L(T) \approx G_g(tL^{1/\nu}). \tag{2.10}$$

with $G_g(u) \to 0$ for $u \to +\infty$ and $G_g(u) \to G(-\infty)$ finite for $u \to -\infty$. When $t = 0$ we have $g_L(T_c) \approx G_g(0)$: the critical temperature can be located by looking at the value of T such that $g_L(T)$ is independent of L. If $G_g(0) > 0$ this independence shows up in the form of the crossing of the plots of $g_L(T)$ as a function of T for various values of L. The value of T for which this crossing occours is then T_c.

Once we know T_c we can find the critical exponents though eq. (2.7) which says that there is a well defined functional dependence between $y = L^{-x_\mathcal{O}/\nu}\mathcal{O}_L$ and $x = tL^{1/\nu}$. We can then try to estimate values of $x_\mathcal{O}$ and ν such that the set of points (x_n, y_n) gathered from experiments collapse on a single curve irrespective of T and L. Of course this can approximately happen only for T near enough at T_c (for the scaling hypotesis to hold) and for L large enough (so that corrections to FSS are small): this is the *critical region*.

2.2.2 Correlation length FSS

Following e.g. [75], instead of replacing ξ_∞ with t in FSS relations we can proceed by inverting the functional relation expressed by eq. (2.6) to obtain

$$\frac{\xi_\infty}{L} \approx F_{\xi,3}\left(\frac{\xi_L}{L}\right). \tag{2.11}$$

Plugging this in eq. (2.5) we obtain a relationship which relates only quantities directly measurable in finite systems:

$$\mathcal{O}_L(t) \approx L^{x_\mathcal{O}/\nu} F_{\mathcal{O},3}\left(\frac{\xi_L(t)}{L}\right). \tag{2.12}$$

Taking the ratio of $\mathcal{O}_L$ at two different sizes L and αL we get

$$\frac{\mathcal{O}_{\alpha L}(t)}{\mathcal{O}_L(t)} \approx F_\mathcal{O}\left(\frac{\xi_L(t)}{L}\right), \tag{2.13}$$

where the (unknown) ratio $x_\mathcal{O}/\nu$ disappears.

Let $z = \xi_L/L$ and define

$$z^* = F_{3,\xi}(\infty). \tag{2.14}$$

The value z^* is directly related to the behavior of the finite-size correlation length at the critical point, since $\xi_L(\beta_c) \approx z^* L$. For ordinary phase transitions z^* is finite.

The knowledge of the FSS functions F_ξ and $F_\mathcal{O}$ (whatever the observable $\mathcal{O}$ is) allow the determination of the exponents ν and $x_\mathcal{O}$ without any knowledge of the critical temperature. Indeed, at the critical point (wherever it is), it holds

$$\mathcal{O}_L(\beta_c) \sim L^{\gamma_\mathcal{O}/\nu}. \tag{2.15}$$

Then, it must be

$$F_\mathcal{O}(z^*) = \frac{\mathcal{O}_{\alpha L}(\beta_c)}{\mathcal{O}_L(\beta_c)} = \alpha^{\gamma_\mathcal{O}/\nu}, \tag{2.16}$$

and therefore

$$\frac{\gamma_\mathcal{O}}{\nu} = \frac{\log F_\mathcal{O}(z^*)}{\log \alpha}. \tag{2.17}$$

where z^* is determined solving the equation $F_\xi(z^*) = \alpha$. Now, if we let $u = tL^{1/\nu}$, $z = \xi_L/L$, then $z = G_\xi(u)$ and

$$\begin{aligned}\frac{d}{du}F_\xi(z) &\approx \frac{d}{dz}\frac{\xi_{\alpha L}}{\xi_{\alpha L}} \approx \alpha \frac{d}{du}\frac{G_\xi(\alpha^{1/\nu}u)}{G_\xi(u)} \\ &= \alpha^{1+1/\nu}\frac{G'_\xi(\alpha^{1/\nu}u)}{G_\xi(u)} - \alpha\frac{G_\xi(\alpha^{1/\nu}u)\,G'_\xi(\alpha^{1/\nu}u)}{G_\xi(u)^2}.\end{aligned}$$

The Taylor expansion for $F_\xi(z)$ around z^* (that is, around $u = 0$) is

$$\begin{aligned}F_\xi(z) &= F_\xi(z^*) + \left[\left(\frac{dz}{du}\right)^{-1}\frac{dF_\xi(z)}{du}\right]_{z=z^*}(z - z^*) + \mathrm{O}((z-z^*)^2) \\ &= \alpha\left(1 + (\alpha^{1/\nu} - 1)\left(\frac{z}{z^*} - 1\right)\right) + \mathrm{O}((z-z^*)^2)\end{aligned}$$

since $G_\xi(0) = z^*$. We conclude that the exponent ν can be recovered from the FSS function F_ξ as

$$z\frac{d}{dz}\log F_\xi(z)\bigg|_{z=z^*} = \alpha^{1/\nu} - 1. \tag{2.18}$$

Another very powerful application of FSS in the form of eq. (2.13) is to the determination of the thermodynamic limit for the observables. Assume we know F_ξ and $F_\mathcal{O}$ for $\alpha > 1$ and that we measure ξ_L and $\mathcal{O}_L$ from a finite simple of size L and we are in a regime where FSS it is proven to hold (up to negligible corrections). Then using eq. (2.13) we can compute the values of $\xi_{\alpha L}$ and $\mathcal{O}_{\alpha L}$ as

$$\xi_{\alpha L} = \xi_L F_\xi\left(\frac{\xi_L}{L}\right) \qquad \mathcal{O}_{\alpha L} = \mathcal{O}_L F_\mathcal{O}\left(\frac{\xi_L}{L}\right)$$

which means that we are able also to predict $\xi_{\alpha^n L}$ and $\xi_{\mathcal{O}^n L}$ for arbitary n until the limiting values ξ_∞ and $\mathcal{O}_\infty$ are attained (up to numerical and statistical errors).

The shape factor. FSS is a statement about the behaviour of the thermodynamic quantities as $L, \xi_\infty \to \infty$ with $z = \xi_\infty/L$ (or equivalently $u = tL^{1/\nu}$) constant. This holds true provided the only length scale characterizing the finite box is L. If however the system is in a box with two different linear sizes L, M then by extending the previous arguments it is possible to argue that all the FSS functions depend also on the *shape factor* $S = M/L$, e.g.

$$\begin{aligned}\mathcal{O}_{L,M}(t) &\approx F_{\mathcal{O},0}(\xi_\infty(t), L, M)\\ &= \xi_\infty(t)^{y_\mathcal{O}} F_{\mathcal{O},0}(1, L/\xi_\infty(t), M/\xi_\infty(t))\\ &= \xi_\infty(t)^{y_\mathcal{O}} F_{\mathcal{O},1}(\xi_\infty(t)/L, S)\\ &= L^{y_\mathcal{O}} F_{\mathcal{O},2}(\xi_\infty(t)/L, S).\end{aligned}$$

At the critical point we get, for example,

$$\chi_{L,M}(T_c) = L^{\gamma/\nu} F_{\chi,2}(0, S) = (LM)^{\gamma/2\nu} F_{\chi,4}(S)$$

where $F_{\chi,4}(x)$ is a distinguished function such that $F_{\chi,4}(x) = F_{\chi,4}(1/x)$ using the isotropy assumption (even if the model itself is not isotropic we can argue starting from a microscopically isotropic model in the same universality class). This prediction is confirmed by conformal field theory for two dimensional models (and can be verified by exact computations both in $O(\infty)$ vector-model and in the $2d$ Ising model).

2.3 Anisotropic FSS

In intrinsically anisotropic systems it could happens that the (infinite-volume, exponential) correlation length diverges at the critical point with different critical exponents in different directions[3]. Some examples are uniaxial systems with strong dipolar forces [5], the Kasteleyn model of dimers on the brick lattice [74][4], anisotropic Lifshitz points and, of course, field theories associated to driven-diffusive systems and (by numerical evidences) the KLS model. An analogous situation is that of dynamic critical behaviour where there are two different exponents related the decay of correlations in the spatial and temporal directions.

Consider an anisotropic system in which there exists a local observable Ψ (the order parameter) for which two different exponential correlation lengths exist: $\xi_{\parallel,\infty}$ in the direction of the first coordinate axis and $\xi_{\perp,\infty}$ in the directions transverse to that axis. Let us assume that these correlation lengths diverge at criticality with different exponents, resp. $\nu_\parallel$ and $\nu_\perp$, in particular

$$\xi_{\parallel,\infty}(t) \sim \xi_{\perp,\infty}(t)^{1+\Delta}$$

with $\Delta = \nu_\parallel/\nu_\perp - 1$.

In the specific case of DLG, continuum field theories introduced (see sec. 1.5) to describe its critical singularities predicts indeed a nontrivial *anisotropy exponent* Δ (see tab. 1.1). For example, the scaling form of the critical two-point function for the DLG should have the form (see eq. (1.22) in section 1.4, and section 2.5)

$$\tilde{G}(\boldsymbol{k}_\perp, k_\parallel) \approx \mu^{-2+\eta}\tilde{G}(\mu\boldsymbol{k}_\perp, \mu^{1+\Delta}k_\parallel), \tag{2.19}$$

where η is the anomalous dimension of the order parameter.

In a finite box of sizes (M, L), where M is the linear dimension in the direction of the first axis and L that in the perpendicular directions, we can argue that a generic long-range observable $\mathcal{O}$ will behave as

$$\mathcal{O}_{M,L}(t) \approx \xi_{\perp,\infty}^{x_\mathcal{O}/\nu_\perp} F_{\mathcal{O},\perp,1}\left(\frac{\xi_{\perp,\infty}(t)}{L}, S_\Delta\right) \tag{2.20}$$

where we introduced the *anisotropic shape factor* $S_\Delta = M/L^{1+\Delta}$ which should be kept constant while performing the limit $\xi_\perp, \xi_\parallel, L, M \to \infty$. To justify this FSS form we need strong assumptions, in particular it is not really clear why there appears the ratio $z = \xi_{\perp,\infty}/L$ and not e.g. $\xi_{\perp,\infty}/L^\rho$

[3] These systems are called *strongly anisotropic* in the literature to distinguish them from those *weakly anisotropic* systems in which the microscopic anisotropy is an irrelevant perturbation of the critical theory and has effects only on the non-universal metric factors which appears in the scaling laws near criticality [20].

[4] Here the presence of strong anisotropies in the critical regime is probed by indirect means.

for some $\rho \neq 1$. In section **(Quale?)** we will discuss some examples in which this is indeed the right form for anisotropic FSS.

Here we would like to give a simple heuristic argument to support our conjecture. Assume the generic FSS form

$$\mathcal{O}_{M,L}(t) \approx \xi_{\perp,\infty}^{x_{\mathcal{O}}/\nu_\perp} F_{\mathcal{O},\perp,1}\left(\frac{\xi_{\perp,\infty}(t)}{L^\rho}, S_\delta\right) \tag{2.21}$$

with δ and ρ possibly different from what we expect. The function $F_{\mathcal{O},\perp,1}(x,s)$ is assumed to have a *regular* (i.e. finite and non-zero) limit for $x \to 0$ and s fixed and moreover that the themodynamic limit can be interchanged with the FSS limit. This imply necessarily that the prefactor in eq. (2.21) should be $\xi_{\perp,\infty}^{x_{\mathcal{O}}/\nu_\perp}$.

If we let $S_\delta \to \infty$ in eq. (2.21) keeping $z_\rho = \xi_{\perp,\infty}(t)/L^\rho$ constant we expect that the limit is regular and given by

$$\mathcal{O}_{M,L}(t) \approx \xi_{\perp,\infty}^{x_{\mathcal{O}}/\nu_\perp} F_{\mathcal{O},\perp,1}\left(z_\rho, \infty\right). \tag{2.22}$$

since in this case we are sending $M \to \infty$ faster than what required to keep S_δ constant and thus the finite-size effects associated with M should disappear in the limit. Moreover this limit should coincide with the FSS form of the system in the strip geometry (∞, L):

$$\mathcal{O}_{\infty,L}(t) \approx \xi_{\perp,\infty}^{x_{\mathcal{O}}/\nu_\perp} F_{\mathcal{O},\perp}^{\text{strip}}(z).$$

which is obtained by sending first $M \to \infty$ and then performing the FSS limit (with z constant – here appears $z = z_1$ since only one finite lenght L it is present in the strip geometry). so that

$$F_{\mathcal{O},\perp,1}\left(z_\rho, \infty\right) = F_{\mathcal{O},\perp}^{\text{strip}}(z).$$

which implies that $\rho = 1$ and $F_{\mathcal{O},\perp,1}\left(x, \infty\right) = F_{\mathcal{O},\perp}^{\text{strip}}(x)$. By an analogous argument another regular limit is obtained for $S_\delta \to 0$ in the FSS form

$$\mathcal{O}_{M,L}(t) \approx \xi_{\parallel,\infty}^{x_{\mathcal{O}}/\nu_\parallel} \widetilde{F}_{\mathcal{O},\parallel,1}\left(\frac{\xi_{\parallel,\infty}}{L^{\rho(1+\Delta)}}, S_\delta\right) = \xi_{\parallel,\infty}^{x_{\mathcal{O}}/\nu_\parallel} F_{\mathcal{O},\parallel,1}\left(\frac{\xi_{\parallel,\infty}}{M^{\rho_1}}, S_\delta\right). \tag{2.23}$$

obtained from (2.21) with the substitution $\xi_{\parallel,\infty} \sim \xi_{\parallel,\infty}^{1+\Delta}$ and where $\rho_1 = \rho(1+\Delta)/(1+\delta)$, giving

$$F_{\mathcal{O},\parallel,1}\left(\frac{\xi_{\parallel,\infty}}{M^{\rho_1}}, 0\right) = F_{\mathcal{O},\parallel}^{\text{strip}}\left(\frac{\xi_{\parallel,\infty}}{M}\right). \tag{2.24}$$

where $F_{\mathcal{O},\parallel}^{\text{strip}}$ is the FSS function associated to the vertical strip (M, ∞) by

$$\mathcal{O}_{M,\infty}(t) \approx \xi_{\parallel,\infty}^{x_{\mathcal{O}}/\nu_\parallel} F_{\mathcal{O},\parallel}^{\text{strip}}\left(\frac{\xi_{\parallel,\infty}}{M}\right). \tag{2.25}$$

Then eq. (2.24) implies that $\rho_1 = 1$ and $F_{\mathcal{O},\|,1}(x,0) = F^{\text{strip}}_{\mathcal{O},\|}(x)$. As a conclusion we get $\rho = 1$ and $\delta = \Delta$.

As we have seen in the previous section on isotropic FSS, the FSS ansatz eq. (2.20) can be used to estimate universal quantities from the analisys of finite-sample data. In the isotropic situation a common way to proceed is to gather data from experiments in boxes of linear size L in all directions. This procedure is guaranteed by the fact that all the geometries taken into account have the same (isotropic) shape factor $S = S_0$ which is simply the ratio of linear sizes in (two) different directions[5]

In the application of FSS to anisotropic critical phenomena a key difficulty if that of find out the right shape of the finite-sistems to keep S_Δ constant and being able to apply eq. (2.20). Indeed the exponent Δ is not known in advance and there arise the problem of understanding what happens to FSS when we do not keep S_Δ constant in the limiting procedure.

2.4 Shape mismatch

Assume the FSS limit is performed keeping constant S_δ with $\delta \neq \Delta$. What happens? Depending on being $\delta > \Delta$ or $\delta < \Delta$ we have that $S_\Delta \to 0$ or $S_\Delta \to \infty$, respectively. Then we are led to study the asymptotic behaviour of FSS forms like eq. (2.20). We already remarked that in some cases we expect that the limit will behave in a regular way (i.e. that the FSS functions have a regular limit): see for example eq. (2.22). However we do not expect this to be always true. Let $S_\Delta \to 0$ in the FSS form (eq. (2.20)):

$$\mathcal{O}_{M,L}(t) \approx \xi_{\perp,\infty}^{x_\mathcal{O}/\nu_\perp} F_{\mathcal{O},\perp,1}\left(\frac{\xi_{\perp,\infty}(t)}{L}, S_\Delta\right). \tag{2.26}$$

That this limit cannot be regular is implied by the assumed regularity of the limiting FSS when $z_\| = \xi_\|/M$ is kept constant (eq. (2.23)). Indeed, if we assume that the limit for $S_\Delta \to 0$ of eq. (2.26) is regular we should have

$$\mathcal{O}_{M,L}(t) \approx \xi_{\perp,\infty}^{x_\mathcal{O}/\nu_\perp} F_{\mathcal{O},\perp,1}\left(\frac{\xi_{\perp,\infty}(t)}{L}, 0\right).$$

where if we let $L \to \infty$ we obtain (assuming there are no problems in taking the thermodynamic limit at this point)

$$\mathcal{O}_{M,\infty}(t) \approx \xi_{\perp,\infty}^{x_\mathcal{O}/\nu_\perp} F_{\mathcal{O},\perp,1}(0,0)$$

which does not make any sense in view of eq. (2.25).

[5] In general in a d-dimensional box with linear sizes $L_1, \ldots, L_d$ there are $d-1$ isotropic shape factors $S^{(i)} = L_{i+1}/L_i$, $i = 1, \ldots, d-1$ which appears in FSS functions.

So we are led to conjecture (cfr. Leung [39, 40], Binder and Wang [46]) that the limit $S_\Delta \to 0$ in eq. (2.26) leads to multiplicative singularities in the form

$$\mathcal{O}_{M,L}(t) \approx \xi_{\perp,\infty}^{x_\mathcal{O}/\nu_\perp} S_\Delta^{\alpha_1} F^{\#}_{\mathcal{O},\perp}\left(\frac{\xi_{\perp,\infty}(t)}{L} S_\Delta^{\alpha_2}\right). \tag{2.27}$$

that, after a comparision with eq. (2.23), leads to the identifications $\alpha_1 = 0$, $\alpha_2 = -1/(1+\Delta)$ and $F^{\#}_{\mathcal{O},\perp}(x^{1/(1+\Delta)}) = F^{\text{strip}}_{\mathcal{O},\parallel}(x)$. Note a small subtlety of this reasoning: the two limits involved are different, the strip limit is obtained for M fixed and $L \to \infty$ keeping $\xi_\perp/M^{1/(1+\Delta)}$ fixed while this second limit was obtained keeping $\xi_\perp/L$ fixed while sending L to infinity faster than $M^{1/(1+\Delta)}$. Another charactertistic of this result is that the FFS function $F^{\#}_{\mathcal{O},\perp}$ does not depend on the specific value of δ (as long as $\delta > \Delta$).

This arguments are confirmed by the exact computations in chap. 3 where the case of shape mismatch in the FSS limit of the $O(\infty)$ model with short and long range anisotropic interactions is considered.

Another confirmation is given by extact computations of Bhattacharjee and Nagle [74] for the Kasteleyn model of dimers on the brick lattice. This model is isomorphic to an anisotropic domain-wall model and features generic long-range correlations in the disordered phase due to a conservation law and a second-order phase transition. Note however that this is a genuinely equilibrium system. They found that in a finite box of sizes $2N \times 2M$, where $2N$ is the number of lattice sites in the direction perpendicular to the preferred axis for the domain walls and $2M$ is the size of the transverse direction, the specific heat $C_{N,M}(t)$ as a function of the reduced temperature t takes the asymptotic form

$$C_{N,M}(t) \approx \mathcal{M}^{1/2} \mathcal{P}(t\mathcal{M}, \mathcal{S}) \tag{2.28}$$

where

$$\mathcal{S} = \frac{N^2}{M} \qquad \mathcal{M} := M\frac{\mathcal{S}}{1+\mathcal{S}} = \frac{MN^2}{M+N^2}$$

And where the function $\mathcal{P}(x,y)$ has well defined limits for $y \to 0$ and $y \to \infty$. When $\mathcal{S} \to 0$ we have $\mathcal{M} \to N^2$ while for $\mathcal{S} \to \infty$ we obtain $\mathcal{M} \to M$, correspondingly the FSS function converges to the FSS function in the geometry $2N \times \infty$ or $\infty \times 2M$ respectively. A remarkable feature is that no other nontrivial FSS limits are possible. So in case of shape mismatch the systems behaves effectively as a stripe for what concerns FSS.

Note that the anisotropic FSS theory envisaged by Binder and Wang in [46] has essentially the same features (when hyperscaling holds). By euristic arguments they find that in two-dimensional anisotropic models in a finite box with periodic boundary conditions we should have at criticality:

$$\chi(T_c) \propto L_\perp^{\gamma/\nu_\perp} \qquad \text{for } S_\Delta \to \infty,$$

and

$$\chi(T_c) \propto L_{\parallel}^{\gamma/\nu_{\parallel}} \qquad \text{for } S_\Delta \to 0.$$

as expected using eq. (2.27).

2.5 Field-theory of the DLG in a finite box

In section 1.4 we explain why a lattice model as the DLG may be described, in the critical region, with suitable field theories, outlining its derivation in section 1.5. Here we want to draw further conclusions from the theory (1.21).

For the structure factor the renormalization-group analysis gives the scaling form (see Eq. (1.22))

$$\tilde{G}(k_\parallel, \boldsymbol{k}_\perp; \tau) = \mu^{-2+\eta} \tilde{G}(k_\parallel \mu^{-1-\Delta}, \boldsymbol{k}_\perp \mu^{-1}; \tau \mu^{-1/\nu}), \tag{2.29}$$

where, in d dimensions (see Tab. 1.1),

$$\eta = 0, \tag{2.30}$$

$$\nu = \frac{1}{2}, \tag{2.31}$$

$$\Delta = \frac{1}{3}(8-d), \tag{2.32}$$

and $\tau \propto T - T_c$. In two dimensions, for the transverse structure factor, this implies the simple scaling form

$$\tilde{G}_\perp(\boldsymbol{k}; \tau) = \tau^{-1} f(|\boldsymbol{k}|^2/\tau). \tag{2.33}$$

Thus, in infinite volume we have, by using definition (1.18),

$$\xi_{ij} \sim \tau^{-\nu}, \qquad \chi \sim \tau^{-\gamma}, \tag{2.34}$$

where ν is given in Eq. (2.31) and

$$\gamma = 1. \tag{2.35}$$

The function $f(x)$ defined in Eq. (2.33) is trivial. Indeed, keeping into account causality and the form of the interaction vertex one can see that for $k_\parallel = 0$ there are no loop contributions to the two-point function (and also to the response function $\langle \tilde{\varphi}_0 \varphi_{\boldsymbol{x}} \rangle$). Thus, for all $2 \le d \le 5$, $\tilde{G}_\perp(k, \tau)$ is simply given by the tree-level expression

$$\tilde{G}_\perp(\boldsymbol{k}; \tau) = \frac{1}{|\boldsymbol{k}|^2 + \tau}. \tag{2.36}$$

Two observation are here in order. First it is usually assumed that τ is an analytic function of t such that $\tau = 0$ for $t = 0$; thus, $\tau = bt$ for $t \to 0$ with

b positive constant. Second, the function that appears in Eq. (2.36) refers to the coarse-grained fields, which, in the critical limit, differ by a finite renormalization from the lattice ones. Thus, for the lattice function we are interested in, in the scaling limit $t \to 0$, $k \to 0$, with $|\boldsymbol{k}|^2/t$ fixed, we have

$$\tilde{G}_{\perp,\mathrm{latt}}(\boldsymbol{k};t) = \frac{Z}{|\boldsymbol{k}|^2 + bt}, \tag{2.37}$$

where Z and b are positive constants. Eq. (2.37) implies the exponential decay of

$$G_{\perp,\mathrm{latt}}(\boldsymbol{x}_\perp;t) = \int d^{d-1}\boldsymbol{k}\, e^{i\boldsymbol{k}\cdot\boldsymbol{x}_\perp}\ \tilde{G}_{\perp,\mathrm{latt}}(\boldsymbol{k};t), \tag{2.38}$$

which fully justifies our definition of transverse correlation length.

In section 4.2, we study the FSS behaviour of the model by means of numerical simulations. Here, we want to analyze the corresponding continuum field theory in a finite geometry following the method applied in equilibrium spin systems (see, e.g. ref. [5, chap. 36] and references therein). The idea is quite simple. Consider the system in a finite box with periodic boundary conditions. The finite geometry has the only effect of quantizing the momenta. Thus, the perturbative finite-volume correlation functions are obtained by replacing momentum integrals by lattice sums. Ultraviolet divergences are not affected by the presence of the box [66] and thus one can use the infinite-volume renormalization constants [71, 72]. Once the renormalization is carried out, geometry-dependent finite-size correlation functions are obtained.

Following this idea, if we consider a finite box of size $L_\parallel \times L_\perp^{d-1}$, Eq. (2.29) becomes

$$\tilde{G}(k_\parallel, \boldsymbol{k}_\perp; \tau; L_\parallel, L_\perp) = \mu^{-2}\tilde{G}(k_\parallel \mu^{-1-\Delta}, \boldsymbol{k}_\perp\mu^{-1}; \tau\mu^{-2}; L_\parallel\mu^{-1-\Delta}, L_\perp\mu^{-1}), \tag{2.39}$$

which shows that at $T = T_c$

$$\xi_{ij}(T_c) \sim L_\perp, \qquad\qquad \chi(T_c) \sim L_\perp^{\gamma/\nu} \sim L_\perp^2. \tag{2.40}$$

Moreover, Eq. (2.36) holds in finite volume. Keeping again into account the relation between coarse-grained and lattice quantities, we obtain for the lattice correlation function in a finite volume in the continuum limit (i.e. in the FSS limit with $\boldsymbol{k} \to 0$ keeping $|\boldsymbol{k}|^2/t$ fixed)

$$\tilde{G}_{\perp,\mathrm{latt}}(\boldsymbol{k};t;L_\parallel,L_\perp) = \frac{Z(t;L_\parallel,L_\perp)}{|\boldsymbol{k}|^2 + \tau(t;L_\parallel,L_\perp)}, \tag{2.41}$$

where Z and τ are analytic functions of their arguments. In the FSS limit, we expect

$$Z(t;L_\parallel,L_\perp) = \tilde{Z}(tL_\perp^2, S_\Delta), \tag{2.42}$$

$$\tau(t;L_\parallel,L_\perp) = L_\perp^{-2}\,\tilde{\tau}(tL_\perp^2, S_\Delta). \tag{2.43}$$

Using these expressions, in the FSS limit we find

$$\frac{\xi_{13}(t;L_\parallel,L_\perp)}{L_\perp} = \left((2\pi)^2+\tilde\tau(tL_\perp^2,S_\Delta)\right)^{-1/2}, \tag{2.44}$$

$$A_{13} := \frac{\xi_{13}^2(t;L_\parallel,L_\perp)}{\chi(t;L_\parallel,L_\perp)} = \left[\tilde Z(tL_\perp^2,S_\Delta)\right]^{-1}, \tag{2.45}$$

valid for $t\to 0$, $L_\parallel, L_\perp\to\infty$ with S_2 and $tL_\perp^2$ fixed. Therefore, from the scaling of the correlation length and of the amplitude A_{13} we can derive the scaling functions $\tilde Z$ and $\tilde\tau$.

If we make the simplest approximations

$$\tilde Z(tL_\perp^2,S_\Delta)=\text{const} \qquad \text{and} \qquad \tilde\tau(tL_\perp^2,S_\Delta)= \text{ const } \times tL_\perp^2,$$

we obtain for the scaling functions defined in eq. (2.13) the approximate forms

$$F_\xi(z) = \left[1-\left(1-\alpha^{-2}\right)(2\pi)^2 z^2\right]^{-1/2}, \tag{2.46}$$

$$F_\chi(z) = F_\xi^2(z) = \left[1-\left(1-\alpha^{-2}\right)(2\pi)^2 z^2\right]^{-1}. \tag{2.47}$$

As we shall see, these expressions provide reasonably good approximations to our data, but do not describe the data exactly: The functions $\tilde\tau$ and $\tilde Z$ that are determined from the data are nontrivial (see chap. 4).

As we know from the field-theoretical analysis, a peculiarity of this model is the presence of an operator which is dangerously irrelevant for $2<d<5$ and becomes marginal at $d=2$ (recall that scaling dimensions of the operators at the fixed-point are knows at all orders in the ϵ-expansion). Is this operator which fix the magnetization exponent to its mean-field value of $\beta=1/2$. It is well known that a dangerous irrelevant operator may cause violation of FSS, e.g.: the $O(N)$ vector model above four dimensions [66, 71]. Some care should be exercized to treat it in the proper way.

In general the presence of this dangerous operator could modify the scaling relations (2.29), (2.33), and (2.39). Considering, for example, $\tilde G_\perp(k)$ we have

$$\tilde G_\perp(\boldsymbol{k};\tau;L_\parallel,L_\perp;u) = L_\perp^2\tilde G_\perp\left(\boldsymbol{k}L_\perp;\tau L_\perp^2;L_\parallel/L_\perp^{1+\Delta},1;L_\perp^{-2\sigma}u\right), \tag{2.48}$$

where $\sigma=(d-2)/3$ and u is the coupling of the dangerous operator. If the function $\tilde G_\perp(k;\tau;L_\parallel,L_\perp;u)$ is singular for $u\to 0$ then we cannot neglect the contributions coming form the irrelevant operator. To understand the effects of the dangerous operator on the FSS behaviour we will parallel the analysis of Brezin and Zinn-Justin [71] of the FSS behaviour of the $O(N)$-vector model above four dimensions.

At the fixed point the eigenoperator A associated with the irrelevant coupling is [26]

$$uA = \widetilde\varphi\Delta_\perp(u_1\dot\varphi + u_2\Delta_\perp^2 + u_3\varphi^3) \tag{2.49}$$

so that the renormalized dynamic functional near the fixed-point has the form

$$\mathcal{J}(\tilde{\varphi},\varphi) \simeq \mathcal{J}_*(\tilde{\varphi},\varphi) + uA + O(u^2)$$

where $\mathcal{J}_*$ is the fixed point dynamic functional and we neglected all the other irrelevant operators. Let $\psi := \varphi(\boldsymbol{k}_{0,1})$, $\tilde{\psi} := \tilde{\varphi}(\boldsymbol{k}_{0,1})$ (when $d > 2$ choose one of the equivalent modes).

$$e^{-\Sigma(\tilde{\psi},\psi)} = \int' e^{-\mathcal{J}(\tilde{\varphi},\varphi)} d\tilde{\varphi} d\varphi$$

where the prime on the integration is to remember to leave out the modes corresponding to $\psi, \tilde{\psi}$. At the leading order we can simply neglect all the other $\boldsymbol{k} \neq \boldsymbol{k}_{0,1}$ modes and obtain

$$\begin{aligned}\Sigma(\tilde{\psi},\psi) = L_\perp^{d-1} L_\parallel \tilde{\psi} \Big\{ & (1 + u_1 \boldsymbol{k}_{0,1}^2)\dot{\psi} \\ & + \boldsymbol{k}_{0,1}^2 \left[(\boldsymbol{k}_{0,1}^2 + \tau + u_2 \boldsymbol{k}_{0,1}^4)\psi + u_3 |\psi|^2 \psi \right] + n_\perp \boldsymbol{k}_{0,1}^2 \tilde{\psi} \Big\}\end{aligned}$$

This effective dynamic functional can be exaclty integrated to give the stationary probability distribution of ψ

$$P(\psi) = Z^{-1} \exp(-S_{\text{eff}}(\psi)) d\psi \tag{2.50}$$

with

$$S_{\text{eff}}(\psi) = L_\perp^{d-1} L_\parallel \left[\frac{1}{2} (\boldsymbol{k}_{0,1}^2 + \tau + u_2 \boldsymbol{k}_{0,1}^4) |\psi|^2 + \frac{u_3}{4} |\psi|^4 \right] \tag{2.51}$$

Let

$$E_n = \langle |\psi|^n \rangle = \frac{\int |\psi|^n \exp(-S_{\text{eff}}(\psi)) d\psi}{\int \exp(-S_{\text{eff}}(\psi)) d\psi} = (u_3/4)^{-n/4} M_n \left(\frac{\boldsymbol{k}_{0,1}^2 + \tau + u_2 \boldsymbol{k}_{0,1}^4}{\sqrt{u_3}} \right)$$

Using RG arguments (see [71]) we know that we can compute the distribution of ψ in the box $(L_\parallel, L_\perp)$ using the box of transverse lenght $L_\perp = 1$ by substituting $t \mapsto t L_\perp^2$, $u \mapsto u L_\perp^{-2\sigma}$ and $\varphi \mapsto L_\perp^{(d-1+\eta)/2} \varphi$:

$$\begin{aligned} S_{\text{eff}}(\psi) &= S_\Delta \left[\frac{1}{2} ((2\pi)^2 + \tau L^2 + u_2 L_\perp^{-2\sigma} (2\pi)^4) |\psi|^2 + \frac{u_3 L_\perp^{-2\sigma}}{4} |\psi|^4 \right] \\ &= S_\Delta \left[\frac{1}{2} ((L_\perp/\xi_L)^2 + u_2 L_\perp^{-2\sigma} (2\pi)^4) |\psi|^2 + \frac{u_3 L_\perp^{-2\sigma}}{4} |\psi|^4 \right] \end{aligned} \tag{2.52}$$

and

$$\begin{aligned} E_n &= L_\perp^{n(d-1+\eta-\sigma)/2} (u_3/4)^{-n/4} M_n \left(\sqrt{S_\Delta} \frac{(L_\perp/\xi_L)^2 + u_2 L^{-2\sigma} (2\pi)^4}{\sqrt{u_3 L_\perp^{-2\sigma}}} \right) \\ &= L_\perp^{nd/2} (u_3/4)^{-n/4} M_n \left(\sqrt{S_\Delta} \frac{(L_\perp/\xi_L)^2 L^\sigma + u_2 L_\perp^{-\sigma} (2\pi)^4}{\sqrt{u_3}} \right) \end{aligned} \tag{2.53}$$

Note that in the high temperature region ξ_L/L is bounded from above by $1/2\pi$ uniformly and for $L_\perp \to \infty$ we are allowed to approximate

$$\frac{(L_\perp/\xi_L)^2 L^\sigma + u_2 L_\perp^{-\sigma}(2\pi)^4}{\sqrt{u_3}} \approx \frac{(L_\perp/\xi_L)^2 L^\sigma}{\sqrt{u_3}}$$

which goes to infinity if we keep ξ_L/L fixed. Then, in the FSS limit, we obtain

$$\begin{aligned} E_n &\approx L_\perp^{nd/2}(u_3/4)^{-n/4} M_n\left(\frac{(L_\perp/\xi_L)^2 L^\sigma}{\sqrt{u_3}}\right) \\ &\approx L_\perp^{nd/2}(u_3/4)^{-n/4}\left(\frac{(L_\perp/\xi_L)^2 L^\sigma}{\sqrt{u_3}}\right)^{-n/2} \\ &\propto L_\perp^{n(d-1+\eta)/2}(L_\perp/\xi_L)^{-n} \end{aligned} \tag{2.54}$$

which means that the dangerous irrelevant coupling of the infinite-volume theory is actually not dangerous – and can be asimptotically neglected – for what concerns the FSS behaviour of the model in the disordered phase. Note that this is a peculiarity which stems from the absence of the zero mode[6].

For $d = 2$ the dangerous operator becomes marginal and we loose the control on the scaling behaviour of the field theory. However, if we assume that the operator will be marginally irrelevant (as it seems the case from the results of chap. 4), then the above considerations apply, provided we substitute for the factors $L_\perp^\sigma$ the true asymptotic behaviour of the operator: e.g. logaritms in the form $(\log L_\perp)^a$ for some, unknown, power $a > 0$. This suggest that, in numerical simulations, can be hard to test the asymptotic regime described by eq. (2.54). To analize the possible presence of these logaritmic corrections we note that the values E_n, in the approximation we considered, are functions of the ratio

$$z^\# := \frac{(L_\perp/\xi_L)^2 Y_L + u_2 Y_L^{-1}(2\pi)^4}{\sqrt{u_3}}$$

where there are unknown amplitudes u_2 and u_3 and where $Y_L = L_\perp^\sigma$ for $2 < d < 5$ and maybe $Y_L = \log(L_\perp)^a$ with $a > 0$ for $d = 2$. Adimensional ratios of E_ns should be functions of $z^\#$: in particular

$$g_L = 2 - \frac{\langle|\psi|^4\rangle}{\langle|\psi|^2\rangle^2} = 2 - \frac{M_4(z^\#)}{M_2(z^\#)^2} =: M_g(z^\#) \tag{2.55}$$

and

$$X_L := L_\perp^{d-1} L_\parallel \frac{m^2}{\chi} = \frac{\langle|\psi|\rangle^2}{\langle|\psi|^2\rangle} = \frac{M_1(z^\#)^2}{M_2(z^\#)} =: M_X(z^\#). \tag{2.56}$$

[6]In the corresponding treatment of the $O(N)$ model above four dimensions instead of xi_L^2/L^2 we would have tL^2 which cannot be bounded away from zero uniformly in all the high-T region.

This analisys shows that for $2 < d < 5$ the standard observables we considered (like g, χ, m) should not show anomalous finite-size behaviour. This is ultimately due to the absence of the zero mode which allows the perturbative handling of perturbations of the gaussian effective theory for the transverse modes. This feature has been overlook in literature (see [46, 40]) where it was assumed that, above two dimensions, the dangerously irrelevant operator should induce violations of FSS even in the high-T region. The analysis of the finite-size behaviour of the model in the low-temperature phase should, of course, take into account the rôle of the dangerous operator in stabilizing the order parameter. At this time we feel that a deeper understanding of FSS behaviour of models without zero modes above their upper critical dimension is needed. To our knowledge, apart from our work on the proper definition of correlation lenght [95], only a work of Eisenriegler and Tomaschiz [93] on the ϕ^4 model with fixed magnatization below the upper critical dimension deals with finite-volume effects without zero mode.

Chapter 3

Shape mismatch in the $O(\infty)$ model

In this chapter we analyze the finite-size scaling behaviour of the $O(N)$-vector model in the $N \to \infty$ limit where the model is exaclty solvable [5]. This model has been a classical example in FSS investigations, starting from the seminal work of Brezin [66]. Recently a very nice book on FSS [98] analized systematically finite-size effects in the spherical model (equivalent to the $O(\infty)$ vector model) for a wide range of modifications, including presence of long-range correlations and of boundary effects. We will consider a general class of $O(\infty)$ models which includes the classical isotropic short-range and long-range cases but also models where the correlation function decay with different power-laws in different lattice directions. This will induce a strongly anisotropic phase transition. For these models we analyze the effects on FSS functions of shape mismatch, i.e. of using finite boxes with arbitrary shape factors. As we will see, our result will confirm the phenomenological picture outlined in sec. 2.4.

3.1 The models

Let us recall in this section some basic facts about the model we are going to study. We consider a d-dimensional hypercubic lattice Λ of finite extent M in the first q directions (called the "parallel" directions) and L in the remaining p directions (with $d = q + p$) volume $V = M^q L^p$ and unit N-vector spins $\boldsymbol{\sigma}$ defined at the sites of the lattice interacting with Hamiltonian

$$\mathcal{H} = -N \sum_{\boldsymbol{x},\boldsymbol{y}} J(\boldsymbol{x} - \boldsymbol{y}) \boldsymbol{\sigma}_{\boldsymbol{x}} \cdot \boldsymbol{\sigma}_{\boldsymbol{y}} - Nh \sum_{\boldsymbol{x}} \sigma^1_{\boldsymbol{x}}, \tag{3.1}$$

where $J(\boldsymbol{x})$ is a coupling potential whose Fourier transform $\widehat{J}(\boldsymbol{q})$ has the asymptotic form

$$\widehat{J}(\boldsymbol{q}) \simeq \widehat{J}(\boldsymbol{0}) + |\boldsymbol{q}_\perp|^{2\rho} + |\boldsymbol{q}_\parallel|^{2\sigma}, \qquad \text{for } |\boldsymbol{q}| \to 0$$

with $0 < \sigma \leq 1$. The partition function is simply

$$Z = \int \prod_{\boldsymbol{x}} [d\boldsymbol{\sigma}_{\boldsymbol{x}}\, \delta(\boldsymbol{\sigma}_{\boldsymbol{x}}^2 - 1)]\; e^{-\beta \mathcal{H}}. \tag{3.2}$$

In tha large-N limit, assuming periodic boundary conditions and $h = 0$, the theory is solved in terms of the gap equations ($\beta = 1/T$)

$$\lambda_V \sigma_V = 0, \qquad \beta = \beta \sigma_V^2 + \frac{1}{L^p M^q} \sum_{\boldsymbol{q} \in \Lambda_V^*} \frac{1}{K(\boldsymbol{q}) + \lambda_V}, \tag{3.3}$$

where $K(\boldsymbol{q}) = -2(\widehat{J}(\boldsymbol{q}) - \widehat{J}(\boldsymbol{0}))$ and Λ_V^* is the lattice

$$\Lambda_V^* = \left(2\pi M^{-1}\, \mathbb{Z}_M^q, 2\pi L^{-1}\, \mathbb{Z}_L^p, \right). \tag{3.4}$$

In the infinite volume, the same equations holds, with the simple substitution of the summation with the normalized integral over the first Brillouin zone $[-\pi, \pi]^d$.

The meaning of the parameters λ_V and σ_V is clarified by considering the magnetization and the two-point function. If $\langle \cdot \rangle_V$ is the mean value for a system of volume V, we define

$$M_V = \langle \sigma^1 \rangle_V, \qquad G_V(\boldsymbol{x}) = \langle \boldsymbol{\sigma}_{\boldsymbol{0}} \cdot \boldsymbol{\sigma}_{\boldsymbol{x}} \rangle_V. \tag{3.5}$$

Then

$$M_V = \sigma_V, \qquad \widehat{G}_V(\boldsymbol{q}) = \frac{\beta^{-1}}{K(\boldsymbol{q}) + \lambda_V}, \tag{3.6}$$

where $\widehat{G}(q)$ is the Fourier transform of $G(x)$. As we show in sec. A.2 the correlation function, in the thermodynamic limit, has the form

$$G_\infty(\boldsymbol{x}) = \xi_\perp^{\rho(2-D)} \widetilde{G}_\infty(\boldsymbol{x}_\perp / \xi_{\perp,\infty}, \boldsymbol{x}_\parallel / \xi_{\parallel,\infty})$$

where

$$\xi_{\perp,\infty} = \lambda_\infty^{-1/2\rho}, \qquad \xi_{\parallel,\infty} = \lambda_\infty^{-1/2\sigma}.$$

So even if the model has long-range correlations in the high-T phase it is sensible to look at $\xi_{\perp,\infty}$ and $\xi_{\parallel,\infty}$ as appropriate typical length-scales of the system. For simplicity we will refer to them respectively as transverse and longitudinal correlation lenghts. They are linked by the obvious relation

$$\xi_{\parallel,\infty} = \xi_{\perp,\infty}^{\rho/\sigma}$$

and in the following we will write $\xi_\infty := \xi_{\perp,\infty}$. The critical point is characterized by a vanishing mass gap, i.e. $\xi_\infty^{-1} = 0$ and by vanishing magnetization, $\sigma_\infty = 0$ so that critical temperature is given by (see Eq. (3.3))

$$\beta_c = \int_{-\pi}^{\pi} \frac{d^d \boldsymbol{p}}{(2\pi)^d} \frac{1}{K(\boldsymbol{p})} \tag{3.7}$$

which is finite whenever the effective dimensionality $D := p/\rho + q/\sigma$ is greater than 2 and infinite for $D \leq 2$ (the system undergoes a zero-temperature phase transition). Moreover, given we will be interested in finite volume properties, we have $M_V = 0$, for all values of β, so that we can set $\sigma_V = 0$ in the gap equation.

3.2 Anisotropic FSS

We do not address here the problem of the definition of a finite volume correlation length and we will use simply

$$\xi_{\perp,V} = \lambda_V^{-1/2\rho}, \qquad \xi_{\parallel,V} = \lambda_V^{-1/2\sigma}.$$

Both $\xi_\perp$ and $\xi_\parallel$ have an infinite volume limit $\xi_{\perp,\infty}$ and $\xi_{\parallel,\infty}$ respectively so they are bona-fide finite-volume correlations lenghts. For brevity ξ_V will mean $\xi_{\perp,V}$.

In the appendix A we show that, in the limit where $L, M \to \infty$ with $z = (4\pi)^{-\rho/2}(L/\xi_V)^\rho$ and $S = M/L^{\rho/\sigma}$ constant, the gap equation take the form

$$(4\pi)^{\rho+(d-\rho D)/2}(\beta - \beta_c)L^{\rho(D-2)} = -(4\pi)^{\rho d/2}A + I(z, S) \tag{3.8}$$

where $\beta = 1/T$, β_c is given in Eq. (3.7). Then we can take $\Delta = \sigma/\rho - 1$ so that $S = S_\Delta$. Moreover the two-point function, in the FSS limit with $|\boldsymbol{x}_\perp|/L$ and $|\boldsymbol{x}_\parallel|/M$ constant, becomes (cfr. eq. (A.7))

$$G_V(\boldsymbol{x}) \approx \xi_\perp^{\rho(2-D)} \widetilde{G}_\infty(\boldsymbol{x}_\perp/\xi_{\perp,V}, \boldsymbol{x}_\parallel/\xi_{\parallel,V}, S, \xi_{\perp,V}/L).$$

Now a simple question arises: is it possible to have a nontrivial FSS function even if the scaling is performed keeping constant the anisotropic aspect ratio

$$S_\delta = \frac{M}{L^{1+\delta}}$$

(we set, in the following $S_\delta = 1$) with $\delta \neq \Delta$? We consider in the following only the case $\delta > 0$, given that the case $-1 < \delta < 0$ is obtained performing, in the formulas below, the substitutions

$$p \leftrightarrow q, \quad L \leftrightarrow M, \quad \rho \leftrightarrow \sigma, \quad \delta \to -\delta/(1+\delta).$$

If S_δ is kept constant ($\delta > \Delta$), we have $S_\Delta \to \infty$ for $L \to \infty$. As shown sec. A.3, in this limit and for $D > 2$ the gap equation takes the form

$$\begin{aligned}(4\pi)^{\rho+(d-\rho D)/2}(\beta - \beta_c)L^{\rho(D-2)} &= -(4\pi)^{\rho d/2}Az^{D-2} \\ &+ r^{\sigma-q/2}\mathcal{J}_1(z^2 r^\sigma) + \mathcal{J}_2(z^2) + C_{\sigma,p}\int_1^{r^\sigma} dt\, e^{-z^2 t} t^{-q/2\sigma}\end{aligned} \tag{3.9}$$

where β_c is given in Eq. (3.7), $r = (4\pi)^{\rho/\sigma-1}S^2$ and

$$\begin{aligned}\mathcal{J}_1(x) &= \frac{e^{-x}}{x} + \mathcal{G}_{\sigma,q}(x)\\ \mathcal{J}_2(x) &= -C_{\sigma,q}C_{\rho,p}\int_1^\infty dt\, t^{-D/2}e^{-xt} + \mathcal{G}_{\rho,p}(x)\end{aligned} \tag{3.10}$$

where

$$\mathcal{G}_{\sigma,q}(x) := \int_1^\infty dt\, e^{-xt}\left[B^q(\tau_t) - 1\right] + \int_0^1 dt\, e^{-xt}\tau_t^{-q/2}\left[B^q\left(\tau_t^{-1}\right) - 1\right].$$

In Eq. (3.9) we have to explicit the dependence of the last term on the variables z and zS. We have

$$\int_1^{r^\sigma} e^{-z^2t}t^{-q/2\sigma}\,dt = \begin{cases} z^{-2+q/\sigma}\displaystyle\int_0^{r^\sigma z^2} e^{-t}t^{-q/2\sigma}\,dt - \int_0^1 e^{-zt}t^{-q/2\sigma}\,dt \\ \qquad\qquad\qquad\qquad \text{for } 0 < q/\sigma < 2 \\ \displaystyle\int_1^\infty e^{-z^2t}t^{-q/2\sigma}\,dt - r^{\sigma-q/2}\int_1^\infty e^{-r^\sigma z^2t}t^{-q/2\sigma}\,dt \\ \qquad\qquad\qquad\qquad \text{for } q/\sigma \geq 2 \end{cases} \tag{3.11}$$

Then, according to the fact that $0 < q/\sigma < 2$ or otherwise, we are led to two different forms of the gap equation suitable for taking limits:

- $0 < q/\sigma < 2$: the gap equation is

$$\begin{aligned}(4\pi)^{\rho+(d-\rho D)/2}(\beta-\beta_c)L^{\rho(D-2)} &= -(4\pi)^{\rho d/2}Az^{D-2} + r^{\sigma-q/2}\mathcal{J}_1(z^2r^\sigma)\\ &+ \mathcal{J}_2(z^2) - C_{\sigma,p}\int_0^1 e^{-zt}t^{-q/2\sigma} + C_{\sigma,p}z^{-2+q/\sigma}\int_0^{r^\sigma z^2} e^{-t}t^{-q/2\sigma}\,dt\end{aligned} \tag{3.12}$$

- $q/\sigma \geq 2$: in this case, instead

$$\begin{aligned}(4\pi)^{\rho+(d-\rho D)/2}(\beta-\beta_c)L^{\rho(D-2)} &= -(4\pi)^{\rho d/2}Az^{D-2} + \mathcal{J}_2(z^2)\\ &+ C_{\sigma,p}\int_1^\infty e^{-z^2t}t^{-q/2\sigma}\,dt\\ &+ r^{\sigma-q/2}\left[\mathcal{J}_1(z^2r^\sigma) - C_{\sigma,p}\int_1^\infty e^{-r^\sigma z^2t}t^{-q/2\sigma}\,dt\right]\end{aligned} \tag{3.13}$$

Scaling M as $L^{1+\delta}$ corresponds to consider more and more elongated geometries, in which the first q dimensions approaches infinity faster than the remaining p. Two possible interesting limits should be considered (we recall that $z \sim (L/\xi_V)^\rho$, $zS^\sigma \sim (M/\xi_{\|,V})^\sigma$)

(a) If one keeps constant, doing the FSS limit, the ratio $\xi_V/L \sim z^{-1/\rho}$, then we expect the final "effective" geometry should be $\infty^q \times L^p$ and the FSS be that of a "layer". In terms of the parameters appearing in the previous expressions this limt corresponds to

$$zS^\sigma \to \infty, \qquad z \text{ constant};$$

(b) Also $\xi_{\parallel,V}/M$ can be kept constant in FSS. The expected "effective" geometry should be that of an q-dimensional hypercube with linear size M ($M^q \times 0^p$), and thus we should observe the corresponding FSS. This limits corresponds to

$$zS^\sigma \text{ constant}, \qquad z \to 0.$$

3.3 $\xi_V \sim L$

Assume that $0 < q/\sigma < 2$. Consider the term $r^{\sigma-q/2}\mathcal{J}_1(r^\sigma z^2)$, we have

$$r^{\sigma-q/2}\mathcal{J}_1(r^\sigma z^2) \sim \begin{cases} r^{\sigma-q/2}e^{-r^\sigma z^2} & \text{for } \sigma = 1 \\ r^{\sigma-q/2}(r^\sigma z^2)^{-2} & \text{for } 0 < \sigma < 1 \end{cases}$$

and thus is negligible in this limit with respect to the others terms. Moreover (given that $zS \to \infty$)

$$\begin{aligned} z^{-2+q/\sigma}\int_0^{r^\sigma z^2} e^{-t}t^{-q/2\sigma}\,dt &= z^{-2+q/\sigma}\int_0^\infty e^{-t}t^{-q/2\sigma}\,dt + \cdots \\ &= \int_0^\infty e^{-z^2 t}t^{-q/2\sigma}\,dt + \cdots \end{aligned}$$

thus the gap equation becomes

$$4\pi(\beta-\beta_c)L^{d-2} = -(4\pi)^{\rho d/2}Az^{D-2} + \mathcal{J}_2(z^2) + C_{\sigma,p}\int_1^\infty e^{-z^2 t}t^{-q/2\sigma}\,dt \quad (3.14)$$

which is, as expected, the gap equation for a layered geometry $\infty^q \times L^p$. From the scaling form, the exponent ν is easily identified as $1/\nu = D-2$, expected for a bulk system in D (effective) dimensions. Note that for $q/\sigma > 2$, taking into account Eq (3.13) and the fact that the last two terms are exponentially small for $zS \to \infty$, the gap equation is exactly the same as eq. (3.14), as expected.

3.4 $\xi_{\parallel,V} \sim M$

Case $0 < q/\sigma < 2$

We observe that $\mathcal{J}_2(z^2)$ has a finite limit for $z \to 0$. The same is true for the second integral on the r.h.s. of Eq. (3.11). The gap equation is Eq. (3.12),

i. e.

$$(4\pi)^{\rho+(d-\rho D)/2}(\beta-\beta_c)L^{\rho(D-2)} = -(4\pi)^{\rho d/2}Az^{D-2} + r^{\sigma-q/2}\mathcal{J}_1(z^2r^\sigma) + \mathcal{J}_2(z^2) - C_{\sigma,p}\int_0^1 e^{-zt}t^{-q/2\sigma} + C_{\sigma,p}z^{-2+q/\sigma}\int_0^{r^\sigma z^2} e^{-t}t^{-q/2\sigma}\,dt \tag{3.15}$$

Given that $z \to 0$, the last term on the r.h.s. is greater than the sum of those on the first line of r.h.s., at least when

$$\frac{z^{2-q/\sigma}}{C_{\sigma,p}}\left|-(4\pi)^{\rho d/2}Az^{D-2} + \mathcal{J}_2(z^2) - C_{\sigma,p}\int_0^1 e^{-zt}t^{-q/2\sigma}dt\right| \ll \int_0^{r^\sigma z^2} e^{-t}t^{-q/2\sigma}\,dt$$

so that the gap equation may be rewritten in the form

$$(4\pi)^{\rho+(d-\rho D)/2}(\beta-\beta_c)L^{\rho(D-2)}r^{q/2-\sigma} = \mathcal{J}_1(z^2r^\sigma) + C_{\sigma,p}(r^\sigma z^2)^{q/2\sigma-1}\int_0^{r^\sigma z^2} e^{-t}t^{-q/2\sigma}\,dt \tag{3.16}$$

We note, first, that this scaling is possible only for $\beta > \beta_c$, given the r.h.s. is a positive function. Given that M is scaled according to $M \sim L^{1+\delta}$, then an effective exponent $\tilde{\nu}(\delta)$ can be identified from the power of M on the l.h.s.

$$L^{D-2}r^{q/2-\sigma} \sim M^{\frac{\rho(D-2)+(\delta-\Delta)(q-2\sigma)}{1+\delta}}$$

giving

$$\frac{1}{\tilde{\nu}(\delta)} = \frac{\rho/\nu_D + (\delta-\Delta)\sigma/\nu_{q/\sigma}}{1+\delta} \tag{3.17}$$

where $\nu_d^{-1}{:=}d-2$ is the exponent of a d-dimensional system (at least when $d > 2$). Moreover the gap equation can be rewritten as (see app. A)

$$(4\pi)^{\rho+(d-\rho D)/2}(\beta-\beta_c)L^{1/\tilde{\nu}(\delta)} = \int_0^\infty dt\,\Psi_\sigma(r^\sigma z^2 t)t^{-q/2\sigma}B^q\left(t^{-1/\sigma}\right) \tag{3.18}$$

Which has the same form of the gap equation for an hypercubic systems with geometry M^q (i.e. $(p=0)$) when $q/\sigma < 2$ (i. e. below the l.c.d. of the model):

$$(4\pi)^\sigma\beta M^{q-2\sigma} = \int_0^\infty dt\,\Psi_\sigma(r^\sigma z^2 t)t^{-q/2\sigma}B^q\left(t^{-1/\sigma}\right). \tag{3.19}$$

The FSS properties in this particular limit are influenced by the exponent with which the scaling is performed. In the limit of small δ the standard

scaling exponent is recovered. For $\delta \to \infty$, a sort of crossover towards a finite q-dimensional systems occours, as one could naïvely expect. Note, however, that we have assumed $q/\sigma < 2$, that is the eventual effective geometry has a dimensionality below the lower critical dimension of the reduced model, and we have $\nu_{q/\sigma}^{-1} < 0$. As a consequence the FSS is singular when $\tilde{\nu}^{-1}(\delta) = 0$, i.e. $\delta = \rho(D-2)/(2\sigma - q) > 0$.

Thermodynamic limit

We observe that Eq. (3.15) may be rewritten as

$$(\beta - \beta_c) M^{\tilde{\nu}^{-1}(\delta)} = \Phi_0(M/\xi_{\parallel,V}) + S^{q-2\sigma}\Phi_1(L/\xi_V) \tag{3.20}$$

If $M/\xi_{\parallel,V}$ is kept constant (as in the scaling we are interested in), given that $\Phi_1(x) \sim 1$ for $x \to 0$, the second term on r.h.s.

$$S^{q-2\sigma}\Phi_1(L^\rho/\xi_V) = S^{q-2\sigma}\Phi_1(M^\sigma/\xi_V S^{-1}) \sim S^{q-2\sigma}$$

is negligible compared to the first one for $L, M \to \infty$, so the FSS form

$$(\beta - \beta_c) M^{\tilde{\nu}^{-1}} = \Phi_0(M/\xi_{\parallel,V}) \tag{3.21}$$

holds. This scaling form is apparently inconsistent with the requirement of a well-defined infinite volume limit. Indeed to cancel out, for ξ finite ($\beta \neq \beta_c$) and $M \to \infty$, the dependence on M, we have to suppose that $\Phi_0(x) \sim x^{1/\tilde{\nu}}$ for $x \to \infty$, so that $\xi_\infty \sim (\beta - \beta_c)^{-\tilde{\nu}}$, in contrast with the expected thermodynamic limit $\xi_{\parallel,\infty} \sim (\beta - \beta_c)^{-1/\sigma(D-2)}$.

To recover correctly the thermodynamic limit we have to take into account that those terms which are negligible for $M \to \infty$ with $\xi_{\parallel,V}/M$ kept constant may be not negligible when $\xi_{\parallel,V}$ is bounded and $M \to \infty$. Indeed, going back to Eq. (3.20), given that $\Phi_0(x) \sim 0$ while $\Phi_1(x) \sim x^{\rho(D-2)}$ for $x \to \infty$, we get $S^{q-2\sigma}\Phi_1(L/\xi_V) \sim M^{\tilde{\nu}^{-1}} \xi_{\parallel,V}^{\sigma(2-D)}$ and thus the dependence of Eq. (3.20) on M cancels and $\xi_{\parallel,\infty} \sim (\beta - \beta_c)^{-1/\sigma(D-2)}$, as expected.

Case $q/\sigma \geq 2$

The gap equation is given in Eq. (3.13), i. e.

$$\begin{aligned}(4\pi)^{\rho+(d-\rho D)/2}(\beta - \beta_c)L^{\rho(D-2)} &= -(4\pi)^{\rho d/2} A z^{D-2} + \mathcal{J}_2(z^2) \\ &+ C_{\sigma,p}\int_1^\infty e^{-z^2 t} t^{-q/2\sigma}\, dt + r^{\sigma - q/2}\left[\mathcal{J}_1(z^2 r^\sigma) - C_{\sigma,p}\int_1^\infty e^{-r^\sigma z^2 t} t^{-q/2\sigma}\, dt\right]\end{aligned} \tag{3.22}$$

From this expression it is easy to see that for fixed $z^2 r^\sigma$ (zS) and r large enough, the second line is negligible with respect to the first line, which has

a finite limit for $z \to 0$. Thus no nontrivial scaling emerges. We can observe, however, that there is a way out, by noting that, for $1 < b < 2$, $a > 0$

$$\int_1^\infty \mathrm{d}t e^{-at} t^{-b} = \frac{1}{b-1} + \Gamma(1-b) a^{b-1} + O(a)$$

thus, the gap equation may be also written as ($2 < q/\sigma < D < 4$)

$$\begin{aligned}(4\pi)^{\rho+(d-\rho D)/2}(\beta-\beta_c)L^{\rho(D-2)} - K = \mathrm{O}(z^{D-2}) + C_{\sigma,p} z^{q/\sigma-2}\Gamma(1-q/2\sigma) \\ + r^{\sigma-q/2}\left[\mathcal{J}_1(z^2 r^\sigma) - C_{\sigma,p}\int_1^\infty e^{-r^\sigma z^2 t} t^{-q/2\sigma}\, dt\right]\end{aligned} \tag{3.23}$$

where

$$K = \mathcal{J}_2(0) + C_{\sigma,p}\frac{1}{q/2\sigma - 1}$$

now, in terms of a shifted temperature we can recover a sensible scaling with zS_0 constant, i.e.

$$\begin{aligned}(4\pi)^{\rho+(d-\rho D)/2}\left(\beta - \beta_c - \frac{\widetilde{K}}{L^{\rho(D-2)}}\right) L^{\rho(D-2)} r^{q/2-\sigma} = C_{\sigma,p}(r^\sigma z^2)^{q/2\sigma-1}\Gamma(1-q/2\sigma) \\ + \mathcal{J}_1(z^2 r^\sigma) - C_{\sigma,p}\int_1^\infty e^{-r^\sigma z^2 t} t^{-q/2\sigma}\, dt + \mathrm{O}(z^{p/2\rho})\end{aligned} \tag{3.24}$$

This can be rewritten as (see section A.3 in the appendix)

$$(4\pi)^{\rho+(d-\rho D)/2}(\beta - \tilde{\beta}_c(L))L^{1/\tilde{\nu}(\delta)} = \int_0^\infty dt\, \Psi_\sigma(r^\sigma z^2 t) t^{-q/2\sigma}\left[B^q\left(t^{-1/\sigma}\right) - 1\right] \tag{3.25}$$

where

$$\tilde{\beta}_c(L) = \beta_c + \frac{\widetilde{K}}{L^{\rho(D-2)}}.$$

Again this is the same gap equation of the lower (M^q) dimensional system (above the l.c.d. of the model: $q/2\sigma \geq 2$):

$$(4\pi)^\sigma(\beta - \beta_c^{\mathrm{low}})M^{q-2\sigma} = \int_0^\infty dt\, \Psi_\sigma(r^\sigma z^2 t) t^{-q/2\sigma}\left[B^q\left(t^{-1/\sigma}\right) - 1\right]. \tag{3.26}$$

where β_c^{low} is the corresponding critical temperature. It is easy to see that the l.h.s of the previous equation is the same as that of Eq. (3.14) with $q = 0$, $p \mapsto q$ and $z \mapsto zS_0$, i.e. as the r.h.s. of the gap equation for a finite hypercubic system in geometry L^q. The effective exponent $\tilde{\nu}(\delta)$ appears also in this case in the FSS.

3.5 Which one is the correct exponent?

Using the result from previous section we would like to address here the problem of the "phenomenological" determination of the critical exponents (we consider the case of $\nu_\perp$ and $\nu_\parallel$ for the model we are dealing with) without any *a priori* knowledge of the right value of Δ. First of all we note that, calling $\nu'_\perp$, $\nu'_\parallel$ the exponents deduced from data collapse according to the FSS relations

$$tM^{1/\nu'_\parallel} = F_{\parallel,\delta}(\xi_{\parallel,V}/M, S_\delta)$$

and

$$tL^{1/\nu'_\perp} = F_{\perp,\delta}(\xi_{\perp,V}/L, S_\delta)$$

we have

$$1/\nu'_\perp = \begin{cases} \rho(D-2) & \delta > 0 \\ \frac{\sigma/\nu_D + (\delta-\Delta)\rho/\nu_{p/\rho}}{1+\delta} & \delta < 0 \end{cases} , \tag{3.27}$$

and

$$1/\nu'_\parallel = \begin{cases} \frac{\rho/\nu_D + (\delta-\Delta)\sigma/\nu_{q/\sigma}}{1+\delta} & \delta > 0 \\ \sigma(D-2) & \delta < 0 \end{cases} . \tag{3.28}$$

Whatever scaling is performed (i.e. $\xi_V \sim L$, $\xi_V \sim M$), there is a range of δ for which the exponent ν'_* extracted from the data does not depend on δ and $\nu'_* = \nu_*$. Moreover the scaling function one finds differs from the one determined for $\delta = \Delta$, the former being that of a *layer* geometry. This behaviour is fully consistent with our discussion of shape mismatch in sec. 2.4. To our opinion the other nontrivial FSS limits in which the exponents ν'_* are function of δ, and which can be realized only in the low temperature phase are a perculiarity of the $O(\infty)$ model due to the fact that in low temperature the finite-volume correlation lenght can diverge faster than the corresponding dimension of the lattice.

This analysis suggest that, in simulations where the exact value of Δ is not known, one can proceed by using a sequence of increasing values of δ and estimate critical exponents by FSS with S_δ fixed until the estimates do not change anymore with δ. This provided it is possible to measure the correlation lenght of the system in the "transverse" direction so to be able to keep $\xi_{\perp,V}/L$ fixed.

Chapter 4

Numerical experiments

4.1 Setup

We studied the phase transition of the DLG in two dimensions by Monte Carlo simulations. Our aim was to check the validity of the FSS assumptions and eventually to use FSS to compute the critical exponents. The observables we took into account are those described in Section 1.3. We used the dynamics described in Sec. 1.1, with Metropolis rates, i.e. we set

$$w(x) = \min\,(1, e^{-x}). \tag{4.1}$$

Simulations were performed at infinite driving field E: therefore, forward (backward) jumps in the direction of the field are always accepted (rejected).

The dynamics of the DLG is diffusive and the dynamic critical exponent is expected [26] to be $z_\perp = 4$. Thus, it is important to have an efficient implementation of the Monte Carlo sampling algorithm in order to cope with the severe critical slowing down.

For the pseudo random-numbers we used the congruential generator of Parisi-Rapuano which is a 32 bit shift-register generator based on

$$a_n = (a_{n-24} + a_{n-55})\,\mathrm{XOR}\,a_{n-61}$$

where a is an array of 256 unsigned 32−bit integers. To initialize the array we used the congruential generator $x = x{*}31167285{+}1$ (see [64]) with 48−bit integers to make it independent of the computer architecture (suggested by A. Sokal). The same random number generator is used to choose the links to flip and to perform the Metropolis rejection step.

A multi-spin coding technique is used to evolve simultaneously many independent configurations. The number of spin configuration to evolve it is chosen to be 128 optimizing the number of single-spin sweeps per second. Indeed we observed that on Pentium or PowerPC processors there is an abrupt change of performances increasing the number of spins in the multi-spin implementation, e.g. on a Pentium processor with 32 spins we have

updating at a speed of $1.3 \cdot 10^8$ spin-flip/sec, raising to $2.7 \cdot 10^8$ for 128 spins, while it drops to $2.0 \cdot 10^8$ for 192 spins; after that it starts to raise againg (with the number of spins) to reach $3.8 \cdot 10^8$ for 960 spins. This behaviour can be traced to optimal allocation of the various level of cache memory present in this architectures.

Our first aim has been to test the theoretical prediction of the standard field theory for the DLG, see sec. 1.4. This implies that the correct FSS limit must be achieved with $S_2 = L_\parallel / L_\perp^3$ constant. The following geometries were taken into account $(L_\parallel, L_\perp)$: $(21, 14)$, $(32, 16)$, $(46, 18)$, $(64, 20)$, $(88, 22)$, $(110, 24)$, $(168, 28)$,$(216, 30)$, $(262, 32)$, $(373, 36)$, $(512, 40)$, $(592, 42)$, $(681, 44)$, $(778, 46)$, $(884, 48)$, for which $S_2 \simeq 0.2$; and the following values of β: 0.28, 0.29, 0.3, 0.305, 0.3075, 0.31, 0.3105, 0.311, 0.31125, 0.3115, 0.31175 0.312, which lies all in the disordered phase (albeit very near to the critical line).

It is very important to be sure that the system has reached the steady-state distribution before sampling. Metastable configurations in which the Markov chain could be trapped for times much longer than typical relaxation times in the steady state are a dangerous source of bias. In the DLG, configurations in which multiple stripes aligned with the external field are present are very long-lived and it is possible that they persist for times of the order of those of typical simulation runs, thus effectively inducing a spurious geometry on the system. To avoid the formation of stripes, we took care to initialize the larger systems by suitably rescaled thermalized configurations of smaller systems (where the stripes decay faster) at the same temperature and value of S_2.

We computed the autocorrelation time τ_χ for the susceptibility χ. Such an observable is expected to have a good overlap with the slowest modes of the system, so that τ_χ should give a good indication of the number of sweeps necessary to generate independent configurations. We found that, for one of the lowest temperature we considered ($\beta = 0.311$), $\tau_\chi \approx 900$, 1400, 2700 sweeps, for $L = 20, 24, 28$ respectively, where a MC sweep is conventionally defined as the number of moves equal to the volume of the lattice. For this reason, in order to have approximately independent configurations, we measured once every 1500 sweeps for every value of β.

For each geometry and β we collected approximately $3 \cdot 10^5$ measures, sometimes more. The raw data are reported in Tables B.1, B.2.

The statistical variance of the observables is estimated by using the jackknife method [65]. To take into account the possible residual correlations of the samples, we used a blocking technique in the jackknife analysis. In the standard jackknife method the estimator for the variance is obtained discarding single data points. In the blocking technique, several variance estimators are considered, discarding blocks of data of increasing length and monitoring the estimated variance until it reaches a maximum.

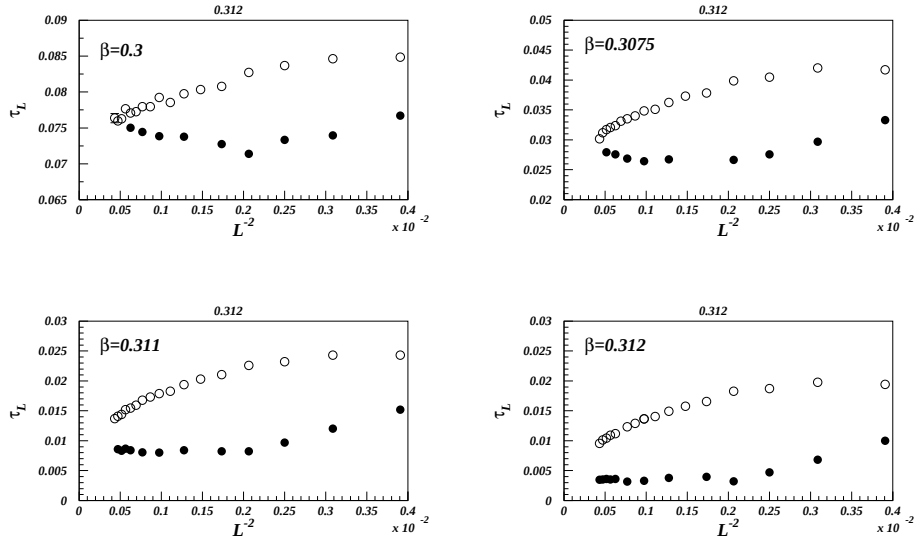

Figure 4.1: τ_L for different geometries as a function of the inverse temperature β. Filled (respectively empty) points refer to geometries with aspect ratio S_2 (respectively S_1) fixed. Here $S_2 \approx 0.200$, $S_1 \approx 0.106$. Errors are smaller than the size of the points.

4.2 Finite-size scaling

First we checked that the correlation lenght ξ_{13} (which in the following will be called ξ) has a good thermodynamic limit indipendently from the chosen geometry. In this respect we considered also a sequence of systems for which S_1 were constant and with $L_\perp$ going form 14 to 48 as above. With the aim to test the theoretical prediction on the finite-size correction to the correlation lenght:

$$\xi_L(\beta)^{-2} = \xi_\infty(\beta)^{-2} + 4\pi^2 L^{-2} + \mathrm{O}(L^{-4}) \tag{4.2}$$

we introduce the following quantity

$$\tau_L(\beta) = \xi_L(\beta)^{-2} - 4\pi^2 L^{-2}. \tag{4.3}$$

A good behaviour of ξ_L as $L \to \infty$ is reflected in a good behaviour of τ_L and viceversa. Moreover we expect from (4.2) that τ_L will be constant for large L when the shape factor S_2 is kept constant, but not otherwise. Indeed, as figure 4.1 shows, a good thermodynamic limit seem to exists for every value of β. As expected, when the temperature approaches the critical value, it is necessary to use larger and larger lattices to see the convergence to the infinite-volume limit. At β fixed we expect the convergence to become eventually exponential in L. However, for lattices with S_2 fixed we observed an intermediate region of values of L in which τ_L is apparently constant.

β	$L_{\min}$	N	R^2	R_c^2	τ_∞	a
0.28	22	4	3.12	9.49	0.2397(13)	-5.44(87)
0.29	22	4	2.76	9.49	0.15309(87)	-4.19(56)
0.3	22	4	5.09	9.49	0.07607(35)	-2.02(24)
0.3025	22	4	5.19	9.49	0.05864(36)	-1.30(25)
0.305	24	8	14.63	15.50	0.04382(26)	-1.91(26)
0.3075	26	2	0.70	6.00	0.02961(52)	-3.33(67)
0.31	22	4	8.29	9.49	0.01309(11)	0.310(74)
0.3105	22	4	7.57	9.49	0.01069(18)	0.09(13)
0.311	24	7	14.78	14.08	0.00852(21)	-0.17(18)
0.31125	22	4	2.65	9.49	0.00703(11)	-0.012(72)
0.3115	22	4	8.56	9.49	0.00586(14)	0.01(13)
0.31175	24	3	9.21	7.82	0.00421(20)	0.49(19)
0.312	28	6	11.46	12.59	0.00348(16)	0.01(20)

Table 4.1: Fit of $\tau_L(\beta)$ with $\tau_\infty + aL^{-2}$ (for S_2 constant): $L_{\min}$ is the minimum value of L allowed in the fit, N are the degrees of freedom, R^2 is the sum of square residuals and R_c^2 is the critical value for R^2 at the 95% confidence level based on a χ^2 distribution with N degrees of freedom.

Such a region widens as β approaches the critical point and is therefore consistent with the relation (4.2), that is

$$\frac{1}{\xi_\infty^2(\beta)} \approx \frac{1}{\xi_L^2(\beta)} - \frac{4\pi^2}{L^2},$$

in the FSS limit $L \to \infty$, $T \to T_c$. But this only happens for the geometries with S_2 constant. Note also that for the geometries with S_1 constant the corrections to the infinite volume limit are larger, which is what expected since the geometries with S_1 constant tend to be smaller than those with S_2 constant when comparing system with the same transverse size, as we do here.

The good behaviour of τ_L hints to the possibility of extracting the infinite volume limit τ_∞ directly by fitting τ_L, for large enough L, with the constant value $\tau_\infty = 1/\xi_\infty^2$.

Table 4.1 shows the results of fitting $\tau_L(\beta)$ as a function of L with the linear model $\tau_\infty(\beta) + a(\beta)L^{-2}$ discarding the observations with $L < L_{\min}$ where $L_{\min}$ is chosen to have a reasonable value of the sum of squared residuals R^2. In the table are also reported critical values of R^2 at the 95% confidence level based on the χ^2 statistics which shows that almost all the fits are consistent (only two of them have $R^2 > R_c^2$ and this is statistically compatible with the 95% confidence level). The value of the parameter $\tau_\infty(\beta)$ gives then our preferred estimate for the infinite volume correlation lenght $\xi_\infty(\beta) = 1/\sqrt{\tau_\infty(\beta)}$.

Performing the same kind of analisys on the data obtained in the geometries with S_1 constant is not reliable since these data are clearly affected by larger corrections and thus a straigth extrapolation would be questionable.

A simple argument shows that the formula (4.2) implies that $\nu = 1/2$. Then, given the values of $\tau_\infty(\beta)$ we can check the expected value of ν and estimate the critical value of β.

We fitted

$$\tau_\infty(\beta) = A \left| \frac{\beta}{\beta_c} - 1 \right|^{2\nu}$$

for $\beta > \beta_{\min}$ choosing for $\beta_{\min}$ the lowest value for which $R^2 < R_c^2$ (here and in the following we will use always critical values at the 95% confidence level) and we obtained $\beta_{\min} = 0.31$, $N = 4$, $R^2 = 4.2$ ($p = 0.38$, $R_c^2 = 9.48$), $A = 1.09(31)$, $2\nu = 0.921(65)$, $\beta_c = 0.312557(93)$. Adding analytic corrections to scaling does not produce better results.

A better estimate of β_c is obtained by fixing $\nu = 1/2$. In this case $\beta_{\min} = 0.31$, $N = 5$, $R^2 = 5.56$ ($p = 0.35$, $R_c^2 = 11.07$), $A = 1.540(24)$, $\beta_c = 0.312670(26)$. Adding the first analytic correction to scaling (with the same value of $\beta_{\min} = 0.31$) gives $N = 4$, $R^2 = 4.02$ ($p = 0.40$, $R_c^2 = 11.07$), $A = 1.70(13)$, $\beta_c = 0.312603(54)$ and $B = -15(12)$.

The we will consider as out best estimate of the critical temperature:

$$\beta_c \quad = 0.312603(54). \tag{4.4}$$

The result for β_c should be compared with the existing determinations:

$$\beta_c = \begin{cases} 0.3108(11) & \text{(Ref. [39])}; \\ 0.3125(13) & \text{(Ref. [41])}. \end{cases} \tag{4.5}$$

Our result (4.4) is in fairly good agreement with both estimates, although more precise.

The good FSS behaviour of the correlation lenght is witnessed by the plot of ξ_{2L}/ξ_L vs. ξ_L/L in fig. 4.2. The solid line is the theoretical prediction. It is clear that as the size of the systems increase the points converge towards the theoretical line. We would like to emphasize that in this plot *there are no tunable parameters involved*. So the observed collapse is very remarkable. To get rid of the small corrections to FSS still present, in fig. 4.3 we plotted ξ_{2L}/ξ_L vs. $\xi_{2L}/2L$. The use of data from the larger system for the values in the horizontal axis reduces significantly the corrections in the FSS plot.

Next we checked the FSS behaviour of various observables plotting $\mathcal{O}_{2L}/\mathcal{O}_L$ vs. $\xi_{2L}/2L$. The susceptibility is plotted in fig. 4.5, showing the same features present in the FSS plot for ξ. In fig. 4.4 we report the amplitude A for which the theory predicts no anomalous dimensions, here we have large error-bars (due to the very small range in the vertical axis); the data points shows a right trend towards the theoretical prediction (shown as a dotted line).

The plot for the magnetization of fig. 4.7 shows a good collapse of data points. If we look for the value of the ratio m_{2L}/m_L at the critical point (i.e. when $\xi_{2L}/2L = 1/2\pi \simeq 0.159$ we see that it should be around 0.5 which means that $\beta/\nu \simeq 1$ in accordance with the standard theory.

The behaviour of the Binder parameter reported in fig. 4.6 seems to present a good data collapse and a rough estimate of the anomalous dimensions of g would give in this case $\gamma_g/\nu \simeq -0.4$ meaning that $g = 0$ at the critical point. Even if we conjecture this limit to be true and thus supports the theory which predicts gaussian transverse fluctuations at the critical point, the analysis of the scaling plot could be more sublte and we give some arguments that what we see could be (logarithmic?) corrections to FSS in the next section.

The last plot shows some *preliminary* results about the parallel correlation lenght which can be defined in analogy to the trasverse by looking at the structure function at zero transverse momenta. In this case we used a definition of the correlation lenght base on the first and the second non-zero parallel momenta. Fig. 4.9 report a plot of $\xi_\parallel/L_\parallel$ vs. ξ_L/L. There are huge corrections to FSS but data points seems going to collapse on a well-defined curve.

4.3 Corrections to FSS

Now we would like to exploit the analysis of sec. 2.5 to check for the presence of logarithmic corrections to FSS. In the upper plot in fig. 4.10 we report X_L versus g_L according to the data compared to the theoretical prediction which says that

$$X^{\text{th}} = M_1(z^\#)^2/M_2(z^\#), \qquad g^{\text{th}} = 2 - M_1(z^\#)/M_2(z^\#)^2 \tag{4.6}$$

to achieve this purpose, for each data point we determined $z_L^\#(\beta)$ such that

$$g_L(\beta) = 2 - M_1(z_L^\#(\beta))/M_2(z_L^\#(\beta))^2$$

and then plugged this into the first of the eqns. (4.6) to obtain X^{th} as a function of $g_L(\beta)$. It is clear from the second plot in fig. 4.10 that deviations (even if somewhat systematic) are very small and compatible with statistical errors. Note that $g \to 0$ is the gaussian limit where $X \to 4/\pi \approx 0.785$ and that $g \approx 0.43$ corresponds to the strongly anharmonic limit were our approximation is no more justified. Note also that using an effective action S_{eff} with a different kind of interaction (e.g. φ^n, $n \neq 4$) gives result incompatible with statistical errors.

Using the values of $z_L^\#(\beta)$ as determined from the cumulant $g_L(\beta)$ we proceeded to fit them to the form

$$z_L^\#(\beta) = a_1 \left(\frac{L}{\xi_L(\beta)}\right)^2 (\log L)^{a_2} + a_3 (\log L)^{-a_2}$$

to mimic the structure of the corrections above two dimensions and assuming logarithmic behaviour for the marginally irrelevant coupling. The fit is unreliable and cannot be used to confirm this palusible L dependence of the corrections. However, estimated parameters can be used to provide an explicit example showing how logaritmic corrections to FSS can generate an FSS plot like that of fig. 4.6 which almost looks like a good scaling plot. In this example, reported in fig. 4.11, we set $a_1 = 0.0103$, $a_3 = -8.55$, $a_2 = 1.42$ and used the observed values of $\xi_L(\beta), \xi_{2L}(\beta)$ to evaluate the theoretical prediction for g_{2L}/g_L. This look indistinguishable from the observed data.

4.4 FSS for S_1 fixed

Here we report preliminary results about a series of simulations with geometries with fixed value of $S_1 = L_\parallel/L_\perp^2$ with the aim of understanding the effects of shape mismatch in this model. Indeed, by the results reviewed in the previous sections, we are fairly confident that S_2 is the right shape factor for the DLG – the one which should appear in FSS functions. Then keeping S_1 constant while doing the FSS limit means that $S_2 \to 0$. If we try to keep $\xi_{\perp,L}/L_\perp$ constant in this limit we should expect a singular behaviour of the FSS functions as argued in sec. 2.4.

We considered the following geometries with $S_1 \approx 0.106$ constant: $(20, 14)$, $(27, 16)$, $(34, 18)$, $(42, 20)$, $(51, 22)$, $(61, 24)$, $(72, 26)$, $(83, 28)$, $(96, 30)$, $(109, 132)$, $(123, 34)$, $(138, 36)$, $(154, 38)$, $(170, 40)$, $(188, 42)$, $(206, 44)$, $(225, 46)$, $(245, 48)$. And the following values of β: 0.27, 0.28, 0.29, 0.3, 0.305, 0.3075, 0.31, 0.3105, 0.311, 0.312. Raw data are reported in table B.3 and table B.4.

In fig. 4.12 we reported the (2L/L) plot for ξ in the case of fixed S_1. It shows larger corrections compared to that obtained with S_2 constant – however this is somewhat natural given that the geometries considered are smaller with respect to the corresponding geometries for S_2 constant. In any case, the most relevant feature of the plot is that it is clear that $\xi_{2L}/\xi_L \leq 1.85$. Note in fact that the set of β considered for these geometries is the same of those with S_2 constant and we have data up to $\beta = 0.312$, quite near to $\beta_c \approx 0.3126$. To understand the scaling behaviour of ξ_L at β_c we took the data with $\beta = 0.312$ and assuming $\xi_L(\beta_c) \propto L_\xi^a$ tried to estimate a_ξ. To do this we proceeded as follows: given that L_n is an increasing sequence of values of L at our disposal we computed the ratios

$$r_n = \frac{\log(\xi_{L_{n+1}}(\beta)) - \log(\xi_{L_n}(\beta))}{\log(L_{n+1}) - \log(L_n)}$$

with the corresponding statistical errors: note that if $\xi_{L_n} \propto L_n^{a_\xi}$ we have $r_n = a_\xi$. We estimated a from the r_n by doing a constant fit. The best fit is obtained considering data with $L \geq L_{\min} = 24$ and gives $a_\xi = 0.847(13)$

with $R^2 = 3.765$ and $N = 10$. Repeating the same procedure for χ with the same value of $L_{\min}$ we got: $a_\chi = 1.676(16)$ with $R^2 = 6.210$ and $N = 10$. For m (again same $L_{\min}$): $a_m = -0.6787(91)$ with $R^2 = 8.260$ and $N = 10$.

Note that the determinations of a_ξ,a_χ and a_m are consistent with the equations $a_\chi = 2a_\xi$, $a_m = a_\chi/2 - 3/2$ obtained from the relations

$$\chi_L \propto \xi_L^2, \qquad m_L^2 \propto \frac{\chi_L}{L_\parallel L_\perp}$$

valid for the mean-field theory.

This suggests that the appropriate FSS form in this case should be

$$\xi_L/L_{\text{eff}} = F_\xi^\flat(\xi_\infty/L_{\text{eff}}), \qquad \chi_L/L_{\text{eff}} = F_\chi^\flat(\xi_\infty/L_{\text{eff}}) \tag{4.7}$$

where $L_{\text{eff}} = L^{a_\xi}$ is an effective lenght-scale entering the FSS functions. Note that a similar result was found (in the same limit $S_2 \to 0$) by Leung [39, 40] which by theoretical arguments and analysis of finite-size data was led to the conclusion that

$$\chi_L(t) = L_\parallel^{1/3} L_\perp H_\chi(\dot{t} L_\parallel^{1/2} L_\perp^{1/2})$$

where $\dot{t}$ is a shifted reduced temperature. The exponents in this results are not exact but approximate values consistent with the data at his disposal. However they partially agree with our observations. Indeed for S_1 constant $L_\parallel \propto L_\perp^2$ and Leung's results become

$$\chi_L(t) = L_\perp^{5/3} H_\chi(\dot{t} L_\perp^{3/2})$$

which shows that, near criticality, $\chi_L \propto L_\perp^{5/3}$ in agreement with our observation that $a_\chi \approx 1.676$.

We think that this situation is not very clear, first of all because we where expecting that in the limit of $S_\Delta \to 0$ FSS would hold with $\xi_L/L_\parallel^{1/3} \propto \xi_L/L_\perp^{2/3}$ constant[1] which would give an exponent too small to be consistent with our data.

For reference we reported also the (2L/L) FSS plots for the other observables χ, m, g resp. in fig. 4.13, 4.14, 4.15. However we are prevented to interpret them by the strange scaling behaviour of the correlation length.

We used $a_\xi \approx 0.847$ to check eq. (4.7) by plotting ξ_L/L^{a_ξ} versus $(L^{a_\xi}/\xi_\infty)^2$ as determined by the extrapolation in the previous section. This is reported in fig. 4.19. The solid line is the function $F_\xi^\flat$ defined by

$$F_\xi^\flat(x) = A_0 H^*(x/\sqrt{A_0})$$

[1]This is appropriate for the strip geometry where $L_\perp \to \infty$ and consistent with exact solutions, our findings in the $O(\infty)$ model and also with the phenomenological FSS analysis of Binder and Wang [46].

where A_0 is a non-universal amplitute fitted (by eyes) to the data and H^* is the FSS function for the correlation lenght of the 1d Ising model:

$$\xi_L^{\text{ising}}/L = H^*((L/\xi_\infty^{\text{ising}})^2)$$

where ξ_L^{ising} is related to the mass gap of the 1d Ising model of L sites as usual and $\xi_\infty^{\text{ising}}$ is the corresponding infinite-volume limit. This particular choice of the FSS function can be justified heuristically by noting that when $S_2 \ll 1$ and $\xi_\parallel \gg L_\perp$ the system behaves as effectively one-dimensional and the discrete model resembles a 1d Ising model. As can be seen, the result is not really bad (remember that we have at our disposal only the parameter A_0) but of course is just an hint for future investigations. Finally, fig. 4.18 reports a plot of ξ_{2L}/ξ_L versus $\xi_{2L}/2L^{a_\xi}$ with again the prediction from the 1d Ising model with the same amplitude estimate before. Here deviations from the prediction are marked.

In fig. 4.20 we check relations between adimensional ratios, in the spirit of fig. 4.10, for S_1 geomeries: the results are very similar to that for the S_2 geometries.

4.5 Conclusions

By the means of a well-behaved transverse correlations lenght we were able to probe the FSS regime of the DLG in much deeper detail than previous works in the literature, first of all avoiding the deprecable tecnique of data collapsing for the determination of critical exponents. Data collapse, indeed, is usually judged by eyes: in doubtful situations like ours, a more quantitative approach to the verification of scaling relations is needed. We want to stress again that simulations at S_2 constant agree fairly well with the theory *without* any tuning of parameters. This give strong evidences that the correct scaling limit can be obtained with S_2 constant. The prediction of ν and γ are thus consistent with the mean-field behaviour of the transverse correlations predicted by the field-theoretical approach of sec. 1.4. By our arguments of sec. 2.4, even if $\Delta < 2$, the FSS scaling of the transverse correlation function is not modified by shape mismatch, indeed we expect that the relation

$$\frac{\xi_{2L}}{\xi_L} \approx F_\xi\left(\frac{\xi_L(t)}{L}, S_\Delta\right),$$

has a regular limit for $S_\Delta \to \infty$ (this is what happens if we keep S_2 constant and $\Delta < 2$). In particular our analysis applies also to the case $\Delta = 1$.

Another novelty of our approach is the different perspective on the rôle of the dangerous operator in the FSS behaviour of the standard field-theory for the DLG, and thus on the KLS model if we assume the standard picture to be correct. Indeed we showed how this dangerous operator does not lead to violations of FSS above two dimensions and in high temperature due to

the absence of the zero-mode. This ultimately means that the standard set of observables in finite-volume is not suited for capturing the anomalous behaviour expected from the analysis of the infinite-volume field-theory. A better understanding of this phenomenon, an in particular of the finite-size behaviour of the theory below the critical temperature is under current investigation. Even if we do not still have strong arguments we believe that our data for the Binder cumulant are affected by (logarithmic?) corrections to FSS. If that is the case it would be very difficult to see this logarithmic nature by MC simulations due to the need of simulating prohibitively large boxes. In any case the method of crossing of g to find the critical temperature should not be used in this situation.

An analisys of the data from geometries at S_1 constant is under consideration to understand the discrepancy between the recent claims made in the literature [57] with our results.

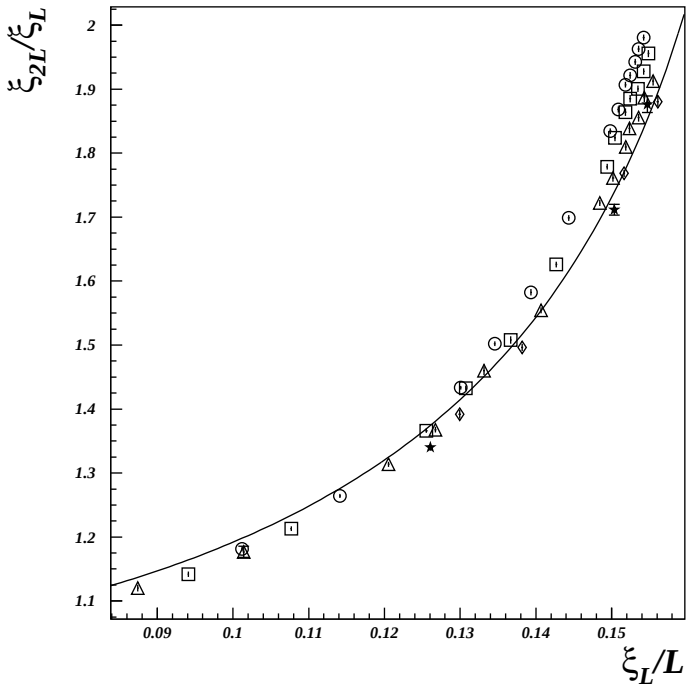

Figure 4.2: FSS plot for ξ with $\alpha = 2$. Marks are as follows : $L = 16(\circ)$, $18(\square)$, $20(\triangle)$, $22(\Diamond)$, $24(\bigstar)$. On the right ξ_{2L}/ξ_L is plotted against $\xi_{2L}/(2L)$ to reduce the effects of corrections to FSS. The lines are the theoretical prediction.

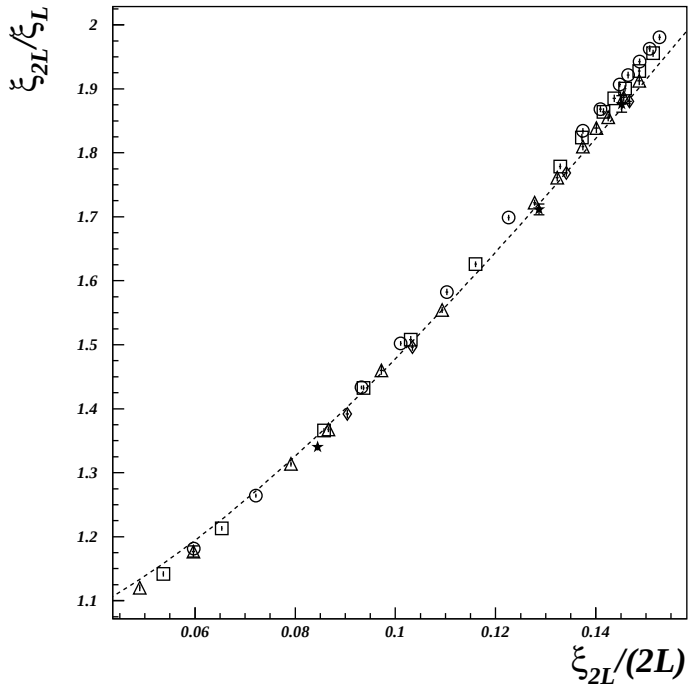

Figure 4.3: FSS plot for ξ. Marks are as in fig. 4.2. ξ_{2L}/ξ_L is plotted against $\xi_{2L}/(2L)$ to reduce the effects of corrections to FSS. The line is the theoretical prediction.

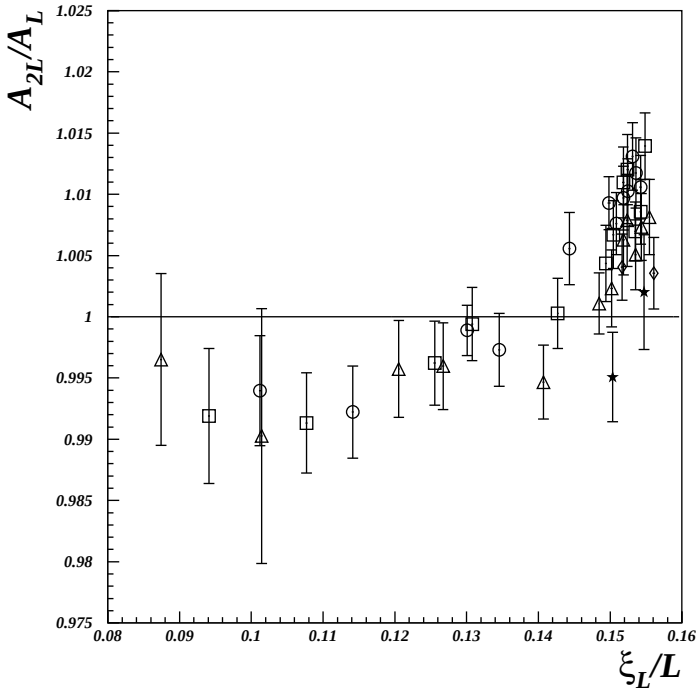

Figure 4.4: FSS plot for A. Marks are as in fig. 4.2. The solid line is the theoretical prediction.

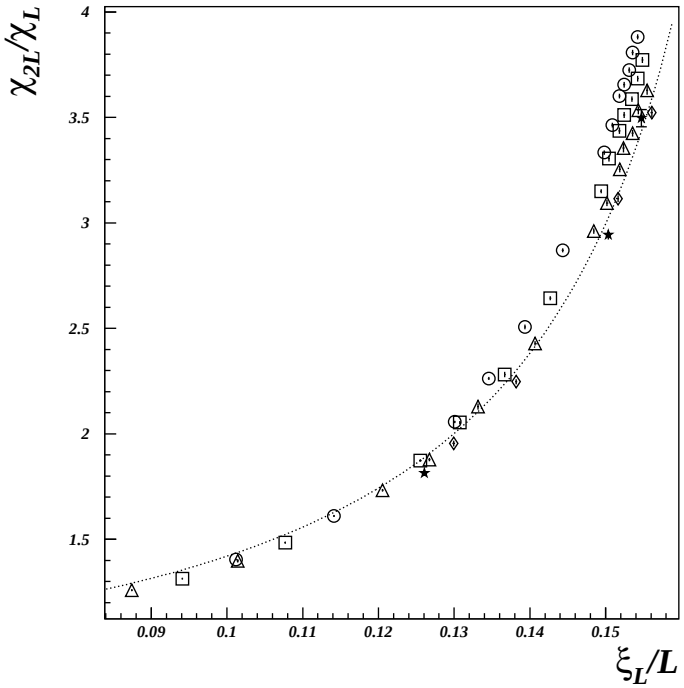

Figure 4.5: FSS plot for χ. Marks are as in fig. 4.2. The line is the theoretical prediction.

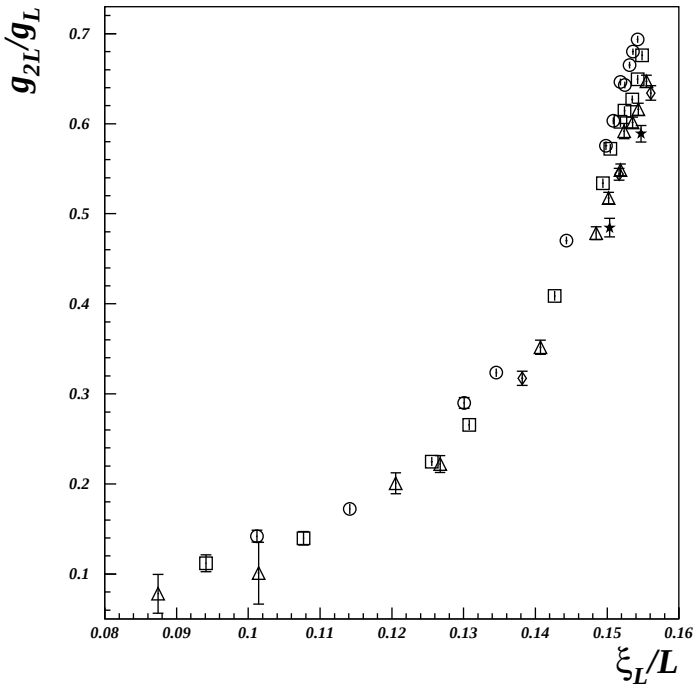

Figure 4.6: FSS plot for g. Marks are as in fig. 4.2.

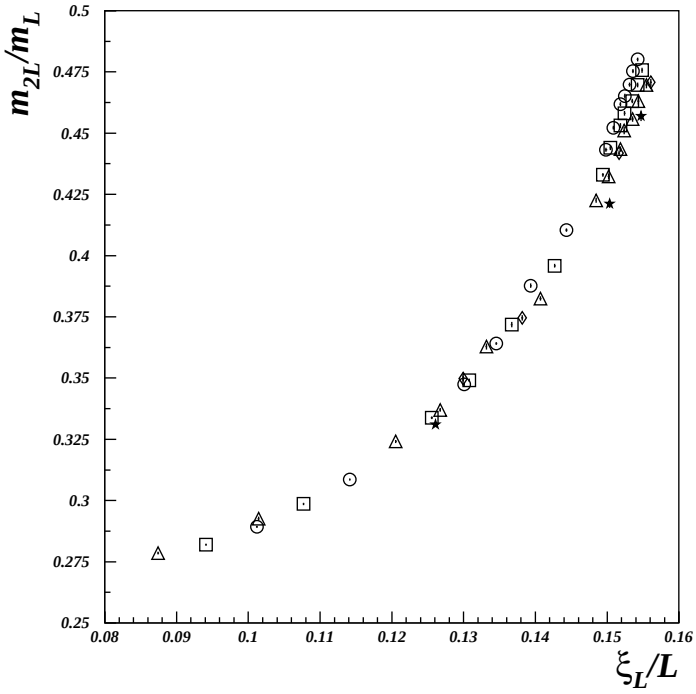

Figure 4.7: FSS plot for m. Marks are as in fig. 4.2.

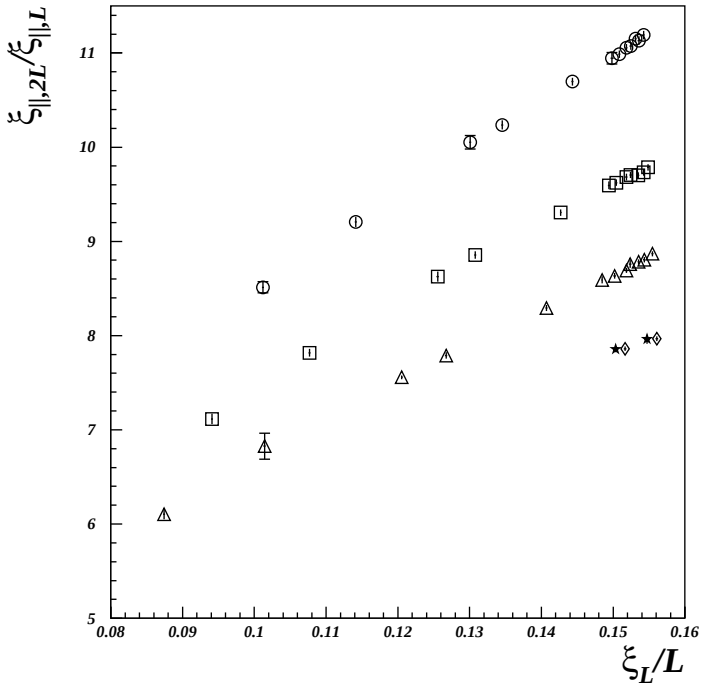

Figure 4.8: FSS plot for $\xi_{\parallel}$. Marks are as in fig. 4.2.

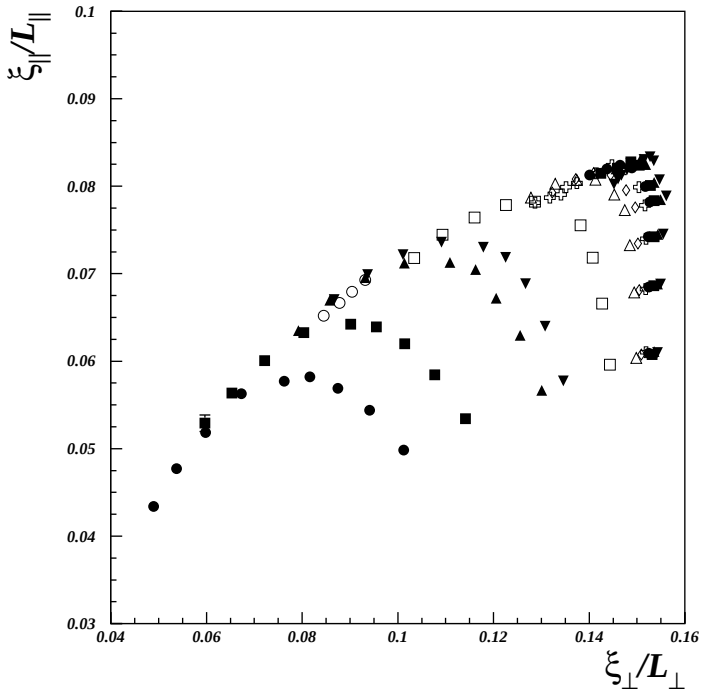

Figure 4.9: FSS plot of $\xi_{\parallel}/L_{\parallel}$ versus ξ/L. All the data points are shown. For the same value of β (same marker) the larger geometries are on the left of smaller ones. The plot clearly shows that corrections to FSS dies out as L increases.

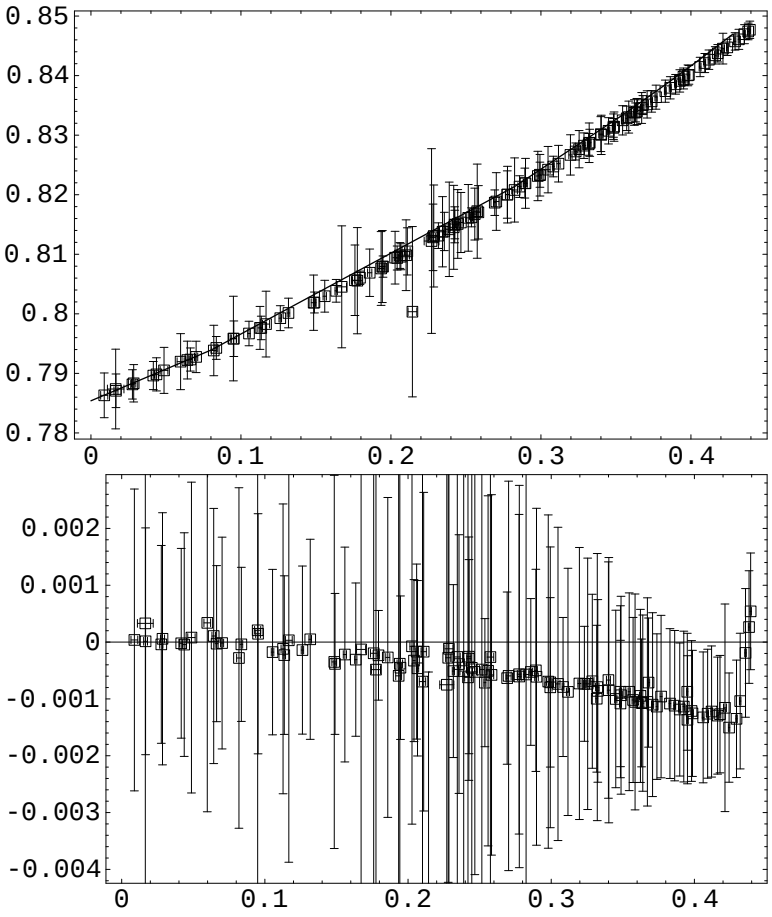

Figure 4.10: Check of FSS corrections: upper figure is the plot of X_L vs. g_L (see sect. 2.2.2) and a plot of the theoretical prediction, they are indistinguishable in this scale. Lower figure reports $X_L - X_L^{\rm th}$ vs. g_L, deviations are seen for $g_L \simeq 0.43$ (the limit of large quartic coupling).

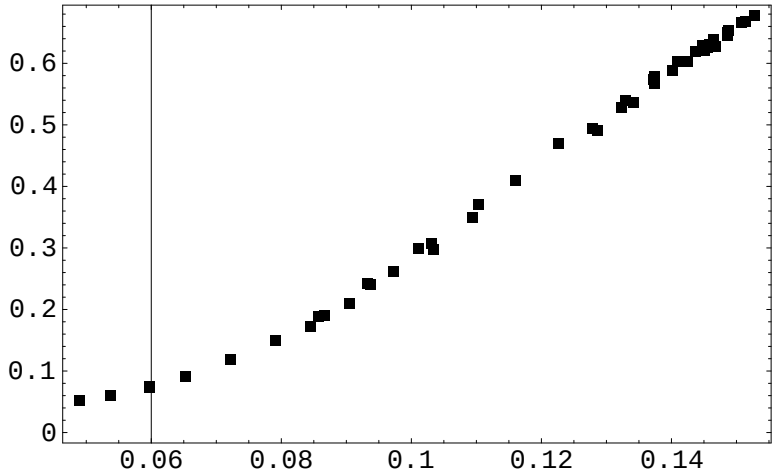

Figure 4.11: Check of FSS corrections: here it is shown how the FSS plot for g, i.e. g_{2L}/g_L vs ξ_L/L looks like assuming a specific pattern for the L dependence of the corrections. In this case it is indistinguishable from the real data.

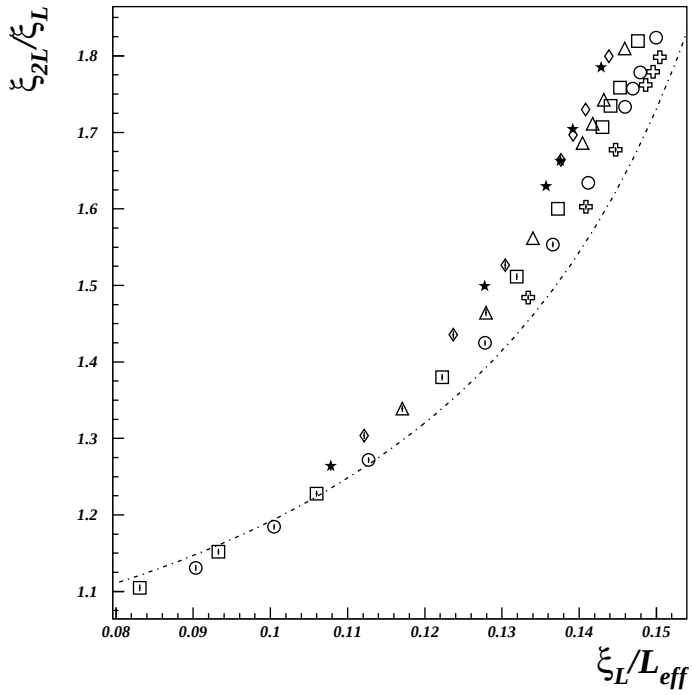

Figure 4.12: FSS plot for ξ with S_1 fixed. Marks are as in fig. 4.2.The line is the theoretical prediction of FSS with S_2 fixed, for comparison.

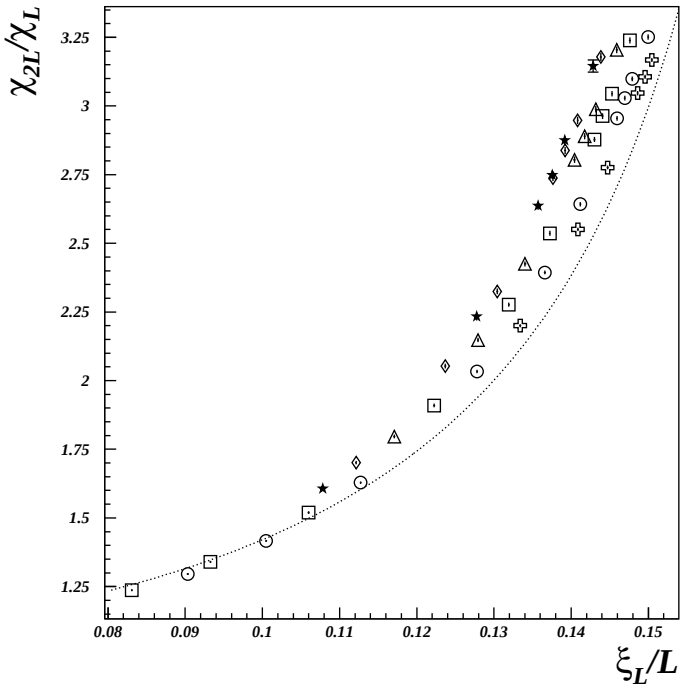

Figure 4.13: FSS plot for χ with S_1 fixed. Marks are as in fig. 4.2. The line is the theoretical prediction of FSS with S_2 fixed, for comparison.

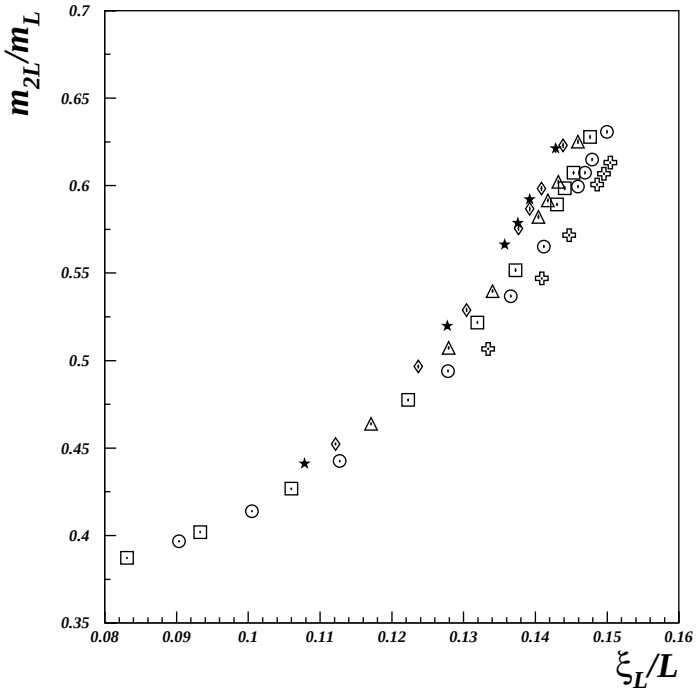

Figure 4.14: FSS plot for m with S_1 fixed. Marks are as in fig. 4.2.

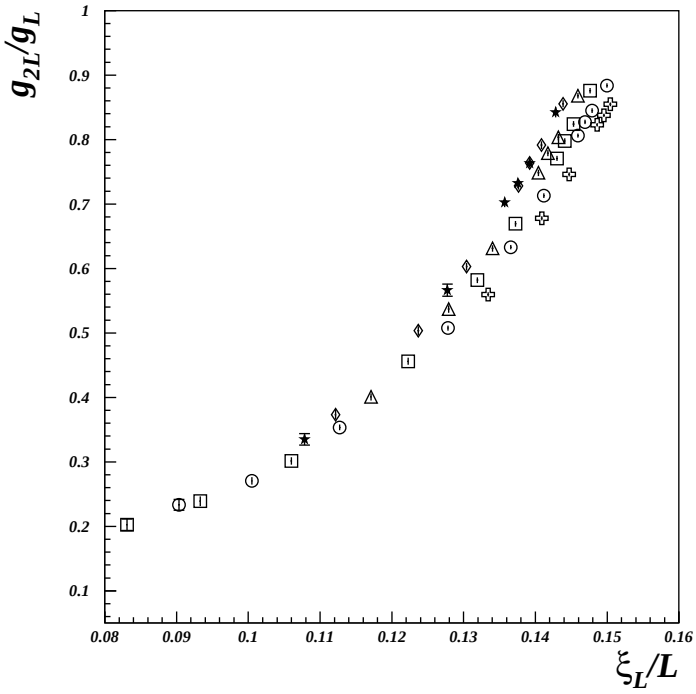

Figure 4.15: FSS plot for g with S_1 fixed. Marks are as in fig. 4.2.

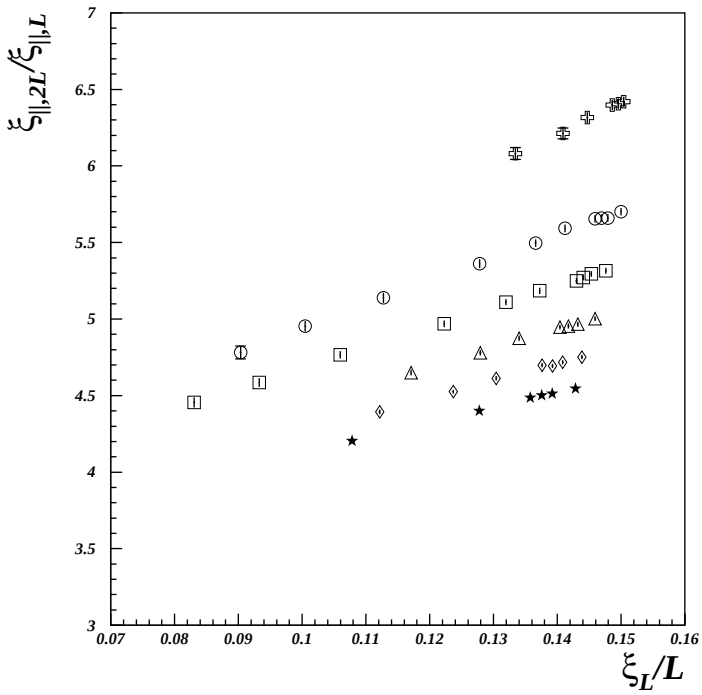

Figure 4.16: FSS plot for $\xi_{\parallel}$ with S_1 fixed. Marks are as in fig. 4.2.

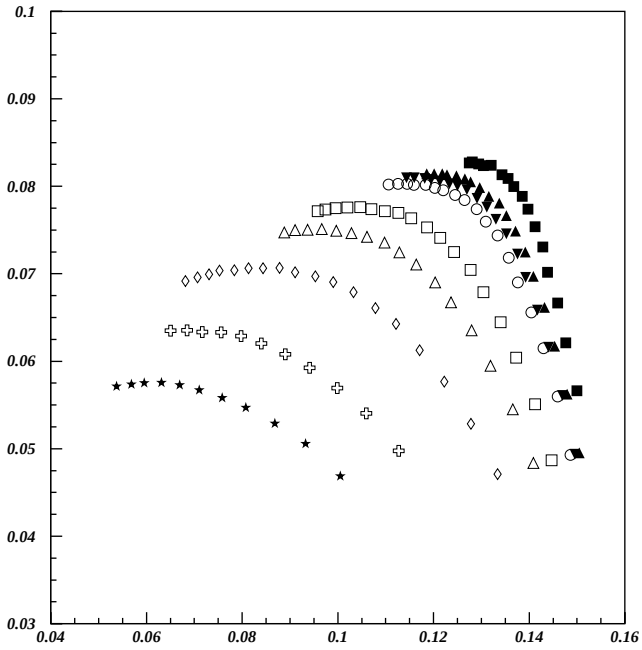

Figure 4.17: FSS plot of $\xi_{\|}/L_{\|}$ versus ξ/L for S_1 geometries. All the data points are shown. For the same value of β (same marker) the larger geometries are on the left of smaller ones.

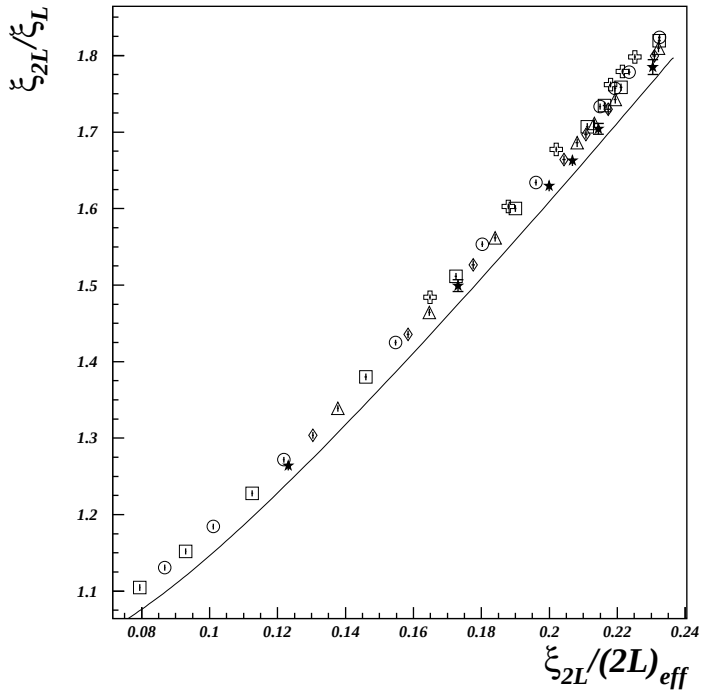

Figure 4.18: FSS plot for ξ with S_1 fixed . Marks are as in fig. 4.2. Here $L_{\text{eff}} = L_{\perp}^{a_\xi}$ ($a_\xi = 0.847$). The solid line is the FSS curve of the one dimensional Ising model with one adjustable parameter to account for non-universal metric factor.

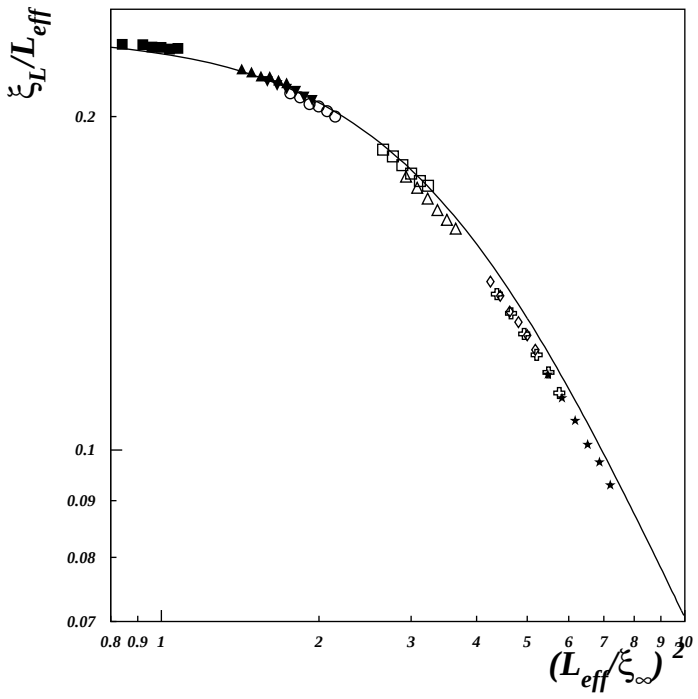

Figure 4.19: Plot of ξ_L/L_{eff} vs $(L_{\text{eff}}/\xi_\infty)^2$ with $L_{\text{eff}} = L_\perp^{a_\xi}$ ($a_\xi = 0.847$); for each β the six largest geometries are shown, different marks stay for different temperatures. The solid line is the FSS curve of the one dimensional Ising model with one adjustable parameter to account for non-universal metric factor.

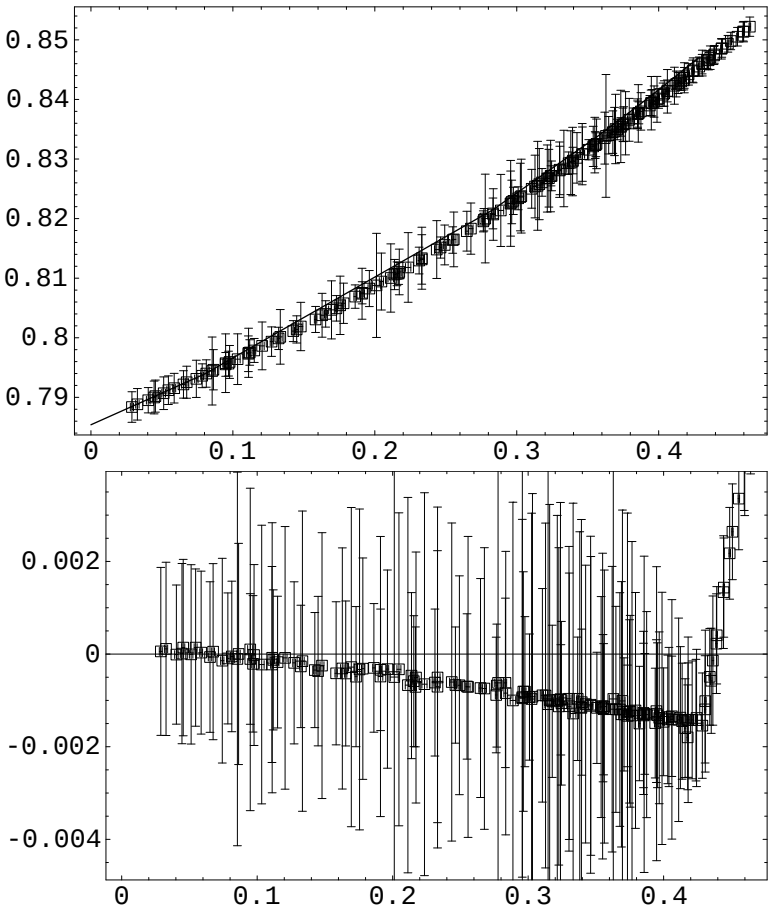

Figure 4.20: Check of FSS corrections for the geometries with S_1 constant: upper figure is the plot of X_L vs. g_L (see sect. 2.2.2) and a plot of the theoretical prediction, they are indistingushable in this scale. Lower figure reports $X_L - X_L^{\rm th}$.

Appendix A

Computations in the $O(\infty)$ model

A.1 FSS of the gap equation

By standard arguments (see eq. [66]), the gap equation can be approximated with

$$\beta - \beta_c \approx -\lambda_V \int_{[-\pi,\pi]^d} \frac{d^d\boldsymbol{p}}{(2\pi)^d} \frac{1}{K(\boldsymbol{p})(K(\boldsymbol{p})+\lambda_V)} + \Sigma' \approx -\lambda_V^{D/2-1} A + \Sigma'. \tag{A.1}$$

with $K(\boldsymbol{p}) = |\boldsymbol{p}_\perp|^{2\rho} + |\boldsymbol{p}_\parallel|^{2\sigma}$ where $0 < \sigma \leq 1$, $0 < \rho \leq 1$ and where $D = p/\rho + q/\sigma$,

$$A := \int_{\mathbb{R}^d} \frac{d^d\boldsymbol{p}}{(2\pi)^d} \frac{1}{K(\boldsymbol{p})(K(\boldsymbol{p})+1)}$$

and

$$\Sigma' := \frac{1}{V} \sum_{\boldsymbol{p}\in\Lambda_V^*} \frac{1}{K(\boldsymbol{p})+\lambda_V} - \int_{[-\pi,\pi]^d} \frac{d^d\boldsymbol{p}}{(2\pi)^d} \frac{1}{K(\boldsymbol{p})+\lambda_V}.$$

Using Poisson summation formula

$$\sum_{n=a}^{b} f(n) = \sum_k \int_a^b dn f(n) e^{i2\pi nk} + \frac{1}{2}\left(f(a)+f(b)\right)$$

we have

$$\frac{1}{V} \sum_{\boldsymbol{p}\in\Lambda_V^*} f(\boldsymbol{p}) = \sum_{\boldsymbol{n}} \int_{[-\pi,\pi]^d} \frac{d^d\boldsymbol{p}}{(2\pi)^d} f(\boldsymbol{p}) e^{i\boldsymbol{p}_\parallel \boldsymbol{n}_\parallel M + i\boldsymbol{p}_\perp \boldsymbol{n}_\perp L} + \mathrm{O}(L^{-1}|f(\pi)+f(-\pi)|). \tag{A.2}$$

so that

$$\begin{aligned}\Sigma' &\approx \sum_{\boldsymbol{n}\neq\boldsymbol{0}} \int_{[-\pi,\pi]^d} \frac{d^d\boldsymbol{p}}{(2\pi)^d} \frac{e^{i\boldsymbol{p}_\parallel \boldsymbol{n}_\parallel M + i\boldsymbol{p}_\perp \boldsymbol{n}_\perp L}}{K(\boldsymbol{p})+\lambda_V} \\ &\approx \sum_{\boldsymbol{n}\neq\boldsymbol{0}} \int_{\mathbb{R}^d} \frac{d^d\boldsymbol{p}}{(2\pi)^d} \frac{e^{i\boldsymbol{p}_\parallel \boldsymbol{n}_\parallel M + i\boldsymbol{p}_\perp \boldsymbol{n}_\perp L}}{K(\boldsymbol{p})+\lambda_V}\end{aligned} \tag{A.3}$$

where we have extended the integration to all the space, convergence being guaranteed by the oscillating phase factor.

Introduce the function

$$B(s) := \sum_{n\in\mathbb{Z}} e^{-\pi n^2 s}, \quad \text{with} \quad B(s) = s^{-1/2}B(1/s).$$

To deal with the particular form of the propagator it will be useful to introduce auxiliary integrations. It happens that actually these integrations are mean values according to particular probability ditribution. Then, in the following, we will denote with $\mathbb{E}$ the probabilistic mean value. Since the random variables we introduce are just a trick to perform computations if r.v. appears in final results the operation of taking the mean will be understood whenever not present.

Recall that a *subordinator* X_t (for detail see e.g. [15]) of order α, for $0<\alpha<1$ is a positive and increasing jump process over $\mathbb{R}_+$ with stationary independent increments and such that

$$\mathbb{E}\, e^{-uX_t} = e^{-tu^\alpha}$$

for $u>0$. It holds that $\mathbb{E}\, X_t^\beta < \infty$ for $\beta<\alpha$ and that $X_{\ell t} \stackrel{d}{=} \ell^{1/\alpha}\tau_t$ where equality means equality in ditribution. The law of X_1 is then an α-stable law supported on the positive semiaxis, its density $f_\alpha(x)$ with respect of Lebesgue measure on $\mathbb{R}_+$ has the asymptotic behaviour

$$f_\alpha(x) \sim x^{-(1+\alpha)}, \qquad \text{for } x\to+\infty.$$

and

$$f_\alpha(x) \sim \exp\left(-Cx^{-\alpha/(1-\alpha)}\right), \qquad \text{for } x\to 0+,$$

where C is a positive constant.

We can consider the case $\alpha=1$ as a limiting situation in with the process X_t becomes deterministic and ballistic: $X_t = t$.

Introducing auxiliary integrations over a parameter t and over the distribution of independent subordinators η_t and τ_t of respective order ρ and σ (with $0<\sigma\leq 1$ and $0<\rho\leq 1$), is possible to factorize the multiple

summations in eq. (A.3) as follows:

$$\begin{aligned}
\Sigma' &= \sum_{\boldsymbol{n}\neq\boldsymbol{0}} \int_{\mathbb{R}^d} \frac{d^d\boldsymbol{p}}{(2\pi)^d} \int_0^\infty dt\, e^{-\lambda_V t - t|\boldsymbol{p}_\perp|^{2\rho} - t|\boldsymbol{p}_\parallel|^{2\sigma} + i\boldsymbol{p}_\perp\cdot\boldsymbol{n}_\perp L + i\boldsymbol{p}_\parallel \boldsymbol{n}_\parallel M} \\
&= \mathbb{E} \sum_{\boldsymbol{n}\neq\boldsymbol{0}} \int_{\mathbb{R}^d} \frac{d^d\boldsymbol{p}}{(2\pi)^d} \int_0^\infty dt\, e^{-\lambda_V t - \eta_t|\boldsymbol{p}_\perp|^{2} - \tau_t|\boldsymbol{p}_\parallel|^{2} + i\boldsymbol{p}_\perp\cdot\boldsymbol{n}_\perp L + i\boldsymbol{p}_\parallel \boldsymbol{n}_\parallel M} \\
&= \mathbb{E}\, \frac{1}{(4\pi)^{d/2}} \sum_{\boldsymbol{n}\neq\boldsymbol{0}} \int_0^\infty dt\, \eta_t^{-p/2} \tau_t^{-q/2} e^{-\lambda_V t - (\boldsymbol{n}_\perp L)^2/(4\eta_t) - (\boldsymbol{n}_\parallel M)^2/(4\tau_t)} \\
&= \mathbb{E}\, \frac{L^{(2-D)\rho}}{(4\pi)^{\rho+(d-\rho D)/2}} \int_0^\infty dt\, \eta_t^{-p/2} \tau_t^{-q/2} e^{-z^2 t} \left[B^p\left(\frac{1}{\eta_t}\right) B^q\left(\frac{r}{\tau_t}\right) - 1 \right]
\end{aligned}$$

with $S = M/L^{\rho/\sigma}$, $r = (4\pi)^{\rho/\sigma-1} S^2$, $z = L^\rho \sqrt{\lambda/(4\pi)^\rho}$, $D = p/\rho + q/\sigma$. We see that the r.v. τ_t and η_t can be interpreted as auxiliary random times replacing the unique deterministic auxiliary time variable (Schwinger's proper-time) appearing in the treatment of short-range case ($\sigma = \rho = 1$). This allows a unified treatment of a whole host of models.

This last expression readly implies that in the FSS limit with S constant we obtain the gap equation

$$(4\pi)^{\rho+(d-\rho D)/2} (\beta - \beta_c) L^{\rho(D-2)} = -(4\pi)^{\rho d/2} A + I(z, S) \tag{A.4}$$

where $\beta = 1/T$, β_c is given in Eq. (3.7), $z = (4\pi)^{-\rho/2} (L/\xi_V)^\rho$.

In the low temperature regime ($\beta > \beta_c$ fixed) we have

$$\beta - \beta_c = -\lambda_V^{D/2-1} A + \Sigma' > 0$$

which implies that Σ' must remain constant in the limit $L, M \to \infty$ and thus z is forced to go to zero. Then

$$\begin{aligned}
\frac{(4\pi)^{\rho+(d-\rho D)/2}}{L^{\rho(2-D)}} \Sigma' &= \int_0^\infty dt\, \eta_t^{-p/2} \tau_t^{-q/2} e^{-z^2 t} B^p\left(\frac{1}{\eta_t}\right) B^q\left(\frac{r}{\tau_t}\right) \\
&\quad - \int_0^\infty dt\, \eta_t^{-p/2} \tau_t^{-q/2} e^{-z^2 t} \\
&= \int_0^\infty dt\, e^{-z^2 t} B^p(\eta_t)\, B^q(\tau_t) - \int_0^\infty dt\, \eta_t^{-p/2} \tau_t^{-q/2} e^{-z^2 t} \\
&= \int_0^\infty dt\, e^{-z^2 t} B^p(\eta_t)\, B^q(\tau_t) - \int_0^\infty dt\, \eta_t^{-p/2} \tau_t^{-q/2} e^{-z^2 t} \\
&\simeq z^{-2}
\end{aligned}$$

which implies that in the infinite volume limit

$$\xi_V \sim L^{\rho D/2}. \tag{A.5}$$

A.2 FSS of the correlation function

Now we consider the FSS limit for the (real-space) correlation function $G_V(\boldsymbol{x})$:

$$G_V(\boldsymbol{x}) = \frac{1}{V} \sum_{\boldsymbol{p} \in \Lambda_V^*} \frac{e^{i\boldsymbol{p}\cdot\boldsymbol{x}}}{K(\boldsymbol{p}) + \lambda_V} \tag{A.6}$$

Using again the Poisson summation formula of eq. (A.2) we get

$$\begin{aligned}
G_V(\boldsymbol{x}) &= \frac{1}{V} \sum_{\boldsymbol{p} \in \Lambda_V^*} \int_0^\infty dt\, e^{i\boldsymbol{p}\cdot\boldsymbol{x} - t|\boldsymbol{p}_\perp|^{2\rho} - t|\boldsymbol{p}_\parallel|^{2\sigma} - t\lambda_V} \\
&= \frac{1}{V} \sum_{\boldsymbol{p} \in \Lambda_V^*} \int_0^\infty dt\, e^{i\boldsymbol{p}\cdot\boldsymbol{x} - \eta_t|\boldsymbol{p}_\perp|^2 - \tau_t|\boldsymbol{p}_\parallel|^2 - \lambda_V t} \\
&\approx \int_0^\infty dt\, e^{-\lambda_V t} \sum_n \int_{\mathbb{R}^d} \frac{d^d\boldsymbol{p}}{(2\pi)^d} e^{i\boldsymbol{p}_\parallel(\boldsymbol{n}_\parallel M + \boldsymbol{x}_\parallel) + i\boldsymbol{p}_\perp(\boldsymbol{n}_\perp L + \boldsymbol{x}_\perp) - \eta_t|\boldsymbol{p}_\perp|^2 - \tau_t|\boldsymbol{p}_\parallel|^2} \\
&\approx \frac{1}{(4\pi\sqrt{\pi})^d} \int_0^\infty dt\, e^{-\lambda_V t} \tau_t^{-q/2} \eta_t^{p/2} \sum_{\boldsymbol{n} \in \mathbb{Z}^d} e^{-|\boldsymbol{x}_\perp + L\boldsymbol{n}_\perp|^2/(4\eta_t) - |\boldsymbol{x}_\parallel + M\boldsymbol{n}_\parallel|^2/(4\tau_t)}
\end{aligned}$$

($\approx$ means again equality modulo finite-size corrections uniform in T). In the infinite volume limit with x and λ_V fixed only the $\boldsymbol{n} = \boldsymbol{0}$ term is non-vanishing and we get

$$\begin{aligned}
G_V(\boldsymbol{x}) &\approx \frac{1}{(4\pi\sqrt{\pi})^d} \int_0^\infty dt\, e^{-\lambda_V t} \tau_t^{-q/2} \eta_t^{p/2} e^{-|\boldsymbol{x}_\perp|^2/(4\eta_t) - |\boldsymbol{x}_\parallel|^2/(4\tau_t)} \\
&= \int_{\mathbb{R}^d} \frac{d^d\boldsymbol{p}}{(2\pi)^d} \frac{e^{i\boldsymbol{p}\boldsymbol{x}}}{K(\boldsymbol{p}) + \lambda_V} = \xi_\perp^{\rho(2-D)} \widetilde{G}_\infty(\boldsymbol{x}_\perp/\xi_\perp, \boldsymbol{x}_\parallel/\xi_\parallel)
\end{aligned}$$

where

$$\xi_\perp = \lambda^{-1/2\rho}, \qquad \xi_\parallel = \lambda^{-1/2\sigma}.$$

If we perform the limit $L, M \to \infty$ with S, $\xi_\parallel/L$, $x_\perp/L$, $x_\parallel/M$ constant we get instead

$$\begin{aligned}
G_V(\boldsymbol{x}) &\approx \frac{L^{\rho(2-D)}}{(4\pi\sqrt{\pi})^d} \int_0^\infty dt\, e^{-(\lambda_V L^{2\rho})t} \tau_t^{-q/2} \eta_t^{p/2} \\
&\qquad \sum_{\boldsymbol{n} \in \mathbb{Z}^d} e^{-|(\boldsymbol{x}_\perp/L) + \boldsymbol{n}_\perp|^2/(4\eta_t) - S^2|(\boldsymbol{x}_\parallel/M) + \boldsymbol{n}_\parallel|^2/(4\tau_t)} \\
&= L^{\rho(2-D)} F(\boldsymbol{x}_\perp/L, \boldsymbol{x}_\parallel/M, S, \lambda_L L^{2\rho}) \\
&= \xi_\perp^{\rho(2-D)} \widetilde{G}(\boldsymbol{x}_\perp/\xi_\perp, \boldsymbol{x}_\parallel/\xi_\parallel, S, \xi_\perp/L, S)
\end{aligned} \tag{A.7}$$

which is the FSS form of the correlation function.

A.3 Gap equation for $S \to \infty$

Now we will determine the limiting form of the gap equation (A.1) for $L \to \infty$, $M \to \infty$ such that $S \to \infty$ and arbitrary values of $z = L/\xi_V$.

We have

$$\begin{aligned}\frac{(4\pi)^{\rho+(d-\rho D)/2}}{L^{\rho(2-D)}}\Sigma' &= \mathbb{E}\int_1^\infty dt\,\eta_t^{-p/2}\tau_t^{-1/2}e^{-z^2t}\left[B^p\left(\frac{1}{\eta_t}\right)B^q\left(\frac{r}{\tau_t}\right)-1\right]\\ &\quad+\mathbb{E}\int_0^1 dt\,\eta_t^{-p/2}\tau_t^{-q/2}e^{-z^2t}\left[B^p\left(\frac{1}{\eta_t}\right)B^q\left(\frac{r}{\tau_t}\right)-1\right]\\ &=: A+B\end{aligned}$$

where

$$\begin{aligned}A &= \overbrace{\int_1^\infty dt\,e^{-z^2t}r^{-q/2}\left[B^p\left(\eta_t\right)B^q\left(\frac{\tau_t}{r}\right)-1\right]}^{C}+\int_1^\infty dt\,e^{-z^2t}\left[r^{-q/2}-\eta_t^{-p/2}\tau_t^{-q/2}\right]\\ &= C+\frac{r^{-q/2}e^{-z^2}}{z^2}-\int_1^\infty dt\,\eta_t^{-p/2}\tau_t^{-q/2}e^{-z^2t}\end{aligned}$$

with

$$\begin{aligned}C &= r^{\sigma-q/2}\int_{1/r^\sigma}^\infty dt\,e^{-z^2r^\sigma t}\left[B^p(r^{\sigma/\rho}\eta_t)B^q\left(\tau_t\right)-1\right]\\ &= r^{\sigma-q/2}\int_{1/r^\sigma}^1 dt\,e^{-z^2r^\sigma t}\left[B^p\left(r^{\sigma/\rho}\eta_t\right)B^q\left(\tau_t\right)-1\right]\\ &\quad+r^{\sigma-q/2}\int_1^\infty dt\,e^{-z^2r^\sigma t}\left[B^p(r^{\sigma/\rho}\eta_t)B^q\left(\tau_t\right)-1\right]\\ &= r^{\sigma-q/2}\int_{1/r^\sigma}^1 dt\,e^{-z^2r^\sigma t}\tau_t^{-q/2}B^p(r^{\sigma/\rho}\eta_t)B^q\left(\frac{1}{\tau_t}\right)-r^{\sigma-q/2}\int_{1/r^\sigma}^1 dt\,e^{-z^2r^\sigma t}\\ &\quad+r^{\sigma-q/2}\int_1^\infty dt\,e^{-z^2r^\sigma t}\left[B^p(r^{\sigma/\rho}\eta_t)B^q\left(\tau_t\right)-1\right]\\ &= r^{\sigma-q/2}\int_{1/r^\sigma}^1 dt\,e^{-z^2r^\sigma t}\tau_t^{-q/2}B^p(r^{\sigma/\rho}\eta_t)\left[B^q\left(\frac{1}{\tau_t}\right)-1\right]\\ &\quad+\int_1^{r^\sigma} dt\,e^{-z^2t}\tau_t^{-q/2}\left[B^p(\eta_t)-1\right]+\int_1^{r^\sigma} dt\,e^{-z^2t}\tau_t^{-q/2}\\ &\quad-r^{\sigma-q/2}\int_{1/r^\sigma}^1 dt\,e^{-z^2r^\sigma t}+r^{\sigma-q/2}\int_1^\infty dt\,e^{-z^2r^\sigma t}\left[B^p\left(r^{\sigma/\rho}\eta_t\right)B^q\left(\tau_t\right)-1\right]\\ &=: C_1+C_2+C_3+C_4+C_5\end{aligned}$$

We can extend integrations in C_1 and C_2, (eventually substitute $B^p(r^{\sigma/\rho}t) \to$

1 in C_5), perform integration of C_4, to obtain:

$$C \approx r^{\sigma-q/2}\left\{\int_0^1 dt\, e^{-z^2 r^\sigma t}\tau_t^{-q/2}B^p(r^{\sigma/\rho}\eta_t)\left[B^q\left(\frac{1}{\tau_t}\right)-1\right]\right.$$
$$\left.+\int_1^\infty dt\, e^{-z^2 r^\sigma t}\left[B^p(r^{\sigma/\rho}\eta_t)B^q\left(\tau_t\right)-1\right]\right\}^*$$
$$+\int_1^\infty dt\, e^{-z^2 t}\tau_t^{-q/2}\left[B^p(\eta_t)-1\right]+\int_1^{r^\sigma} dt\, e^{-z^2 t}\tau_t^{-q/2}+r^{\sigma-q/2}\frac{e^{-z^2r^\sigma}-e^{-z^2}}{z^2r^\sigma}$$

So

$$A=-C_{\sigma,q}C_{\rho,p}\int_1^\infty dt\, t^{-D/2}e^{-z^2t}+r^{\sigma-1/2}\frac{e^{-z^2r^\sigma}-e^{-z^2}}{z^2r^\sigma}+r^{\sigma-q/2}\frac{e^{-z^2}}{z^2r^\sigma}$$
$$+C_{\sigma,q}\int_1^{r^\sigma} dt\, e^{-z^2t}t^{-q/2\sigma}+C_{\sigma,q}\int_1^\infty dt\, e^{-z^2t}t^{-q/2\sigma}\left[B^p(\eta_t)-1\right]+r^{\sigma-q/2}\underbrace{\{\cdots\}^*}_{I(r,z^2)}$$

and

$$B=C_{\sigma,q}\int_0^1 dt\, e^{-z^2t}\eta_t^{-p/2}t^{-q/2\sigma}\left[B^p\left(\frac{1}{\eta_t}\right)-1\right].$$

Finally

$$\begin{aligned}A+B=\;&C_{\sigma,q}\int_1^{r^\sigma} dt\, e^{-z^2t}t^{-q/2\sigma}-C_{\sigma,q}C_{\rho,p}\int_1^\infty dt\, t^{-D/2}e^{-z^2t}\\&+C_{\sigma,q}\int_1^\infty dt\, e^{-z^2t}t^{-q/2\sigma}\left[B^p(\eta_t)-1\right]\\&+C_{\sigma,q}\int_0^1 dt\, e^{-z^2t}t^{-q/2\sigma}\eta_t^{-p/2}\left[B^p(\eta_t^{-1})-1\right]\\&+r^{\sigma-q/2}\frac{e^{-z^2r^\sigma}}{z^2r^\sigma}\\&+r^{\sigma-q/2}\int_1^\infty dt\, e^{-z^2r^\sigma t}\left[B^q\left(\tau_t\right)-1\right]\\&+r^{\sigma-q/2}\int_0^1 dt\, e^{-z^2r^\sigma t}\tau_t^{-q/2}\left[B^q\left(\tau_t^{-1}\right)-1\right]\\&+r^{\sigma-q/2}\int_0^1 dt\, e^{-z^2r^\sigma t}\tau_t^{-q/2}\left[B^p\left(r^{\sigma/\rho}\eta_t\right)-1\right]\left[B^q\left(\frac{1}{\tau_t}\right)-1\right]\end{aligned}$$

The last term is always negligible in the limit $r\to\infty$ and will be dropped from now on.

Then we can write the gap equation as

$$\begin{aligned}(4\pi)^{\rho+(d-\rho D)/2}(\beta-\beta_c)L^{\rho(D-2)}=&-(4\pi)^{\rho d/2}Az^{D-2}\\&+r^{\sigma-q/2}\mathcal{J}_1(z^2r^\sigma)+\mathcal{J}_2(z^2)+C_{\sigma,p}\int_1^{r^\sigma} dt\, e^{-z^2t}t^{-q/2\sigma}\end{aligned}\tag{A.8}$$

where $\beta = 1/T$, β_c is given in Eq. (3.7), $z = (4\pi)^{-\rho/2}(L^\rho/\xi_V)$ and

$$\begin{aligned} \mathcal{J}_1(x) &:= \frac{e^{-x}}{x} + \mathcal{G}_{\sigma,q}(x) \\ \mathcal{J}_2(x) &:= -C_{\sigma,q}C_{\rho,p}\int_1^\infty dt\, t^{-D/2}e^{-xt} + \mathcal{G}_{\rho,p}(x) \end{aligned} \tag{A.9}$$

where

$$\begin{aligned} \mathcal{G}_{\sigma,q}(x) &:= \int_1^\infty dt\, e^{-xt}\left[B^q\left(\tau_t\right) - 1\right] + \int_0^1 dt\, e^{-xt}\tau_t^{-q/2}\left[B^q\left(\tau_t^{-1}\right) - 1\right] \\ &= \int_0^\infty dt\, e^{-xt}\tau_t^{-q/2}\left[B^q\left(\tau_t^{-1}\right) - 1\right] + \int_1^\infty e^{-xt}(\tau_t^{-q/2} - 1)\, dt \\ &= \int_0^\infty dt\, e^{-\tau_1^{-\sigma}xt}t^{-q/2\sigma}\tau_1^{-\sigma}\left[B^q\left(t^{-1/\sigma}\right) - 1\right] + \int_1^\infty e^{-xt}(\tau_t^{-q/2} - 1)\, dt \\ &= \int_0^\infty dt\, \Psi_\sigma(xt)t^{-q/2\sigma}\left[B^q\left(t^{-1/\sigma}\right) - 1\right] + C_{\sigma,q}\int_1^\infty e^{-xt}t^{-q/2\sigma}\, dt - \frac{e^{-x}}{x} \end{aligned}$$

and $\Psi_\sigma(x) := \mathbb{E}[e^{-\tau_1^{-\sigma}x}\tau_1^{-\sigma}]$. The function $\Psi_\sigma(x)$ has the following asymptotic behaviours if $0 < \sigma < 1$:

$$\Psi_\sigma(x) \sim x^{-2} \qquad \text{for } x \to +\infty$$

and

$$\Psi_\sigma(x) \sim x^{-1}\exp\left(-Cx^{-1/(1-\sigma)}\right) \qquad \text{for } x \to 0+$$

for some positive constant C, while $\Psi_1(x) = e^{-x}$.

Note that when z^2r^σ is constant (for $r \to \infty$) and $q/\sigma < 2$ we get:

$$\begin{aligned} \mathcal{J}_1(r^\sigma z^2) &+ r^{q/2-\sigma}C_{\sigma,p}\int_1^{r^\sigma} dt\, e^{-z^2t}t^{-q/2\sigma} \\ &= \int_0^\infty dt\, \Psi_\sigma(r^\sigma z^2 t)t^{-q/2\sigma}\left[B^q\left(t^{-1/\sigma}\right) - 1\right] + C_{\sigma,q}\int_{1/r^\sigma}^\infty e^{-r^\sigma z^2 t}t^{-q/2\sigma}\, dt \\ &= \int_0^\infty dt\, \Psi_\sigma(r^\sigma z^2 t)t^{-q/2\sigma}B^q\left(t^{-1/\sigma}\right) + C_{\sigma,q}\int_0^{1/r^\sigma} e^{-r^\sigma z^2 t}t^{-q/2\sigma}\, dt \\ &\approx \int_0^\infty dt\, \Psi_\sigma(r^\sigma z^2 t)t^{-q/2\sigma}B^q\left(t^{-1/\sigma}\right). \end{aligned}$$

and this corresponds to the FSS function of the q dimensional system. In the case $q/\sigma \geq 2$ we have simply (see sec. 3.4):

$$\begin{aligned} \mathcal{J}_1(z^2r^\sigma) &- C_{\sigma,p}\int_1^\infty e^{-r^\sigma z^2 t}t^{-q/2\sigma}\, dt \\ &= \int_0^\infty dt\, \Psi_\sigma(r^\sigma z^2 t)t^{-q/2\sigma}\left[B^q\left(t^{-1/\sigma}\right) - 1\right]. \end{aligned}$$

Appendix B

Raw data from simulations

Here we collect all the relevant quantities we measured in MC simulations.

$L_\parallel$	L	ξ	χ	A	m	g	$\xi_\parallel$
		$\beta = 0.28$					
32	16	1.6191(18)	10.758(12)	0.24368(40)	0.130291(73)	0.19471(80)	1.5953(65)
46	18	1.6939(19)	11.782(13)	0.24353(42)	0.106822(60)	0.14899(76)	2.5022(91)
64	20	1.7486(24)	12.577(15)	0.24312(52)	0.088528(55)	0.11355(89)	3.641(10)
88	22	1.7952(23)	13.221(16)	0.24375(45)	0.073648(45)	0.08358(94)	5.122(12)
110	24	1.8295(27)	13.731(17)	0.24375(55)	0.064195(40)	0.0663(11)	6.346(13)
168	28	1.8838(33)	14.568(22)	0.24359(60)	0.049452(37)	0.0416(11)	9.453(23)
262	32	1.9130(38)	15.109(23)	0.24221(70)	0.037688(30)	0.0277(11)	13.582(41)
373	36	1.9339(50)	15.484(28)	0.24155(93)	0.030126(27)	0.0167(13)	17.804(73)
512	40	1.9589(64)	15.839(38)	0.2423(12)	0.024660(29)	0.0089(24)	22.22(13)
		$\beta = 0.29$					
32	16	1.8263(17)	13.231(13)	0.25208(39)	0.145232(73)	0.25367(72)	1.7096(61)
46	18	1.9385(20)	14.892(18)	0.25235(37)	0.120651(76)	0.20415(84)	2.6886(74)
64	20	2.0284(26)	16.334(19)	0.25189(49)	0.101281(61)	0.16350(80)	3.9684(87)
88	22	2.1010(25)	17.559(23)	0.25139(41)	0.085143(56)	0.12623(83)	5.625(10)
110	24	2.1626(26)	18.572(24)	0.25184(41)	0.074864(49)	0.10536(88)	7.064(12)
168	28	2.2486(38)	20.138(33)	0.25108(56)	0.058257(49)	0.0701(11)	10.627(18)
262	32	2.3090(40)	21.315(37)	0.25011(56)	0.044811(40)	0.0437(13)	15.740(35)
373	36	2.3518(49)	22.110(44)	0.25016(66)	0.036028(36)	0.0285(14)	21.017(54)
512	40	2.387(14)	22.84(10)	0.2494(21)	0.029636(61)	0.0165(55)	27.09(49)
		$\beta = 0.3$					
32	16	2.0810(19)	16.654(18)	0.26003(20)	0.16414(12)	0.3287(11)	1.8128(99)
46	18	2.2599(26)	19.612(20)	0.26040(55)	0.139479(84)	0.2857(11)	2.8963(90)
64	20	2.4111(19)	22.351(29)	0.26009(50)	0.119294(98)	0.2426(13)	4.3016(32)
88	22	2.5570(29)	25.083(30)	0.26066(45)	0.102430(75)	0.20601(64)	6.202(16)
110	24	2.6604(17)	27.218(18)	0.26004(21)	0.091161(32)	0.17936(56)	7.8399(71)
168	28	2.8383(41)	31.017(47)	0.25972(43)	0.072636(58)	0.13168(89)	11.964(14)
262	32	2.9828(34)	34.254(60)	0.25974(33)	0.057022(57)	0.0952(16)	18.223(30)
373	36	3.0875(46)	36.748(72)	0.25942(34)	0.046562(47)	0.0643(12)	24.984(81)
512	40	3.1673(69)	38.735(99)	0.25899(53)	0.038667(45)	0.0487(26)	32.511(60)
		$\beta = 0.3025$					
32	16	2.1529(18)	17.656(16)	0.26252(34)	0.169306(83)	0.34838(66)	1.8477(56)
46	18	2.3538(21)	21.087(22)	0.26274(33)	0.144925(78)	0.30826(63)	2.9442(74)
64	20	2.5344(27)	24.444(31)	0.26276(35)	0.125037(84)	0.26921(72)	4.4080(77)
88	22	2.6955(29)	27.681(36)	0.26249(38)	0.107824(73)	0.23164(74)	6.3251(94)
110	24	2.8283(30)	30.490(40)	0.26235(40)	0.096697(67)	0.20661(81)	8.033(11)
168	28	3.0548(37)	35.567(58)	0.26238(41)	0.077917(66)	0.1559(11)	12.367(16)
262	32	3.2340(55)	39.948(89)	0.26181(44)	0.061649(71)	0.1127(14)	18.913(30)
373	36	3.3720(64)	43.30(11)	0.26258(45)	0.050597(68)	0.0819(16)	26.068(50)
512	40	3.4664(82)	45.92(14)	0.26170(58)	0.042138(63)	0.0598(23)	34.334(90)
		$\beta = 0.3050$					
32	16	2.2299(16)	18.781(16)	0.26476(24)	0.175010(84)		
46	18	2.4605(22)	22.815(26)	0.26534(26)	0.151172(96)		
64	20	2.6633(27)	26.749(38)	0.26517(27)	0.13114(10)		
88	22	2.8588(35)	30.793(54)	0.26541(29)	0.11403(11)		
110	24	3.0259(43)	34.462(70)	0.26570(29)	0.10308(11)		
168	28	3.3077(62)	41.22(11)	0.26543(36)	0.08412(12)		
216	30	3.4114(70)	44.06(13)	0.26415(36)	0.07390(12)		
256	32	3.5286(85)	47.07(17)	0.26450(42)	0.06786(13)		
365	36	3.710(11)	52.05(22)	0.26442(50)	0.05621(12)		
500	40	3.888(14)	56.95(29)	0.26548(64)	0.04759(13)		
592	42	3.914(16)	57.93(31)	0.26443(99)	0.04298(12)	0.0714(39)	41.03(19)
681	44	3.979(15)	60.18(30)	0.26308(84)	0.039892(98)	0.0653(30)	46.27(16)
778	46	4.038(10)	61.62(20)	0.26462(57)	0.036916(61)	0.0589(20)	51.86(14)
884	48	4.0554(99)	62.51(19)	0.26310(58)	0.034121(55)	0.0483(24)	57.63(16)
		$\beta = 0.3075$					
32	16	2.3093(21)	19.992(18)	0.26676(35)	0.181034(88)	0.39515(57)	1.9069(49)
46	18	2.5687(19)	24.682(23)	0.26733(32)	0.157657(78)	0.36309(69)	3.0624(65)
64	20	2.8141(24)	29.501(31)	0.26844(33)	0.138181(79)	0.33179(70)	4.5961(80)
88	22	3.0400(30)	34.533(43)	0.26762(32)	0.121188(79)	0.29934(68)	6.6479(79)
168	28	3.6017(45)	48.397(93)	0.26804(31)	0.091505(93)	0.2356(11)	13.145(14)
262	32	3.9228(68)	57.37(14)	0.26825(43)	0.074304(94)	0.1859(14)	20.397(27)
373	36	4.1764(87)	65.23(18)	0.26740(45)	0.062411(92)	0.1485(16)	28.500(45)
512	40	4.374(10)	71.66(24)	0.26701(48)	0.052849(94)	0.1167(24)	38.117(78)
681	44	4.549(14)	77.60(34)	0.26669(54)	0.04540(10)	0.0950(21)	48.88(12)

Table B.1: Observables for S_2 geometries.

$L_\parallel$	L	ξ	χ	A	m	g	$\xi_\parallel$
		$\beta = 0.31$					
32	16	2.3975(28)	21.392(31)	0.26870(25)	0.18784(15)	0.42136(99)	1.9320(82)
46	18	2.6893(22)	26.803(21)	0.26983(48)	0.164882(77)	0.39503(46)	3.1211(84)
64	20	2.9691(13)	32.596(27)	0.27044(27)	0.145826(79)	0.36797(77)	4.6893(89)
88	22	3.2437(43)	39.005(63)	0.26975(63)	0.12933(12)	0.3399(14)	6.7983(51)
110	24	3.4866(24)	44.941(38)	0.27049(21)	0.118671(53)	0.32316(66)	8.6928(80)
168	28	3.9556(44)	57.703(84)	0.27116(28)	0.100412(81)	0.2893(11)	13.564(13)
262	32	4.3976(58)	71.31(12)	0.27119(33)	0.083257(82)	0.2425(15)	21.143(30)
373	36	4.7836(81)	84.43(20)	0.27101(36)	0.071388(92)	0.2109(18)	29.947(46)
512	40	5.112(12)	96.54(34)	0.27073(41)	0.06163(12)	0.1760(23)	40.289(97)
		$\beta = 0.3105$					
32	16	2.4141(18)	21.584(17)	0.27000(31)	0.188709(78)	0.42424(50)	1.9437(49)
46	18	2.7082(23)	27.167(24)	0.26996(34)	0.166028(80)	0.39866(62)	3.1332(61)
64	20	3.0040(30)	33.295(35)	0.27104(40)	0.147436(82)	0.37382(59)	4.7005(70)
88	22	3.2910(33)	39.952(49)	0.27109(35)	0.130987(88)	0.34836(80)	6.8253(92)
110	24	3.5446(38)	46.274(61)	0.27151(37)	0.120523(85)	0.33253(72)	8.749(11)
168	28	4.0443(58)	60.03(12)	0.27247(37)	0.10250(11)	0.2993(12)	13.658(15)
262	32	4.5097(78)	74.75(19)	0.27205(37)	0.08534(12)	0.2559(13)	21.358(23)
373	36	4.940(11)	89.79(30)	0.27177(41)	0.07372(13)	0.2281(18)	30.152(49)
512	40	5.291(13)	103.04(38)	0.27166(45)	0.06374(13)	0.1934(20)	40.584(81)
		$\beta = 0.3110$					
32	16	2.4295(20)	21.876(18)	0.26982(35)	0.190095(85)	0.42942(53)	1.9526(50)
46	18	2.7330(23)	27.666(25)	0.26998(34)	0.167675(85)	0.40611(63)	3.1384(68)
64	20	3.0375(31)	34.004(36)	0.27133(39)	0.149149(86)	0.38293(61)	4.7344(75)
88	22	3.3367(30)	40.949(49)	0.27189(36)	0.132722(85)	0.35717(70)	6.8476(85)
110	24	3.6087(35)	47.810(61)	0.27239(36)	0.122655(85)	0.34509(79)	8.787(10)
168	28	4.1255(52)	62.29(11)	0.27324(33)	0.10453(10)	0.3117(11)	13.767(15)
262	32	4.6328(72)	78.78(19)	0.27243(35)	0.08778(11)	0.2775(12)	21.587(23)
373	36	5.094(12)	95.09(33)	0.27294(44)	0.07597(14)	0.2445(20)	30.390(43)
512	40	5.497(12)	110.66(39)	0.27303(38)	0.06615(13)	0.2101(22)	41.149(65)
592	42	5.675(10)	118.34(32)	0.27217(33)	0.062069(87)	0.2028(15)	47.288(60)
681	44	5.900(14)	127.52(47)	0.27299(37)	0.05864(11)	0.1943(19)	53.826(94)
778	46	6.060(21)	134.56(72)	0.27292(51)	0.05503(16)	0.1776(32)	61.22(17)
884	48	6.176(25)	140.72(88)	0.27105(64)	0.05165(17)	0.1672(32)	69.04(20)
		$\beta = 0.31125$					
32	16	2.4391(21)	22.020(21)	0.27017(34)	0.190759(98)	0.43198(51)	1.9496(46)
46	18	2.7438(24)	27.858(25)	0.27025(36)	0.168324(83)	0.40925(54)	3.1504(59)
64	20	3.0473(30)	34.278(36)	0.27090(40)	0.149801(87)	0.38624(68)	4.7501(71)
88	22	3.3586(35)	41.500(52)	0.27182(35)	0.133692(89)	0.36231(68)	6.880(11)
110	24	3.6414(40)	48.512(68)	0.27334(33)	0.123605(96)	0.34876(90)	8.7956(94)
168	28	4.1695(60)	63.68(13)	0.27298(39)	0.10579(11)	0.3197(11)	13.791(15)
262	32	4.6869(85)	80.48(23)	0.27293(37)	0.08872(13)	0.2777(13)	21.586(26)
373	36	5.172(11)	97.82(33)	0.27350(41)	0.07711(14)	0.2516(17)	30.574(43)
512	40	5.604(19)	115.01(60)	0.27304(62)	0.06757(18)	0.2286(28)	41.61(13)
		$\beta = 0.3115$					
32	16	2.4499(21)	22.206(20)	0.27029(35)	0.191660(94)	0.43570(56)	1.9444(47)
46	18	2.7630(23)	28.101(26)	0.27166(33)	0.169113(85)	0.41200(53)	3.1561(62)
64	20	3.0710(26)	34.685(33)	0.27190(34)	0.150740(77)	0.38977(61)	4.7504(72)
88	22	3.3783(39)	42.010(63)	0.27167(36)	0.13457(11)	0.36717(79)	6.894(10)
110	24	3.6678(42)	49.176(70)	0.27356(39)	0.124528(95)	0.35446(75)	8.8076(88)
168	28	4.2136(58)	64.79(12)	0.27404(38)	0.10677(10)	0.32546(96)	13.840(14)
262	32	4.7588(76)	82.70(20)	0.27383(39)	0.09004(12)	0.2897(13)	21.687(26)
373	36	5.2512(90)	100.80(27)	0.27356(32)	0.07832(11)	0.2583(15)	30.613(44)
512	40	5.698(13)	118.80(42)	0.27327(43)	0.06871(13)	0.2344(20)	41.721(66)
		$\beta = 0.3118$					
32	16	2.4574(22)	22.305(18)	0.27073(38)	0.192139(82)	0.43817(50)	1.9559(55)
46	18	2.7764(21)	28.383(23)	0.27159(31)	0.170033(76)	0.41621(51)	3.1652(61)
64	20	3.0867(27)	35.021(38)	0.27207(32)	0.151519(88)	0.39259(56)	4.7673(68)
88	22	3.4079(36)	42.577(56)	0.27277(35)	0.135525(97)	0.37079(73)	6.9033(91)
110	24	3.6859(45)	49.781(77)	0.27291(38)	0.12533(11)	0.35856(88)	8.846(11)
168	28	4.2503(57)	66.04(13)	0.27352(36)	0.10787(11)	0.3322(12)	13.855(15)
262	32	4.8231(79)	84.93(21)	0.27390(39)	0.09131(12)	0.2979(12)	21.773(29)
373	36	5.3518(97)	104.56(30)	0.27392(40)	0.07985(12)	0.2702(18)	30.811(53)
512	40	5.824(15)	123.75(52)	0.27406(42)	0.07015(16)	0.2419(23)	41.981(78)
		$\beta = 0.312$					
32	16	2.4678(20)	22.462(19)	0.27113(34)	0.192845(85)	0.43929(51)	1.9516(55)
46	18	2.7878(22)	28.602(24)	0.27173(34)	0.170722(77)	0.41788(58)	3.1652(62)
64	20	3.1094(26)	35.444(36)	0.27279(34)	0.152516(82)	0.39803(57)	4.7690(69)
88	22	3.4340(31)	43.148(50)	0.27331(33)	0.136530(86)	0.37673(70)	6.9430(85)
110	24	3.7134(37)	50.531(64)	0.27289(37)	0.126343(86)	0.36395(73)	8.879(11)
168	28	4.2984(63)	67.50(13)	0.27372(39)	0.10914(11)	0.3402(11)	13.924(14)
262	32	4.8875(75)	87.18(20)	0.27400(35)	0.09258(11)	0.3047(14)	21.838(24)
373	36	5.452(11)	107.89(34)	0.27552(39)	0.08121(14)	0.2824(19)	30.973(50)
512	40	5.947(17)	128.62(60)	0.27501(50)	0.07164(18)	0.2575(23)	42.297(66)
592	42	6.211(12)	140.35(42)	0.27490(28)	0.06784(11)	0.2466(17)	48.474(63)
681	44	6.457(19)	151.99(71)	0.27428(46)	0.06427(16)	0.2389(26)	55.32(11)
778	46	6.718(37)	163.8(1.5)	0.27547(67)	0.06097(30)	0.2271(49)	62.87(24)
884	48	6.967(41)	176.7(1.8)	0.27476(44)	0.05773(21)	0.2143(29)	70.94(14)

Table B.2: Observables for S_2 geometries (continued).

$L_\parallel$	L	ξ	χ	A	m	g	$\xi_\parallel$
		$\beta = 0.2700$					
27	16	1.4454(19)	8.862(12)	0.23573(45)	0.128502(86)	0.17296(81)	1.1913(69)
34	18	1.4954(20)	9.470(10)	0.23614(51)	0.111341(62)	0.14255(87)	1.6062(72)
42	20	1.5329(24)	9.967(12)	0.23576(55)	0.097300(62)	0.1151(10)	2.0688(93)
51	22	1.5592(24)	10.346(13)	0.23499(56)	0.085656(57)	0.09695(96)	2.5861(89)
61	24	1.5894(28)	10.710(13)	0.23587(66)	0.076194(48)	0.07837(97)	3.145(11)
72	26	1.6041(31)	10.940(16)	0.23519(68)	0.068041(50)	0.0652(13)	3.734(12)
83	28	1.6228(33)	11.176(17)	0.23564(72)	0.061684(47)	0.0546(11)	4.348(13)
96	30	1.6333(37)	11.347(19)	0.23510(81)	0.055797(48)	0.0454(11)	5.042(14)
109	32	1.6343(36)	11.482(15)	0.23262(84)	0.050981(35)	0.0404(13)	5.696(17)
123	34	1.6522(40)	11.654(19)	0.23424(84)	0.046886(40)	0.0327(12)	6.392(17)
138	36	1.6522(43)	11.713(19)	0.23304(95)	0.043113(35)	0.0289(11)	7.156(20)
		$\beta = 0.2800$					
27	16	1.6078(18)	10.608(12)	0.24371(40)	0.141098(82)	0.21683(73)	1.2656(61)
34	18	1.6790(22)	11.544(14)	0.24421(48)	0.123372(77)	0.18615(89)	1.7196(69)
42	20	1.7372(23)	12.355(16)	0.24425(46)	0.108684(75)	0.15826(85)	2.2208(78)
51	22	1.7773(23)	12.997(15)	0.24303(48)	0.096259(57)	0.13224(88)	2.7900(83)
61	24	1.8204(27)	13.598(18)	0.24371(56)	0.086066(58)	0.11185(85)	3.4055(86)
72	26	1.8476(28)	14.043(18)	0.24308(54)	0.077252(48)	0.09492(89)	4.082(11)
83	28	1.8734(33)	14.431(21)	0.24321(62)	0.070217(51)	0.08127(98)	4.755(11)
96	30	1.8945(34)	14.768(25)	0.24303(58)	0.063750(54)	0.0675(10)	5.526(12)
109	32	1.9043(38)	15.028(23)	0.24131(70)	0.058397(46)	0.0586(10)	6.268(14)
123	34	1.9323(40)	15.331(26)	0.24353(72)	0.053840(47)	0.0512(13)	7.054(15)
138	36	1.9343(43)	15.469(27)	0.24188(77)	0.049596(44)	0.0445(12)	7.884(17)
		$\beta = 0.2900$					
27	16	1.8037(19)	12.916(14)	0.25188(41)	0.156535(86)	0.27642(63)	1.3439(60)
34	18	1.9076(22)	14.419(15)	0.25237(44)	0.138582(78)	0.24633(73)	1.8381(61)
42	20	1.9976(25)	15.785(19)	0.25279(45)	0.123430(78)	0.21559(75)	2.3915(69)
51	22	2.0698(26)	16.985(19)	0.25222(49)	0.110566(65)	0.19109(77)	3.0210(77)
61	24	2.1357(30)	18.064(24)	0.25251(50)	0.099601(70)	0.16537(83)	3.7082(84)
72	26	2.1844(31)	18.968(26)	0.25155(48)	0.090113(65)	0.14495(83)	4.466(10)
83	28	2.2336(34)	19.779(30)	0.25224(51)	0.082481(65)	0.12726(97)	5.219(12)
96	30	2.2689(41)	20.458(38)	0.25164(59)	0.075258(71)	0.1109(10)	6.075(12)
109	32	2.2940(43)	21.033(36)	0.25021(63)	0.069279(61)	0.09770(98)	6.906(13)
123	34	2.3295(50)	21.600(45)	0.25122(66)	0.064065(69)	0.0863(12)	7.816(16)
138	36	2.3419(51)	21.911(42)	0.25032(71)	0.059143(59)	0.0742(12)	8.761(15)
		$\beta = 0.3000$					
20	14	1.8678(18)	13.359(13)	0.26114(36)	0.19981(11)	0.38211(68)	0.9423(43)
27	16	2.0451(18)	16.048(16)	0.26064(35)	0.175755(92)	0.35074(64)	1.4267(55)
34	18	2.2007(23)	18.525(18)	0.26143(42)	0.158235(82)	0.32416(63)	1.9608(59)
42	20	2.3416(25)	20.966(24)	0.26152(38)	0.143360(85)	0.30099(57)	2.5730(67)
51	22	2.4671(26)	23.294(26)	0.26128(41)	0.130462(77)	0.27686(60)	3.2779(66)
61	24	2.5877(34)	25.550(34)	0.26208(47)	0.119365(83)	0.25488(78)	4.0314(76)
72	26	2.6846(33)	27.551(37)	0.26160(42)	0.109383(77)	0.23121(75)	4.8877(86)
83	28	2.7722(39)	29.392(45)	0.26148(47)	0.101252(80)	0.21389(89)	5.7302(99)
96	30	2.8580(44)	31.168(57)	0.26207(48)	0.093527(90)	0.19614(94)	6.6920(86)
109	32	2.9138(52)	32.634(67)	0.26017(51)	0.086828(93)	0.1780(10)	7.648(12)
123	34	2.9866(56)	34.180(77)	0.26097(52)	0.081052(95)	0.1628(13)	8.691(12)
138	36	3.0370(64)	35.371(87)	0.26075(58)	0.075560(98)	0.1479(14)	9.745(14)
154	38	3.0917(75)	36.63(10)	0.26097(62)	0.07077(10)	0.1334(13)	10.877(15)
170	40	3.1348(68)	37.663(93)	0.26091(62)	0.066508(85)	0.1206(14)	11.965(17)
188	42	3.1616(73)	38.480(99)	0.25976(63)	0.062341(81)	0.1111(16)	13.231(17)
206	44	3.2164(77)	39.64(10)	0.26099(66)	0.059016(80)	0.1033(18)	14.405(21)
225	46	3.2507(86)	40.49(12)	0.26100(70)	0.055792(87)	0.0949(19)	15.656(23)
245	48	3.270(11)	41.04(15)	0.26059(91)	0.052654(95)	0.0854(20)	16.949(26)
		$\beta = 0.3050$					
20	14	1.9723(17)	14.656(13)	0.26540(34)	0.21009(10)	0.41775(57)	0.9678(42)
27	16	2.1854(20)	18.010(17)	0.26520(35)	0.187020(96)	0.39378(54)	1.4718(48)
34	18	2.3748(22)	21.200(19)	0.26602(39)	0.170114(82)	0.37334(59)	2.0229(54)
42	20	2.5586(28)	24.546(29)	0.26671(40)	0.155959(97)	0.35571(67)	2.6680(69)
51	22	2.7211(28)	27.834(30)	0.26602(38)	0.143433(84)	0.33657(68)	3.4026(58)
61	24	2.8880(35)	31.164(42)	0.26762(43)	0.132607(97)	0.31780(78)	4.2086(73)
72	26	3.0252(33)	34.280(46)	0.26697(39)	0.122762(89)	0.29762(81)	5.1162(83)
83	28	3.1607(42)	37.379(57)	0.26726(44)	0.114903(93)	0.28322(92)	6.0117(82)
96	30	3.2921(50)	40.442(80)	0.26799(43)	0.10717(11)	0.2648(11)	7.0637(99)
109	32	3.3951(51)	43.112(87)	0.26737(42)	0.10040(10)	0.24926(96)	8.089(10)
123	34	3.4976(66)	45.84(11)	0.26685(47)	0.09441(12)	0.2331(13)	9.183(12)
138	36	3.5890(70)	48.27(11)	0.26688(51)	0.08877(11)	0.2172(13)	10.340(13)
154	38	3.6723(83)	50.59(15)	0.26655(54)	0.08365(13)	0.2046(15)	11.564(14)
170	40	3.7468(78)	52.72(13)	0.26630(54)	0.07912(11)	0.1910(17)	12.752(15)
188	42	3.8238(93)	54.83(16)	0.26664(60)	0.07479(12)	0.1756(15)	14.098(17)
206	44	3.9064(90)	57.14(17)	0.26705(54)	0.07122(11)	0.1695(20)	15.397(18)

Table B.3: Observables for S_1 geometries.

$L_\parallel$	L	ξ	χ	A	m	g	$\xi_\parallel$
		$\beta = 0.3075$					
20	14	2.0260(18)	15.377(14)	0.26693(37)	0.21562(11)	0.43514(58)	0.9739(41)
27	16	2.2591(18)	19.086(17)	0.26741(34)	0.192989(89)	0.41587(57)	1.4878(47)
34	18	2.4703(21)	22.757(22)	0.26815(34)	0.176750(89)	0.40000(53)	2.0536(55)
42	20	2.6805(28)	26.667(28)	0.26944(38)	0.163081(93)	0.38605(61)	2.7072(64)
51	22	2.8694(26)	30.587(30)	0.26919(36)	0.150870(81)	0.37077(59)	3.4618(64)
61	24	3.0660(37)	34.732(45)	0.27065(43)	0.140522(99)	0.35528(71)	4.2969(65)
72	26	3.2320(35)	38.708(50)	0.26986(37)	0.130984(92)	0.33958(81)	5.2175(75)
83	28	3.3983(42)	42.685(62)	0.27054(41)	0.123258(97)	0.32456(88)	6.1509(79)
96	30	3.5586(52)	46.757(90)	0.27085(42)	0.11573(12)	0.31052(84)	7.2287(95)
109	32	3.6914(63)	50.44(11)	0.27017(46)	0.10908(13)	0.2965(11)	8.320(10)
123	34	3.8308(70)	54.23(14)	0.27061(42)	0.10316(14)	0.2835(14)	9.465(10)
138	36	3.9527(77)	57.72(15)	0.27068(48)	0.09751(13)	0.2677(15)	10.647(13)
154	38	4.0672(88)	61.27(17)	0.26999(54)	0.09246(13)	0.2556(15)	11.915(13)
170	40	4.1867(92)	64.66(19)	0.27108(53)	0.08802(14)	0.2436(16)	13.194(16)
188	42	4.2847(91)	67.99(21)	0.27004(47)	0.08368(14)	0.2331(18)	14.581(15)
206	44	4.380(12)	71.10(25)	0.26985(59)	0.07980(15)	0.2235(19)	15.968(18)
225	46	4.480(12)	74.30(25)	0.27012(57)	0.07626(14)	0.2113(19)	17.400(21)
245	48	4.597(19)	77.59(41)	0.27230(87)	0.07305(20)	0.2012(29)	18.905(30)
		$\beta = 0.3100$					
20	14	2.0803(17)	16.099(14)	0.26882(34)	0.22114(11)	0.45550(55)	0.9858(38)
27	16	2.3350(18)	20.249(18)	0.26927(31)	0.199294(92)	0.43898(56)	1.5114(45)
34	18	2.5740(24)	24.454(22)	0.27094(38)	0.183806(91)	0.42857(57)	2.0910(49)
42	20	2.8085(29)	29.010(29)	0.27189(38)	0.170689(92)	0.41803(60)	2.7541(56)
51	22	3.0279(27)	33.728(35)	0.27182(33)	0.159041(90)	0.40608(65)	3.5199(61)
61	24	3.2576(36)	38.830(49)	0.27329(39)	0.14921(10)	0.39540(71)	4.3808(68)
72	26	3.4681(35)	44.015(56)	0.27326(33)	0.140330(95)	0.38513(68)	5.3551(78)
83	28	3.6659(45)	49.047(79)	0.27399(38)	0.13281(12)	0.37484(82)	6.3058(89)
96	30	3.8708(51)	54.601(99)	0.27441(40)	0.12574(12)	0.36477(97)	7.4272(91)
109	32	4.0477(61)	59.83(12)	0.27385(43)	0.11947(13)	0.3539(10)	8.547(10)
123	34	4.2325(72)	65.25(16)	0.27455(39)	0.11381(15)	0.3424(12)	9.720(12)
138	36	4.3939(79)	70.38(17)	0.27433(45)	0.10831(14)	0.3303(13)	10.977(11)
154	38	4.5703(95)	75.93(22)	0.27508(48)	0.10358(16)	0.3227(14)	12.292(13)
170	40	4.735(10)	81.35(25)	0.27561(48)	0.09937(16)	0.3128(17)	13.625(13)
188	42	4.866(13)	86.36(31)	0.27424(59)	0.09492(18)	0.3032(19)	15.069(17)
206	44	5.038(12)	92.33(29)	0.27490(51)	0.09153(16)	0.2957(19)	16.540(21)
225	46	5.180(13)	97.53(35)	0.27508(50)	0.08798(17)	0.2888(20)	18.062(19)
245	48	5.308(16)	102.39(45)	0.27523(60)	0.08450(20)	0.2778(24)	19.649(22)
		$\beta = 0.3105$					
20	14	2.0938(19)	16.262(16)	0.26957(37)	0.22237(12)	0.45986(56)	0.9873(38)
27	16	2.3509(18)	20.494(18)	0.26968(32)	0.200643(93)	0.44444(50)	1.5144(44)
34	18	2.5933(21)	24.793(21)	0.27125(36)	0.185200(84)	0.43405(53)	2.0948(53)
42	20	2.8349(28)	29.515(31)	0.27230(37)	0.172285(98)	0.42387(59)	2.7650(62)
51	22	3.0629(27)	34.435(35)	0.27243(35)	0.160827(88)	0.41367(61)	3.5498(55)
61	24	3.3017(36)	39.732(48)	0.27437(40)	0.151077(100)	0.40393(73)	4.4067(72)
72	26	3.5166(37)	45.117(56)	0.27410(37)	0.142234(97)	0.39465(72)	5.3678(75)
83	28	3.7252(42)	50.504(72)	0.27477(38)	0.13492(10)	0.38514(78)	6.3260(89)
96	30	3.9348(50)	56.272(95)	0.27514(38)	0.12780(12)	0.37533(91)	7.4512(88)
109	32	4.1305(65)	62.08(13)	0.27485(43)	0.12187(14)	0.3677(12)	8.5713(93)
123	34	4.3159(78)	67.64(16)	0.27540(45)	0.11604(15)	0.3562(13)	9.794(11)
138	36	4.4987(89)	73.47(19)	0.27547(47)	0.11084(16)	0.3463(14)	11.044(13)
154	38	4.686(11)	79.62(25)	0.27577(49)	0.10623(18)	0.3381(15)	12.363(15)
170	40	4.8519(98)	85.29(23)	0.27602(50)	0.10192(15)	0.3302(15)	13.698(15)
188	42	5.018(12)	91.28(30)	0.27587(52)	0.09776(17)	0.3215(18)	15.189(16)
206	44	5.197(13)	97.72(34)	0.27643(49)	0.09435(18)	0.3159(19)	16.662(18)
225	46	5.334(13)	103.14(34)	0.27580(51)	0.09060(16)	0.3025(20)	18.216(20)
245	48	5.489(17)	109.22(46)	0.27590(60)	0.08741(20)	0.2957(26)	19.836(22)
		$\beta = 0.3110$					
20	14	2.1061(19)	16.430(15)	0.26998(37)	0.22362(11)	0.46423(55)	0.9908(38)
27	16	2.3666(19)	20.736(16)	0.27011(36)	0.201910(87)	0.44876(57)	1.5182(49)
34	18	2.6156(23)	25.172(21)	0.27178(37)	0.186712(85)	0.43921(53)	2.0986(50)
42	20	2.8638(28)	30.029(28)	0.27312(37)	0.173898(87)	0.43062(52)	2.7792(61)
51	22	3.0987(27)	35.107(36)	0.27350(34)	0.162528(90)	0.42106(58)	3.5550(65)
61	24	3.3405(37)	40.632(50)	0.27464(39)	0.15292(10)	0.41237(68)	4.4207(61)
72	26	3.5649(34)	46.252(52)	0.27476(35)	0.144130(88)	0.40306(72)	5.3925(75)
83	28	3.7869(45)	52.038(78)	0.27557(38)	0.13712(11)	0.39676(82)	6.3605(82)
96	30	4.0117(55)	58.29(11)	0.27609(39)	0.13023(13)	0.38748(97)	7.4973(92)
109	32	4.2089(68)	64.25(13)	0.27570(44)	0.12414(14)	0.3792(12)	8.5935(95)
123	34	4.4081(77)	70.40(16)	0.27602(45)	0.11853(15)	0.3689(13)	9.822(11)
138	36	4.6000(86)	76.64(19)	0.27610(44)	0.11339(16)	0.3620(15)	11.112(12)
154	38	4.8075(96)	83.44(22)	0.27699(46)	0.10894(16)	0.3550(15)	12.449(12)
170	40	4.990(11)	89.74(27)	0.27749(46)	0.10471(17)	0.3461(17)	13.804(15)
188	42	5.157(12)	96.24(32)	0.27639(45)	0.10055(18)	0.3393(21)	15.286(16)
206	44	5.360(15)	103.48(39)	0.27761(59)	0.09725(20)	0.3332(20)	16.773(17)
225	46	5.525(13)	110.00(38)	0.27749(48)	0.09376(18)	0.3239(20)	18.320(20)
245	48	5.693(18)	116.79(51)	0.27751(62)	0.09055(21)	0.3147(24)	19.951(20)

Table B.4: Observables for S_1 geometries (continued).

Bibliography

General references of Statistical Mechanics and Field Theory applied to Critical Phenomena and RG:

[1] P. C. Hoenberg and B. I. Halperin, Rev. Mod. Phys. **49**, 435 (1977).

[2] C. N. Yang and T. D. Lee, Phys. Rev. Lett. **87**, 404 (1952);
Phys. Rev. Lett. **87**, 410 (1952).

[3] T.M. Ligget, *Interacting Particle Systems*, Springer-Verlag, New York, 1985.

[4] D. Ruelle, *Statistical Mechanics: Rigorous Results*, Addison Wesley Publishing Company, New York, 1989.

[5] J. Zinn-Justin, *Quantum Field Theory and Critical Phenomena*, 3 ed. (Oxford Science Publication, Clarendon Press, Oxford, 1996).

[6] Basic concepts of the statistical theory of critical phenomena may be found in the following books:
J. Cardy, *Scaling and Renormalization in Statistical Physics*, Cambridge University Press, Cambridge lecture notes in physics 5 (1996).
S. K. Ma, *Modern Theory of Critical Phenomena*, Addison–Wesley Publishing Company, 12th printing (1994).
K. Huang, *Statistical Mechanics*, John Wiley & Sons, 2nd ed. (1987).
G. Parisi *Statistical Field Theory*(Frontiers in Physics 66), Addison–Wesley, Redwood City (1988).
D. J. Amit *Field Theory, the Renormalization Group, and Critical Phenomena*, 2nd ed., World Scientific, Singapore (1984).
see also Ref. [5].

[7] M. E. Fisher, in *Critical Phenomena, International School of Physics "Enrico Fermi", Course 51*, edited by M. S. Green, Academic Press, New York, 1971.

[8] M. E. Fisher, in *Critical Phenomena*, Lecture Notes in Physics, vol. 186, edited by F. J. W. Hahne (Springer, Berlin, 1983).

[9] R. Kubo, M. Toda, N. Hashitsume, *Statistical Physics*, Springer–Verlag, Berlin, 1985.

[10] N. G. van Kampen, *Stochastic processes in physics and chemistry*, North Holland Publishing Company, Amsterdam, 1983.

Functional approach to dynamical critical phenomena:

[11] P. C. Martin, E. D. Siggia and H. A. Rose, Phys. Rev. A **8**, 423 (1973).

[12] H. K. Janssen, Z. Phys. B **23**, 377 (1976).

[13] R. Bausch, H. K. Janssen, and H. Wagner, Z. Phys. B **24**, 113 (1976).

[14] H. K. Janssen, Field-theoretic method applied to critical dynamics, in *Dynamical Critical Phenomena and Related Topics*, edited by C. P. Enz, Lecture Notes in Physics, Vol. 104, (Springer, Berlin–New York–Tokyo, 1979).

[15] D. Revuz, M. Yor, *Continuous Martingales and Brownian Motion*, Springer-Verlag, Berlin 1994.

General references for Non-equilibrium systems:

[16] M. R. Evans, *Phase Transitions in one–dimensional nonequilibrium systems*, Brazilian Journal of Physics **30**, 42-57 (2000), e-print `cond-mat/0007293`.
M. R. Evans and R. A. Blythe, *Nonequilibrium Dynamics in Low Dimensional Systems*, Lectures at the International Summer School on Fundamental Problems in Statistical Physics X, Aug.-Sept. 2001, Altenberg (Germany), to appear in the Proceedings, e-print `cond-mat/0110630`.

[17] H. Hinrichsen, *Nonequilibrium Critical Phenomena and Phase Transitions into Absorbing States*, Adv. in Phys. **49**, 815-958 (2000), e-print `cond-mat/0001070`.

[18] J. Marro and R. Dickman, *Nonequilibrium Phase Transitions in Lattice Models* (Cambridge University Press, Cambridge, 1999).

[19] G. Grinstein, *Generic scale invariance in classical nonequilibrium systems*, J. App. Phys. **69**, 5441 (1991).

Driven Lattice Gas and Generalizations:

[20] B. Schmittmann and R. P. K. Zia, *Statistical mechanics of driven diffusive systems*, in *Phase Transitions and Critical Phenomena*, edited by C. Domb and J. L. Lebowitz, Vol. 17 (Academic Press, London, 1995).

[21] S. Katz, J. L. Lebowitz, and H. Spohn, Phys. Rev. B **28**, 1655 (1983); J. Stat. Phys. **34**, 497 (1984).

[22] H. van Beijeren and L. S. Schulman, Phys. Rev. Lett. **53**, 806 (1984). J. Krug, J. L. Lebowitz, H. Spohn, and M. Q. Zhang, J. Stat. Phys. **44**, 535 (1986).

[23] G. L. Eyink and F. J. Alexander. Shape-dependent thermodinamics and non-local hydrodynamics in a non-gibbsian steady-state of a drift-diffusion system. *Phys. Rev. E*, 57, 1998.

[24] G. L. Eyink, J. L. Lebowitz, and H. Spohn. Hydrodinamic and fluctuations outside of local equilibrium: Driven diffusive systems. *J. Stat. Phys.*, 83(3/4):385–472, 1996.

Field theoretical studies:

[25] K. Gawedzki and A. Kupiainen, Nucl. Phys. B **269**, 45 (1986).

[26] H. K. Janssen and B. Schmittmann, Z. Phys. B **64**, 503 (1986).

[27] K.-t. Leung and J. L. Cardy, J. Stat. Phys. **44**, 567 (1986); Erratum J. Stat. Phys. **45**, 1087 (1986).

Two temperatures DLG:

[28] P. L. Garrido, J. L. Lebowitz, C. Maes, and H. Spohn, *Long-range correlations for conservative dynamics*, Phys. Rev. A **42**, 1954 (1990).

[29] E. L. Præstgaard, H. Larsen, and R. K. P. Zia, *Finite-Size Scaling in a Two-Temperature Lattice Gas: a Monte Carlo Study of Critical Properties*, Europhys. Lett. **25**(6), 447 (1994).

[30] E. L. Præstgaard, B. Schmittmann, and R. K. P. Zia, *A Lattice Gas Coupled to Two Thermal Reservoirs: Monte Carlo and Field Theoretic Studies*, e-print `cond-mat/0010053`.

Random Field DLG:

[31] B. Schmittmann and R. K. P. Zia, *Critical Properties of a Randomly Driven Diffusive System*, Phys. Rev. Lett. **66**, 357 (1991).
Pay attention to a mistake pointed out in [32], footnote pag. 112.

[32] B. Schmittmann, *Fixed–Point Hamiltonian for a Randomly Driven Diffusive System*,Europhys. Lett. **24**, 109 (1993).

Further generalizations:

[33] K. Oerding and H. K. Janssen, *Surface Critical Behaviour of Driven Diffusive Systems with Open Boundaries*, Phys. Rev. E **58**,1446 (1998), e-print `cond-mat/9805189`.

[34] H. K. Janssen and K. Oerding, *Renormalized Field Theory and Particle Density Profile in Driven Diffusive Systems with Open Boundaries*, Phys. Rev. E **53**, 4544 (1996), e-print `cond-mat/9605175`.

[35] V. Becker, H. K. Janssen, *Field Theory of Critical Behaviour in Driven Diffusive Systems with Quenched Disorder*, e-print `cond-mat/9904216`.

[36] R. A. Monetti and E. V. Albano, *Critical behavior of a non-equilibrium interacting particle system driven by an oscillatory field*, Europhys. Lett. **56**, 400 (2001).

MC, FSS of DLG and alternative Field Theories:

[37] M. Gubinelli, *Leggi di Scala per Fenomeni Critici fuori dall'Equilibrio Termodinamico*, Laurea Thesis, University of Pisa, 1998 (unpublished).

[38] M. Q. Zhang, J.-S. Wang, J. L. Lebowitz, and J. L. Vallés, J. Stat. Phys. **52**, 1461 (1988).

[39] K.-t. Leung, Phys. Rev. Lett. **66**, 453 (1991).
See also [40].

[40] K.-t. Leung, Int. J. Mod. Phys. C **3**, 367 (1992).

[41] J. S. Wang, J. Stat. Phys. **82**, 1409 (1996).

[42] A. Achahbar and J. Marro, *Phase Transitions in a Driven Lattice Gas in Two Planes*, J. Stat. Phys. **78**, 1493 (1995).

[43] K. -t. Leung and R. K. P. Zia, *Subtelties in Data Analysis Related to the Size of Critical Region*, J. Stat. Phys. **83**, 1219 (1996).

[44] J. Marro, A. Achahbar, P. L. Garrido, and J. J. Alonso, *Phase transitions in driven lattice gases*, Phy. Rev. E **53**, 6038 (1996).

[45] K.-t. Leung and J. S. Wang, Int. J. Mod. Phys. C **10**, 853 (1999).

[46] K. Binder and J. S. Wang, J. Stat. Phys. **55**, 87 (1989).

[47] J. L. Vallés and J. Marro, J. Stat. Phys. **43**, 441 (1986); **49**, 89 (1987).

[48] P. L. Garrido, and M. A. Muñoz, *Fokker–Planck equation for nonequilibrium competing dynamics*, Phys. Rev. E **50**, 2458 (1994),
Continuum Description for Nonequilibrium Competing Dynamic Models, Phy. Rev. Lett. **75**, 1875 (1995).

[49] P. L. Garrido, F. de los Santos, and M. A. Muñoz, *Langevin equation for driven diffusive systems*, Phys. Rev. E **57**, 752 (1998).

[50] P. L. Garrido and F. de los Santos, J. Stat. Phys. **96**, 303 (1999), e-print `cond-mat/9805211`.

[51] F. de los Santos and M. A. Muñoz, *Renormalized field theory of driven lattice gases under infinitely fast drive*, Phys. Rev. E **61**, 1161 (2000), e-print `cond-mat/9903053`. Note that e-print version of the paper contains wrong critical exponents, as pointed out in [52, 54].

[52] S. Caracciolo, A. Gambassi, M. Gubinelli and A. Pelissetto, private communication to M. A. Muñoz, November 1999.

[53] P. L. Garrido, M. A. Muñoz, and F. de los Santos, Phys. Rev. E **61**, R4683 (2000), e-print `cond-mat/0001165`.

[54] B. Schmittmann, H. K. Janssen, U. C. Täuber, R. K. P. Zia, K.-t. Leung, and J. L. Cardy Phys. Rev. E **61**, 5977 (2000), e-print `cond-mat/9912286`.

[55] K.-t. Leung, *Heuristic derivation of continuum kinetic equations from microscopic dynamics*, Phys. Rev. E **63**, 016102 (2001), e-print `cond-mat/0006217`.

[56] S. Caracciolo, A. Gambassi, M. Gubinelli and A. Pelissetto, *Finite–Size Critical Behaviour of the Driven Lattice Gas*, e-print `cond-mat/0106221`.

[57] A. Achahbar, P. L. Garrido, J. Marro, and M. A. Muñoz, *Is the Particle Current a Relevant Feature in Driven Lattice Gases?*, Phys. Rev. Lett. **87**, 195702-1 (2001), e-print `cond-mat/0106470`.

Studies on dynamical aspects of the DLG phase transition:

[58] K. Hwang, B. Schmittmann, and R. K. P. Zia, *Three–point correlation functions in uniformly and randomly driven diffusive systems*, Phys. Rev. E **48**, 800 (1993).

[59] A. D. Rutenberg and C. Yeung, *Triangular anisotropies in driven diffusive systems: Reconciliation of up and down*, Phys. Rev. E **60**, 2710 (1999).

[60] E. Levine, Y. Kafri and D. Mukamel, *Ordering dynamics of the driven lattice gas model*, Phys. Rev. E **64**, 026105 (2001), e-print `cond-mat/0101324`.

[61] E. V. Albano and G. Saracco, *Dynamic Behavior of Anisotropic Nonequilibrium Driving Lattice Gases*, *Phys. Rev. Lett.* **88**, 145701 (2002).

General references on MC methods:

[62] A. D. Sokal, *Monte Carlo mehtods in statistical mechanics: Foundations and New Algorithms*, lectures given at the Cours de Troisième Cycle de la Physique en Suisse Romande, Lausanne, Switzerland, Jun 15-29, 1989.

[63] K. Kawasaki, in *Phase Transitions and Critical Phenomena*, edited by C. Domb and M. S. Green, Vol. 2, p. 443 (Academic Press, New York, 1972).

[64] D. E. Knuth, *The Art of Computer Programming, Vol. 2 - Seminumerical Algorithms* (Addison-Wesley, Reading, Massachusetts, 1997).

[65] B. Efron, *The Jackknife, the Bootstrap and Other Resampling Plans*, Regional Conference Series in Applied Mathematics, Vol. 38 (SIAM, Philadelphia, 1982).

FSS (theory and MC):

[66] E. Brézin, J. Physique **43**, 15 (1982).

[67] M. E. Fisher and M. N. Barber, Phys. Rev. Lett. **28**, 1516 (1972).

[68] Y. Imry and B. Bergman, Phys. Rev. A **3**, 1416 (1971).

[69] M. N. Barber, *Finite–Size Scaling*, in *Phase Transitions and Critical Phenomena*, edited by C. Domb and J. L. Lebowitz, Vol. 8 (Academic Press, London, 1983).

[70] K. Binder. Monte Carlo investigations. In C. Domb and M. S. Green, editors, *Phase Transitions and Critical Phenomena*, volume 5. Academic Press, New York, 1976.

[71] E. Brézin and J. Zinn-Justin, Nucl. Phys. B **257** [FS14], 867 (1985).

[72] J. Rudnick, H. Guo, and D. Jasnow, J. Stat. Phys. **41**, 353 (1985).

[73] J. L. Cardy, editor, *Finite-Size Scaling* (North-Holland, Amsterdam, 1988).

[74] S. M. Bhattacharjee and J. F. Nagle, *Finite-size effect for the critical point of an anisotropic dimer model of domain walls*, Phys. Rev. A **31**, 3199 (1985).

[75] S. Caracciolo, R. G. Edwards, S. J. Ferreira, A. Pelissetto, and A. D. Sokal, Phys. Rev. Lett. **74**, 2969 (1995), e-print `hep-lat/9409004`.
A similar method has been introduced in Refs. [76, 77].

[76] M. Lüscher, P. Weisz, and U. Wolff, Nucl. Phys. B **359**, 221 (1991).

[77] J.-K. Kim, Europhys. Lett. **28**, 211 (1994);
Phys. Rev. D **50**, 4663 (1994);
Nucl. Phys. B (Proc. Suppl.) **34**, 702 (1994).

[78] S. Caracciolo, R. G. Edwards, A. Pelissetto, and A. D. Sokal, Phys. Rev. Lett. **75**, 1891 (1995), e-print `hep-lat/9411009`.

[79] S. Caracciolo, R. G. Edwards, T. Mendes, A. Pelissetto, and A. D. Sokal, Nucl. Phys. B (Proc. Suppl.) **47**, 763 (1996), e-print `hep-lat/9509033`.

[80] G. Mana, A. Pelissetto, and A. D. Sokal, Phys. Rev. D **54**, 1252 (1996), e-print `hep-lat/9602015`.

[81] T. Mendes, A. Pelissetto, and A. D. Sokal, Nucl. Phys. B **477**, 203 (1996), e-print `hep-lat/9604015`.

[82] G. Mana, A. Pelissetto, and A. D. Sokal, Phys. Rev. D **55**, 3674 (1997), e-print `hep-lat/9610021`.

[83] S. J. Ferreira and A. D. Sokal, J. Stat. Phys. **96**, 461 (1999), e-print `cond-mat/9811345`.

[84] S. Caracciolo and M. Palassini, Phys. Rev. Lett. **82**, 5128 (1999), e-print `cond-mat/9904246`.

[85] M. Hasenbusch, J. Physique I **3**, 753 (1993).

[86] H. W. J. Blöte and G. Kamieniarz, Physica A **196**, 455 (1993).

[87] H. W. J. Blöte, E. Luijten, and J. R. Heringa, J. Phys. A **28**, 6289 (1995).

[88] J. Salas and A. D. Sokal, J. Stat. Phys. **88**, 567 (1997), hep-lat/9607030.

[89] M. Hasenbusch, K. Pinn, and S. Vinti, Phys. Rev. B **59**, 11471 (1999).

[90] H. G. Ballesteros, L. A. Fernández, V. Martín-Mayor, A. Muñoz Sudupe, G. Parisi, and J. J. Ruiz-Lorenzo, J. Phys. A **32**, 1 (1999).

[91] X. S. Chen and V. Dohm, Eur. Phys. J. B **7**, 183 (1999); **15**, 283 (2000).

[92] V. Privman and M. E. Fisher, *Finite–Size Effects at First–Order Transitions*, J. Stat. Phys. **33**, 385 (1983).

[93] E. Eisenriegler and R. Tomaschiz, Phys. Rev. B **35**, 4876 (1987).

[94] D. Dantchev and J. Rudnick, cond-mat/0010478.

[95] S. Caracciolo, A. Gambassi, M. Gubinelli, and A. Pelissetto, Eur. Phys. J. B **20**, 255 (2001), e-print `cond-mat/0010479`.

[96] A. Gambassi, internal note (2001).

[97] Z. B. Li, L. Schülke, and B. Zheng, *Phys. Rev. Lett.* **74**, 3396 (1995);
K. Okano, L. Schülke, K. Yamagishi, and B. Zheng, *Nucl. Phys. B* **485**, 727 (1997);
B. Zheng, *Int. J. Mod. Phys. B* **12**, 1419 (1998);
Physica A **283**, 80 (2000).

[98] J. G. Brankov, D. M. Danchev, N. S. Tonchev, *Theory of Critical Phenomena in Finite-Size Systems*, World Scientific, Singapore (2000).